Integrated Wireless-PON Access Network Architectures

Milos Milosavljevic

A thesis submitted in partial fulfilment

of the requirements of the University of Hertfordshire

for the degree of Doctor of Philosophy

The programme of research was carried out in the Science and Technology Research Institute (STRI), University of Hertfordshire, United Kingdom.

2010

Abstract

Next generation access networks should be able to cultivate the ongoing evolution in services and applications. Advancements on that front are expected to exhibit the transformation of high definition television (HDTV) and 2D services into ultra-HDTV and individual interactive 3D services. Currently deployed passive optical networks (PONs) have been certified to be able to deliver high quality video and internet services while in parallel broadband wireless standards are increasing their spectral efficiency and subscriber utilisation. Exploiting the benefits of both by providing an integrated infrastructure benefiting from the wireless mobility and ease of scalability and escalating bandwidth of next generation PONs are expected to offer service providers the business models justifying the evolved services. In this direction, this thesis deals with the means of transparent routing of standard worldwide interoperability for microwave access (WiMAX) signal formats over legacy PONs to and from wireless end users based on radio over fibre (RoF). The concept of frequency division multiplexing (FDM) with RoF is used for efficient addressing of individual base stations, bandwidth on-demand provisioning across a cell/sector, simple remote radio heads and no interference with the baseband PON spectrum. Network performance evaluation, initially through simulation, has displayed, in the presence of optical non-linearites and multi-path wireless channels, standard error vector magnitudes (EVMs) at remote radio receivers and bit error rates (BERs) of 1E-4 for typical WiMAX rates bidirectionally. To provide enhanced scalability and dynamicity, a newly applied scheme based on extended wavelength band overlay over the splitter, wireless-enabled PONs has been progressively investigated. This allows for the routing of multiple FDM windows to different wavelengths resulting in significantly reduced optical and electrical component costs and no dispersion compensation over the fibre. This has been implemented through the application of a dense array wave guide grating (AWG) and tuneable filter in the optical line terminal (OLT) and optical network unit/base stations (ONU/BSs) respectively. Although with the use of a splitter the distribution point of the optical network remains largely the same, vertical cavity surface emitting laser (VCSEL) arrays provide colourless upstream transmission. In addition, an overlapping cell concept is developed and adopted for increased wireless spectral efficiency and resilience. Finally, an experimental test-bed using commercially available WiMAX transceivers was produced, which enabled repetition of the simulation outcomes and therefore confirmed the overall network performance.

Acknowledgments

To begin with, I would like to thank my supervisor, colleague and friend Dr. Pandelis Kourtessis for his dedication, professionalism, caring and friendly support throughout the course of my research, particularly for believing in me all the way through.

I would also like to thank my supervisor Prof. John M. Senior for his trust, financial support and allowing me to conduct my research without any limits.

I am also indebted to many of my colleagues including Fabien Delestre, Ali Gliwan and Yuval Shachaf for establishing a friendly working environment and also for giving me valuable advises throughout the whole process.

Many thanks to my best friends Dr. Surosh Pillay, Stratis Sofianos, Satpal Juttla and Riste Petrov for giving me the strength, psychological support, encouragement and their endless respect to what I have been working on for the past years.

This is also a great opportunity to thank Dr. Manoj Thakur and Dr. John Mitchell from University College London (UCL) for allowing me to use their facilities in order to perform experimental investigations and for their help throughout.

The last but not the least, this thesis would not be possible without my parents and my girlfriend who encouraged me to achieve and complete my PhD.

Publications

1. M. Milosavljevic, P. Kourtessis, and J. M. Senior, "**Multi-Wavelength WiMAX-PONs with Overlapping Cells**", IEEE/OSA Journal of Optical Communications and Networking, vol. 3, pp. 172-177, (2011)

2. M. Milosavljevic, P. Kourtessis, W. Lim, and J. M. Senior, "**Optical/Wireless Convergence (invited)**," presented at 13th International Conference on Transparent Optical Networks (ICTON), Sweden, Stockholm, July 2011

3. W. Lim, P. Kourtessis, M. Milosavljevic, and J. M. Senior, "**MAC protocol for the Wireless Enabled OFDMA-PON (invited)**," presented at 13th International Conference on Transparent Optical Networks (ICTON), Sweden, Stockholm, July 2011

4. M. Milosavljevic, P. Kourtessis, and J. M. Senior, "**Wireless Convergence over Next Generation OFDMA-PONs**", to be presented in Access Networks and In-House Communications (ANIC), OSA Technical Digest (CD), Canada, Toronto, (in press), June 2011

5. W. Lim, P. Kourtessis, M. Milosavljevic, and J. M. Senior, "**Dynamic Subcarrier Allocation for OFDMA-PONs with Monitoring Mechanism**", to be presented in Access Networks and In-House Communications (ANIC), OSA Technical Digest (CD), Canada, Toronto, (in press), June 2011

6. M. Milosavljevic, M. P. Thakur , P. Kourtessis , J. E. Mitchell , J. M. Senior, "**A Multi-Wavelength Access Network featuring WiMAX Transmission over GPON Links**", presented at 36th European Conference and Exhibition on Optical Communication (ECOC), Italy, Turin, pp. 1334-1336, September 2010

7. <u>M. Milosavljevic</u>, P. Kourtessis, A. Gliwan, and J. M. Senior, "**Multi-wavelength wireless-PONs (invited)**," presented at 12th International Conference on Transparent Optical Networks (ICTON), Germany, Munich, July 2010

8. <u>M. Milosavljevic</u>, P. Kourtessis, and J. M. Senior, "**Transparent Wireless Transmission over the ACCORDANCE Optical/Wireless Segment**", presented at IEEE/IET International Symposium on Communication Systems, Networks and Digital Signal Processing (CSNDSP), United Kingdom, Newcastle, pp. 138-142, July 2010

9. <u>M. Milosavljevic</u>, P. Kourtessis, and J. M. Senior, "**Wireless-PONs with Extended Wavelength Band Overlay**", presented in Access Networks and In-House Communications (ANIC), OSA Technical Digest (CD), Germany, Karlsruhe, paper AWC6, June 2010

10. <u>M. Milosavljevic</u>, Y. Shachaf, P. Kourtessis, and J. M. Senior, "**Interoperability of GPON and WiMAX for Network Capacity Enhancement and Resilience**", OSA Journal of Optical Networks, vol. 8, pp. 285-294, (2009)

11. <u>M. Milosavljevic</u>, P. Kourtessis, A. Gliwan, and J. M. Senior, "**Advanced PON topologies with wireless connectivity (invited)**," presented at 11th International Conference on Transparent Optical Networks (ICTON) , Azores, Ponta Delgada, July 2009

12. <u>M. Milosavljevic</u>, P. Kourtessis, and J. M. Senior, "**Integrated Wireless Optical Networking**," presented at London Communications Symposium (LCS), UK, London, August 2009

13. <u>M. Milosavljevic</u>, F. Bensali, P. Kourtessis, "**xDSL Network Upgrade Employing FPGAs**," presented at 4th IEEE International Symposium on Electronic Design, Test and Applications (DELTA), Hong Kong, pp. 158 - 162, January 2008

Table of Contents

Chapter 7: Experimental Investigation of WiMAX Transmission over Multi-Wavelength PONs

Chapter 8: Project Achievements and Future Work

List of Figures

List of Tables

Abbreviations

A/D	Analog to digital
ADM	Add/drop multiplexer
APD	Avalanche photodetector
ASE	Amplified spontaneous emission
AWG	Arrayed waveguide grating
AWGN	Additive white Gaussian noise
BER	Bit-error-rate
BTS	Base transceiver station
BPF	Band-pass filter
BS	Base station
BWA	Broadband wireless access
CAPEX	Capital Expenditures
CO	Centre office
CP	Cyclic prefix
CPRI	Common public radio interface
CTB	Composite triple beat
CW	Continuous wave
D/A	Digital to analog
DFB	Distributed feedback
DML	Directly modulated laser
DoF	Digital over fibre
DW	Downstream
EIRP	Effective isotropic radiated power
eNB	Enhanced node B
EPON	Ethernet passive optical network
EVM	Error vector magnitude
ER	Extinction ratio
FDMA	Frequency division multiple access
FDM	Frequency division multiplexing
FEC	Forward error correction
FFT	Fast Fourier transform
FTTB	Fibre to the building
FTTC	Fibre to the curb/cabinet
FTTH	Fibre to the home
FTTX	Fibre to the x
FUSC	Full usage of subcarrier
GPON	Gigabit-capable passive optical network
HDTV	High definition television
HPA	High power amplifier
IEEE	Institute of electrical and electronics engineering
IETF	Internet engineering task force
IFFT	Inverse FFT
IMD	Inter modulation distortion
IM-DD	Intensity modulation with direct detection
IP	Internet protocol
IPTV	Internet protocol television
ISI	Inter-symbol interference
ISP	Internet service provider
ITU-T	International telecommunication union
LAN	Local area network
LO	Local oscillator

LOS	Line of sight
LPF	Low-pass filter
LTE	Long Term Evaluation
MAC	Medium access control
MAN	Metropolitan network
MIMO	Multiple-input multiple-output
MO	Middle office
MPEG	Movie pictures experts group
MZM	Mach-Zehnder modulator
NLOS	Non-line of sight
NRZ	Non-return-to-zero
OBI	Optical beat interferance
ODN	Optical distribution network
ODSB	Optical double sideband
OFDM	Orthogonal frequency division multiplexing
OFM	Optical frequency multiplication
OLT	Optical line terminal
ONU	Optical network unit
OPEX	Operational Expenditure
OSNR	Optical signal to noise ratio
OSSB	Optical single sideband
PAN	Personal area network
P2MP	Point-to-multi-point
P2P	Point-to-point
PBC	Polarisation beam combiner
PBS	Polarisation beam splitter
PDF	Probability density function
PDL	Polarisation-dependent loss
PHY	Physical layer
PLC	Power line communication
PON	Passive optical network
PRBS	Pseudo-random binary sequence
PUSC	Partial usage of subcarriers
PXI	PCI extensions for instrumentation
QAM	Quadrature amplitude modulation
QoS	Quality of service
RCE	Relative constellation error
RE	Radio equipment
REC	Radio equipment control
RoF	Radio over Fibre
RF	Radio frequency
RIN	Relative intensity noise
RSOA	Reflective semiconductor optical amplifier
RTG	Receive transition gap
SER	Symbol error rate
SFDR	Spurious free dynamic range
SNR	Signal to noise ratio
SOA	Semiconductor optical amplifier
SPM	Self phase modulation
SSB	Single sideband
SSMF	Standard single mode fibre
SUI	Stanford university interim
TDMA	Time division multiple access
TDM	Time division multiplexing

TE	Transverse electric
TM	Transverse magnetic
TTG	Transmit transition gap
UHF	Ultra high frequency
UP	Upstream
UWB	Ultra-wideband
VCSEL	Vertical cavity surface emitting laser
VoD	Video on demand
VoIP	Voice-over-IP
VPI	Virtual photonics Inc.
VLC	Visible light communication
WDM	Wavelength division multiple
WiFi	Wireless-fidelity
WiMAX	Worldwide-interoperability-for microwave-access
WMN	Wireless mesh network
XPM	Cross phase modulation

Chapter 1

Introduction – PON and WiMAX Technologies

Contents

This chapter provides an introduction to the rapidly emerging access network services and technologies. It starts with an outline of the escalating bandwidth demand, required to provide the current and future online services, subsequently establishing the justification for the convergence of passive optical networks (PON) and state-of-the-art wireless access network technologies to demonstrate next generation access networks. The introduction concludes with the characteristics of PON worldwide deployments and the interoperability of microwave access (WiMAX) architectures, offering a broad perspective of the diverse trends owing to the different business plans of network operators.

1.1 Network Convergence

This research programme has been widely driven by the deployment and development of PON [1] and WiMAX [2] access technologies aiming to provide transparent integrated network solution while in particular in the latter case transforming into emerging radio standards, such as long term evaluation (LTE) [3]. To a broader extent, next-generation access networks should

demonstrate consolidation between different service platforms, mainly optical, wireless and copper access, a model of which is shown in Figure 1-1 [4].
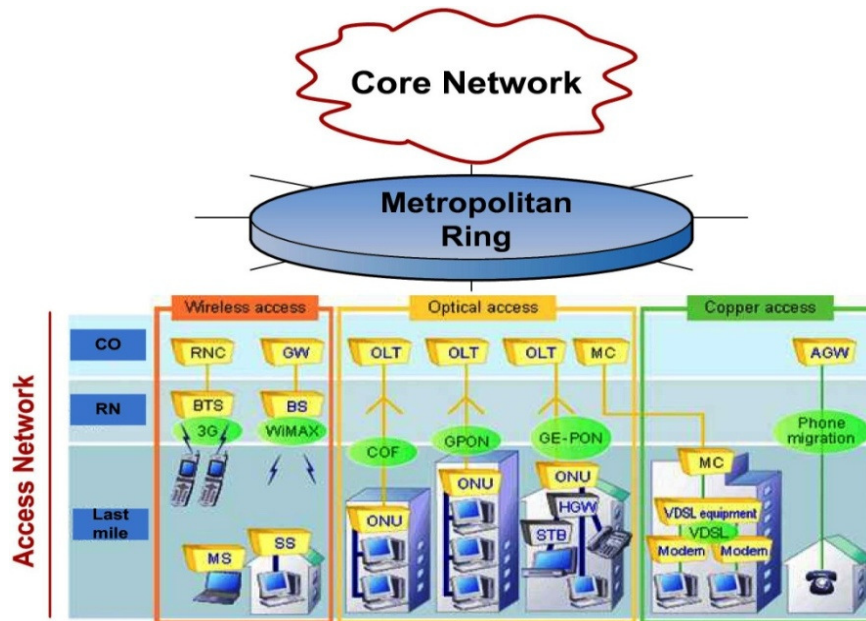
Figure 1-1: A model of next-generation access networks [4]

These networks are unavoidably expected to steer the attention of telecomm operators, providers, vendors and the research community towards state-of-the-art integrated architectural platforms for medium as well as longer term solutions. The former has been naturally generated by the deployment issues risen in the request of accommodating varying network penetration and servicing in the presence of diverse geographical areas while the later driven primarily by researchers and standardisation bodies aiming to provide the next generation converged networks that would lead the way of development from a high-cost and fixed fibre to the home (FTTH)-based networks to cost-effective integrated solutions with enhanced spectral efficiency and resilience, more supported users and most importantly ubiquity and mobility.

In both scenarios characteristics such as optical network transparency to various radio signal formats, scalability, dynamicity and small radio cells are essential ingredients to provide end-users with real-time bandwidth on demand and interactive, multimedia services. From the

operators' point of view, these key network characteristics coupled with the ease of last mile implementation are vital properties to keep capital and operational costs effectively low, particularly since the cost of FTTH-based solutions cannot be currently justified. Towards this direction, the optical network is expected to allow the handling of high data-rates required by the aggregation of traffic originating at the wired and wireless subscribers, whilst the wireless is expected to complement the optical network to enhance flexibility and robustness. Such advantages become more evident in the case of isolated rural areas where optical solutions for broadband internet access become cost ineffective.

1.2 Service Requirements

Over the recent years residential and business customers demand access solutions that have high bandwidth, offering media-rich applications [5, 6] including high-definition television (HDTV), video-on-demand (VoD), online gaming, voice-over-IP (VoIP) and high-speed Internet.

Table 1-1: Bandwidth estimation for a single residential customer [5, 7]

Service	Bandwidth	Comments
3 HDTV channels per residential at 20 Mbit/s each	60 Mbit/s	Three HDTV channels
Education-on-demand, online gaming, Internet	10 Mbit/s	Peer-to-peer require symmetrical bandwidth
Video conference of video phone	2 Mbit/s	Requires symmetrical bandwidth
Remote control and sensing	1 Mbit/s	Requires symmetrical bandwidth
Total	**73 Mbit/s**	**Downstream: 73 Mbit/s** **Upstream: 53 Mbit/s**

As shown in Table 1-1, a single HDTV channel encoded by MPEG2 [7] requires approximately 20 Mbit/s. Consequently, based on an estimation of three television sets per home, it is expected that three HDTV channels operating concurrently will be used by a single residential customer

in addition to services such as high-speed Internet and video phone, allowing for a total bandwidth in the range of 73 Mbit/s that is thought to be sought by subscribers in downstream in the near future [7]. In upstream, mainly driven by symmetrical bandwidth service requirements including online gaming, video-conferencing and education-on-demand in tandem with high-speed Internet and content generation, bandwidth allocations reaching 53 Mbit/s will be needed [7].

In addition, by introducing high TV/Video resolution including future services like UHDTV or 3D TV, real time services (e.g. real time TV/VoD hopping and streaming, cloud 3D gaming and teleworking), individual interactive services (e.g. time shift TV, gaming and peer-to-peer), cloud computing (e.g. personal video recording and web-storage) and business E-Line point-to-point (P2P), the average data rate for a single residential customer or small business is eventually expected to grow symmetrically to more than 300 Mbit/s. Consequently, it becomes apparent that the current estimates given in Table 1-1, if not already, definitely in the forthcoming future, are bound to change.

1.3 State-of-the-Art Access Networks

The deeper penetration of the fibre to subscriber close proximity is considered as an ideal candidate to meet the capacity challenges in the access network at present and in the foreseeable future. Consequently, due to the widespread adoption of the Ethernet protocol in local networks and the increasing demand for high-speed access networks, active Ethernet FTTH architectures have been extensively investigated and standardised [8]. Among these access network architectures, an Ethernet router/switch can be deployed in either the street cabinet for a point to multipoint topology or in the local exchange for a point to point topology, using multimode and single-mode fibres to provide subscribers with data rates in the range of 100 Mbit/s to 1 Gbit/s depending on distances and the type of fibre used. In that sense, placing an active device in the street cabinet requires high capital expenditures (CAPEX) in addition to high operational expenditures (OPEX) due to the need for electrical power monitoring and maintenance of backup batteries in the street cabinet [1]. Moreover, such a network is not transparent to different signal formats and data rates, consequently in case the network is to be upgraded to support higher data rates or different transmission protocols it requires replacing the electronics in the street cabinet [1]. On the contrary, placing the switch in the local exchange results in a large number of fibres reaching the local exchange, though allows virtually unlimited bandwidth per subscriber due to dedicated connections to subscribers and upgradability to higher speeds on subscriber by subscriber basis.

In the meanwhile, PONs have evolved to provide simplicity and low network costs [1]. The PON is a typical point to multipoint optical access network based on FTTH, fibre-to-the-building (FTTB) or fibre-to-the-curb (FTTC) infrastructure, connecting the optical line terminal (OLT) in the local exchange with many residential and business customers by means of passive splitters located in the field. PONs have been largely adopted and deployed mostly in Asia and

North America in contrast to Europe that is moving forward with several fibre deployment projects so far [9]. Consequently, detailed analysis of time division multiplexed (TDM)-PON and its standards will be performed in the following chapter.

The dominance of PON systems is reflected in the chart of Figure 1-2 which compares the connected numbers of PON subscribers to active Ethernet subscribers, showing the significant market advantage of PON systems [10].
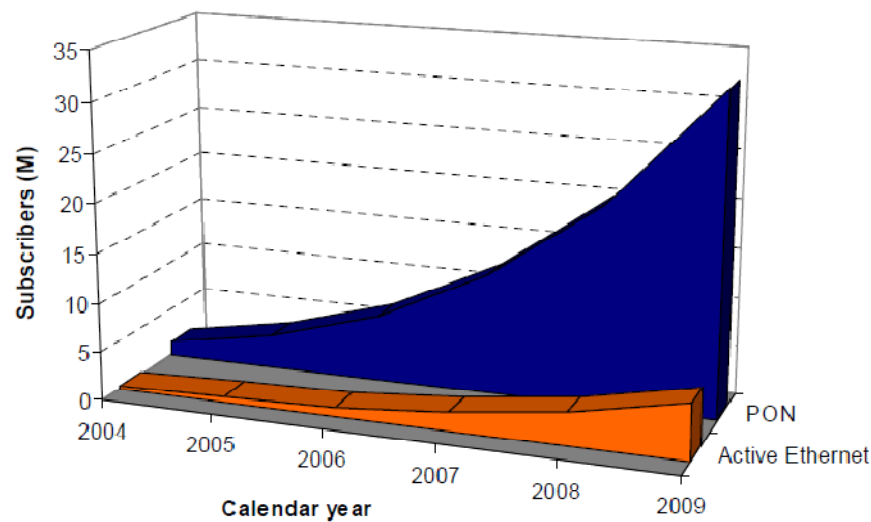
Figure 1-2: PON versus active Ethernet deployment [10]

In parallel with the above, broadband access networks in excessive deployment and increasing development include wireless alternatives, employed to satisfy low field deployment cost and mobility. The two broadband wireless access standards, WiMAX [11, 12] and 3GPP LTE [13], are promising to deliver speeds in the range of hundreds of Mbit/s for point to multipoint wireless broadband communication supporting services required by 4G networks. Nevertheless, these broadband wireless solutions are currently not viable to support high-speed Internet and media-rich video applications since the relatively low aggregate bandwidth is shared among tens to hundreds of users over macro-cellular distances [14]. As with the advancements of novel transmission technologies, such as advanced signal processing techniques and smart antennas,

6

these standards are however continuously upgraded for the delivery of even higher throughputs and therefore enhanced quality of service per a subscriber [2, 15]

From the deployment prospective, WiMAX is considered worldwide for mobile broadband wireless solutions while LTE is expecting delays in deployment due to the limited LTE-enabled devices as further developments are required from the silicon side [16].

Finally, for high-speed local and personal area networks (LAN and PAN), deployed mainly for in-door environments, wireless-fidelity (WiFi) [17, 18] and ultra-wideband (UWB) [19] have emerged from different standardisation bodies as state-of-the-art solutions to offer data rates in the range of 100 Mbit/s to 1 Gbit/s respectively. However, they only provide a very limited mobility and cannot guarantee the required performance to deliver real time multimedia services [20, 21].

1.4 Deployment of FTTH and WiMAX Solutions Worldwide

1.4.1 FTTH

Throughout Europe there are currently more than 1 million FTTH subscribers based on Gigabit-PON (GPON) networks, although the number of connected homes is approximately 2.6 million [22] with a forecast of 4 million FTTH subscribers by the end of 2010 [23]. Currently, as a result of regulatory uncertainties, there are several fibre deployment projects in Europe, initiated both by new network operators and incumbents, mostly located in Sweden, Italy, France, Germany, Denmark, Netherlands and Norway [24].

On the contrary, South Korea has maintained high broadband service penetration rate with rapid growth of approximately 7 million subscribers requesting triple-play services in excess of 50 Mbit/s [7] and as a result approximately 12 million subscribers are expected to be served by 2010 [7, 25]. According to bandwidth demand, cost and future upgradeability, wavelength

division multiplexing (WDM)-PON based FTTH has been chosen to be deployed primarily although has not been standardised yet, in contrast to the rest of Asia and the United States, capable of delivering triple-play services at symmetrical bandwidth of 155 Mbit/s per subscriber [7, 26].

The Japanese broadband market is also entering into a total FTTH age. Although initially FTTH was used only for Internet access, at present, network providers employ mainly EPON systems to provide up to 100 Mbit/s per customer focusing on triple-play services as the main drive to full-scale FTTH [27]. The FTTH market in Japan continues to grow rapidly as the number of both small/medium enterprises and residential customers have exceeded 10 million with a target of serving 30 million customers by 2010 [22, 27] by means of creating attractive applications that are available only on FTTH. Out of the current customer number, the vast majority is residential, demonstrating that FTTH has been accepted not only to provide services to enterprises but also for ordinary consumers [27].

In the Hong Kong region, around 23 percent of households are connected with FTTH [9]. The first provider, Hong Kong Broadband Network Limited (HKBN), to launch FTTH with 100 Mbit/s and 1 Gbit/s services in 2005, has been operating GPON at 2.5 Gbit/s downstream since the beginning of 2008, delivering advanced triple-play services, and is planning to increase its FTTH coverage from 1.4 million to 2 million home connected within the next few years [28].

Finally, in the United States there are more than 10 million FTTH connections with the aim to exceed 18 million households by 2010 [29], out of which nearly 2 million residential and businesses customers are receiving services by Verizon as the main player in addition to other suppliers. Recently, GPON has been receiving more attention and has already been in deployment in undeveloped areas, offering single downstream and upstream speeds at 2.5 Gbit/s and 1.25 Gbit/s respectively for distances of 20 km.

1.4.2 WiMAX

According to the WiMAX forum, an industry-led non-profitable organization formed to certify and promote the compatibility and interoperability of broadband wireless products based upon the harmonized IEEE 802.16/ETSI HiperMAN standards, the second quarter of 2009 WiMAX deployment reached the milestone of 500 networks in more than 145 countries [30]. At the close of second quarter of 2009, over 3.96 million WiMAX subscribers existed that represents a 16% growth from first quarter of 2009 and a 72% growth over quarter two of 2008 [30, 31].

As illustrated in Figure 1-3, the fixed and mobile WiMAX are already available in North America, Europe, Asia, South America, the Middle East, and Africa [32]. In Europe, for instance, WiMAX Telecom AG is a leading cross-border wireless access operator. The company currently has 42 MHz of 3.5 GHz spectrum in Austria, Croatia, Germany, Slovakia, and Switzerland [30]. Also, Danske Telecom in Denmark, holding the license in 3.5GHz spectrum, lunched WiMAX services in 2008 covering about 40% of its population [30].

Figure 1-3: WiMAX deployment worldwide [32]

Furthermore, in 2009 UQ Communications of Japan launched Mobile WiMAX service [30, 33] following the lead of Clearwire of North America and Scartel of Russia, which both started their Mobile WiMAX service in 2008. Clearwire, with the average download speed limited to

3-6 Mbit/s, plans to continue expansion to cover 120 million users, almost half of the U.S. population, by 2010 [32]. Scartel has begun services in Moscow and St. Petersburg, and its 2009 plan included 11 major cities [32].

Finally, in terms of usage cost, WiMAX is the only wireless standard to enable users to use data services at an affordable price today. Currently, major wireless service providers provide 3G data service for laptops at about $60/5Gbytes with additional charges over 5 Gbytes [32]. US operator Clearwire, for instance, offers unlimited data service at $50 [32].

1.5 Motivation and Objectives

The aforementioned networking characteristics will create a more sophisticated communication substratum in which advanced rate control and adaptation mechanisms can be deployed, offering a more enhanced user experience in terms of cutting edge multimedia services. The combination of all these network traits renders the overall PON-WIMAX architecture more self-sustained, since the effective integration of a flexible resource allocation and multi-path wireless access, through novel and effective radio cell techniques, creates a more sophisticated platform that minimizes the necessity for monitoring and corrective interventions. The cost effectiveness of such schemes creates new opportunities for service and network providers since futuristic services can be provided over a more reconfigurable, easily deployable and profitable networking framework.

Furthermore, the design and deployment of wireless networks has mainly been service-driven and has been centred on the end-user satisfaction while on the other hand the main preoccupation pertaining to optical systems evolutions relates to the issue of future-proofness against legacy and emerging services and applications. In view to that, with the ultimate goal of providing access to information when needed, wherever needed, and in whatever format, the

10

vision of technological convergence of wireless and optical networks is not only becoming a necessity but also plays a key role in future communications networks.

Consequently, towards the technical evolution of optical-wireless access networks and the seamless coexistence of both technologies, this research programme focuses on important solutions to problems relating to this direction. The boundary between both worlds will be softer and as the commercial volume increases the cost of components will be driven down thus increasing the widespread and success for feasible and economically affordable deployment and operation of these future integrated architectural platforms.

To that extent, this work is tackling the issue that stem from the coexistence of diverse technologies, PON and WiMAX, within the same infrastructure. It will efficiently exploit the benefits offered by the advantageous combination of these technologies to provide enhanced PON's flexibility and robustness as well as improved WiMAX performance.

To summarise, the main objectives of this research programme are:

➢ Definition of a novel access network architecture achieving convergence among heterogeneous technologies (optical and wireless)

➢ Defining the architectural details and interfaces for embedding the WiMAX into overall network structure

➢ Investigating the analogue transmission of wireless signals based on radio over fibre (RoF) techniques over PONs and wireless channels

➢ Definition of multi-wavelength support over splitter-based PON for enhanced network scalability and dynamicity

➢ Specifications and the investigation of advanced network solutions such as WiMAX overlapping radio cells enabled by the integrated architectural platform

> ➢ Transmission of standard WiMAX channels over multiple wavelengths and overlapping radio cells

1.6 Thesis Outline

Following the review of FTTH and WiMAX worldwide deployment initiatives, chapter 2 concentrates on the operational characteristics of individual PON and WiMAX standards while introducing potential next-generation access network solutions. Subsequently, chapter 3 represents the preliminary criteria to be met with reference to the optical/wireless integration followed by the defining VPI/MATLAB co-simulation requirements for the modelling of WiMAX transmission over PONs.

Chapter 4 follows to describe the principal characteristics of an original network based on RoF and frequency division multiplexing (FDM) to address individual remote base stations by means of transparent wireless signal routing. The designed architecture is progressively enhanced in chapters 5 and 6, following the application of multi-wavelength overlay over the integrated splitter-PON architecture. A complete network was modelled and evaluated drawing performance figures of individual network elements as well as the propagation of wireless and optical signals. For the purpose of validating the simulation work, chapter 7 demonstrates experimentally the transmission of the PON and WiMAX signals for varying network parameters. Finally, chapter 8 serves the purpose of summarising the work conducted throughout this research programme and subsequently discussing the potential evolution and technical challenges this would involve.

References

[1] E. Frank, C. David, H. Onn, K. Glen, L. R. Ding, O. Moshe, and P. Thomas, "An introduction to PON technologies," *IEEE Communication Magazine*, vol. 45, pp. S17-S25, (2007).

[2] S. Ahmadi, "An overview of next-generation mobile WiMAX technology," *IEEE Communications Magazine*, vol. 47, pp. 84-98, (2009).

[3] D. Astely, E. Dahlman, A. Furuskar, Y. Jading, M. Lindstrom, and S. Parkvall, "LTE: the evolution of mobile broadband - LTE part II: 3GPP release 8," *IEEE Communications Magazine*, vol. 47, pp. 44-51, (2009).

[4] *OKI* (Online). Available: http://www.oki.com/en/ngn/solution/access_network.html

[5] M. J. O'Mahony, C. Politi, D. Klonidis, R. Nejabati, and D. Simeonidou, "Future Optical Networks," *J. Lightw. Technol.*, vol. 24, pp. 4684-4696, (2006).

[6] *Cisco Systems: Global IP Traffic Forecast and Methodology* (Online). Available: www.hbtf.org/files/cisco_IPforecast.pdf

[7] C.-H. Lee, S.-M. Lee, K.-M. Choi, J.-H. Moon, S.-G. Mun, K.-T. Jeong, J. H. Kim, and B. Kim, "WDM-PON experiences in Korea (Invited)," *J. Opt. Netw.*, vol. 6, pp. 451-464, (2007).

[8] *Ethernet in the First Mile Task Force*, IEEE 802.3ah, 2004

[9] *FTTH   Council   Europe   General   Presentation*   (Online).   Available: http://www.ftthcouncil.eu/documents/presentation/2007-11-29_FTTH_CE_General_presentation_V.2.1.pdf

[10] *Infonetics Research* (Online). Available: http://www.infonetics.com/

[11] "IEEE Standard for Local and Metropolitan Area Networks Part 16: Air Interface for Fixed Broadband Wireless Access Systems," *IEEE Std 802.16-2004 (Revision of IEEE Std 802.16-2001)*, pp. 0_1-857, (2004).

13

[12] "IEEE Standard for Local and metropolitan area networks Part 16: Air Interface for Fixed and Mobile Broadband Wireless Access Systems Amendment 2: Physical and Medium Access Control Layers for Combined Fixed and Mobile Operation in Licensed Bands and Corrigendum 1," *IEEE Std 802.16e-2005 and IEEE Std 802.16-2004/Cor 1-2005 (Amendment and Corrigendum to IEEE Std 802.16-2004)*, pp. 0_1-822, (2006).

[13] *Evolved Universal Terrestrial Radio Access (E-UTRA): LTE Physical Layer - General description*, 3GPP TS 36.201, 2008

[14] *WiMAX Capacity - White Paper* (Online). Available: http://www.srtelecom.com/uploads/File/whitepapers/WiMAX-Capacity.pdf

[15] Y. Yang, H. Honglin, X. Jing, and M. Guoqiang, "Relay technologies for WiMax and LTE-advanced mobile systems," *IEEE Communications Magazine*, pp. 100-105, (2009).

[16] *WiMAX: The Quientessential Answer to Broadband in India - White Paper* (Online). Available: http://img.en25.com/Web/WiMaxBroadbandSolutions/Protivity-wimax_in_india.pdf

[17] *IEEE Standard for Information technology--Telecommunications and information exchange between systems--Local and metropolitan area networks--Specific requirements Part 11: Wireless LAN Medium Access Control (MAC) and Physical Layer (PHY) Specifications Amendment 5: Enhancements for Higher Throughput*, IEEE Std 802.11n-2009 (Amendment to IEEE Std 802.11-2007 as amended by IEEE Std 802.11k-2008, IEEE Std 802.11r-2008, IEEE Std 802.11y-2008, and IEEE Std 802.11w-2009), 2009

[18] *High Rate 60 GHz PHY, MAC and HDMI PAL* (Online). Available: http://www.ecma-international.org/publications/files/ECMA-ST/Ecma-387.pdf

[19] *IEEE802.15 WPAN Task Group 3c* (Online). Available: http://www.ieee802.org/15/pub/TG3c.html

[20] *LAN/MAN Wireless LANs*, IEEE 802.11 The Working Group for WLAN Standards, 2005

[21] "IEEE standard for information technology - telecommunications and information exchange between systems - local and metropolitan area networks - specific requirements part 15.3: wireless medium access control (MAC) and physical layer (PHY) specifications for high rate wireless personal area networks (WPANs)," *IEEE Std 802.15.3-2003*, pp. 0_1-315, (2003).

[22] P. Chanclou, S. Gosselin, J. F. Palacios, V. L. Álvarez, and E. Zouganeli, "Overview of the Optical Broadband Access Evolution: A Joint Article by Operators in the IST Network of Excellence e-Photon/ONe," *IEEE Communications Magazine*, vol. 44, pp. 29-35, (2006).

[23] *FTTH situation in Europe* (Online). Available: www.idate.fr/pages/download.php?id=371&rub=news_telech&nom=PR_IDATE_FTTH_CONF_2007.pdf

[24] K. Casier, B. Lannoo, J. Van Ooteghem, B. Wouters, S. Verbrugge, D. Colle, M. Pickavet, and P. Demeester, "Game-theoretic evaluation of a municipality FTTH rollout," presented at Conference on Optical Fiber Communication OFC/NFOEC, March, 2009.

[25] *Broadband IT Korea Information* (Online). Available: http://www.mic.go.kr/index.jsp

[26] K. H. Deok, K. Seung-Goo, and L. Chang-Hee, "A low-cost WDM source with an ASE injected Fabry-Perot semiconductor laser," *Photon. Technol. Lett.*, vol. 12, pp. 1067-1069, (2000).

[27] H. Shinohara, "FTTH experiences in Japan (Invited)," *J. Opt. Netw.*, vol. 6, pp. 616-623, (2007).

[28] *Alcatel-Lucent and Hong Kong Broadband Network introduce first carrier-class GPON in Hong Kong* (Online). Available: www.alcatel-lucent.com

[29] F. J. Effenberger, K. McCammon, and V. O'Byrne, "Passive optical network deployment in North America (Invited)," *J. Opt. Netw.*, vol. 6, pp. 808-818, (2007).

[30] *WiMAX forum* (Online). Available: http://www.wimaxforum.org/home/

[31] *The WiMAX and LTE Operator Tracking Service – BWA Research UK* (Online). Available: http://www.4gcounts.com

[32] W. Kim, "Mobile WiMax, the leader of the mobile internet era," *IEEE Communications Magazine*, pp. 11-12, (2009).

[33] *UQ   Communication   Japan*   (Online).   Available: http://www.uqwimax.jp/english/annai/rinen.html

Chapter 2

Next Generation Access Networks

Contents

This chapter concentrates on the functional characteristics of PON and WiMAX topologies and the standards deployed in current access networks. Following the evolution of access networks and the timely developments in online services, e.g. online gaming, video streaming, internet protocol TV (IPTV) etc, potential solutions for enhancing the existing PON and WiMAX standards are reviewed. Finally, the techno-economical aspects of these developments are discussed, leading to the justification of the trend towards converged optical/wireless schemes.

2.1 PON Architecture and Standards

PONs are being deployed to provide broadband access networks due to their simplicity of implementation and low OPEX [1, 2]. Among the possible PON topologies appropriate for the access network [3], the tree architecture, shown in Figure 2-1, is widely deployed since it allows maximum network coverage at minimum split. This would result in reduced attenuation along the fibre link, avoiding the use of power amplifiers. Data transmission in PONs is established

between an OLT and the optical network units (ONUs) [4], with the former being located in the central office, connecting the access network with the metro backbone and the later at either a street cabinet in FTTC architectures, or at the customer premises in FTTH and FTTB architectures. The ONUs are connected to the OLT by means of a feeder fibre through passive components in order to be maintained and managed economically [4].
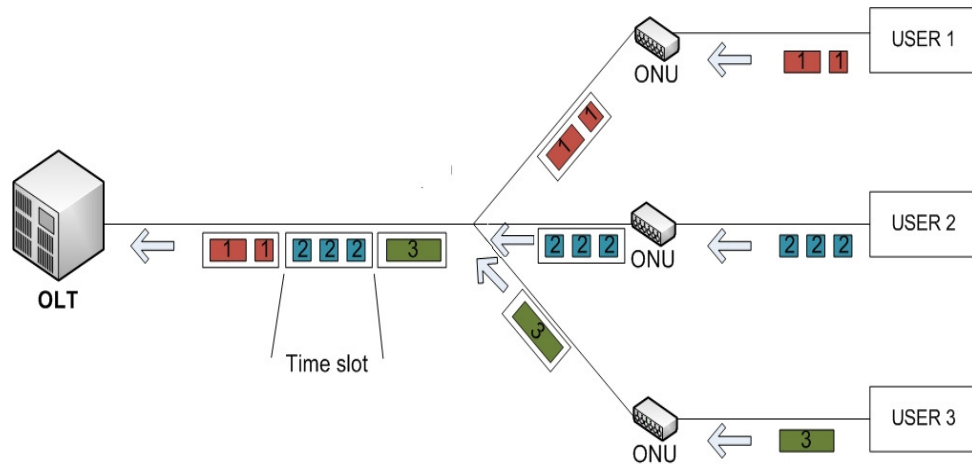
Figure 2-1: Conceptual architecture of a TDM-PON

In downstream, signals communicated from the OLT reach the passive optical splitter and consequently broadcasted to all ONUs. Although, each ONU receives the totality of downstream data, secure channels are established to ensure ONUs recover only their intended data streams [5]. In upstream, as shown in Figure 2-1, the splitter combines all ONU packets in a TDM fashion to avoid collisions in the feeder fibre. Consequently, each ONU has to restrict its transmission only to predefined time-slots administrated by a mandatory access control (MAC) protocol, which can allocate time-slots to ONUs both statically and dynamically.

Currently deployed TDM-PONs allow for the implementation of typical fibre distances of 20 km between the OLT and ONUs, delivering Gbit/s equivalent bandwidth at manageable OPEX and CAPEX [6] while saving in the amount of optical fibre installed [1]. In addition, since downstream transmission is broadcasted, video broadcasting at either analogue or IP can be

demonstrated using a separate wavelength. Finally, being optically transparent end-to-end, due to the agnostic nature of the passive splitter, PONs allow for a smooth upgrade to higher data rates and additional wavelengths [3, 7].

TDM-PON standards include the existing Ethernet-PON (EPON) [8] and GPON [9-11], being the outcome of two different groups of equipment vendors and network operators. The EPON was developed and formalised in the IEEE 802.3ah standard [8] to bring Ethernet to residential and business customers [12]. EPONs have been adopted rapidly, primarily due to their ubiquitous and cost-effective technology, allowing for interoperability with a variety of legacy equipment [3, 12]. They are capable of providing triple-play services [12] at symmetrical 1.25 Gbit/s data rates using the 1490 nm and 1310 nm wavelengths for downstream and upstream transmission respectively. The 1550 nm wavelength is reserved for future extensions or additional services such as analogue video broadcasting for a maximum of 32 ONUs at distances of up to 20 km [3, 13]. In upstream, a typical medium access control (MAC) protocol is used, avoiding data collisions in the distribution network.

To extend the capacity limitation of EPONs by means of data rates and splitting ratios while providing increased bandwidth efficiency, ITU-T has developed the GPON standard by producing the G.984 series [9-11]. GPONs offer technical advantages over their counterparts by accommodating triple-play services at variable data rates reaching up to 2.5 Gbit/s compared to the single 1.25 Gbit/s rate in EPONs. They utilise a similar wavelength assignment, allowing network operators to configure transmission rates according to user requirements. Unlike EPONs, GPONs can support a maximum of 128 ONUs for distances of up to 60 km [14] as well as offering almost double bandwidth efficiency due to less data transmission overheads. To address security issues in downstream, GPON provides an advanced encryption standard. The

encryption key associated with each ONU is sent in the secured upstream data since individual ONUs cannot have access to upstream transmissions of others.

Significantly, with the emerging applications and consequently ever increasing demand for bandwidth, PONs capable of accommodating even higher bandwidth were timely promoted. Towards this direction a task group was formed by IEEE [15, 16] and FSAN [17] and recently standardised what is known as the 10G-EPON, particularly aiming at achieving symmetrical 10 Gbit/s for distances of at least 20 km and 1:32 split [18, 19]. Chromatic dispersion may become significant over the standard single mode fibre (SSMF) at these distances and data rates therefore state-of-the-art transceivers need to be developed [20]. These systems also provide backward compatibility with optical distribution networks currently deployed.

2.2 WiMAX Architecture and Standards

WiMAX is a broadband wireless access network developed to compete with traditional wireline access technologies by providing mobile, high-speed data and telecommunications services comparable to emerging 4G technologies [21]. It can support fixed, nomadic and mobile access based primarily on point-to-multipoint transmission [22]. As illustrated in Figure 2-3 data transmission in WiMAX is carried out between an internet service provider (ISP) and base stations [23], with the former located in the central office, connecting the access network with the internet backbone and the later at subscriber close proximity delivering data to end users.

WiMAX is capable to support relatively high data rates in the range of 75 Mbit/s with 64-QAM modulation in 20 MHz bandwidth. The WiMAX standards also facilitate scalable bandwidth and data rates, adaptive modulation and coding based on received signal-to-noise ratio (SNR) and state-of-the-art forward error correction techniques [24, 25]. In the same time they provide

support for time division multiple access (TDMA) and frequency division multiple access (FDMA) transmission as well as advanced antenna techniques.

The end-to-end services are delivered over an IP architecture allowing WiMAX to ride the declining cost curves of IP processing and facilitate easy convergence with other networks [26].

The base stations, usually equipped with multiple antennas employed in various downlink multi-antenna schemes such as beamforming, spatial multiplexing or spatial diversity coding [23, 26], are connected to the ISP by means of either T1/E1 interfaces, Ethernet or via line-of-sight millimetre-wave connections [27, 28].
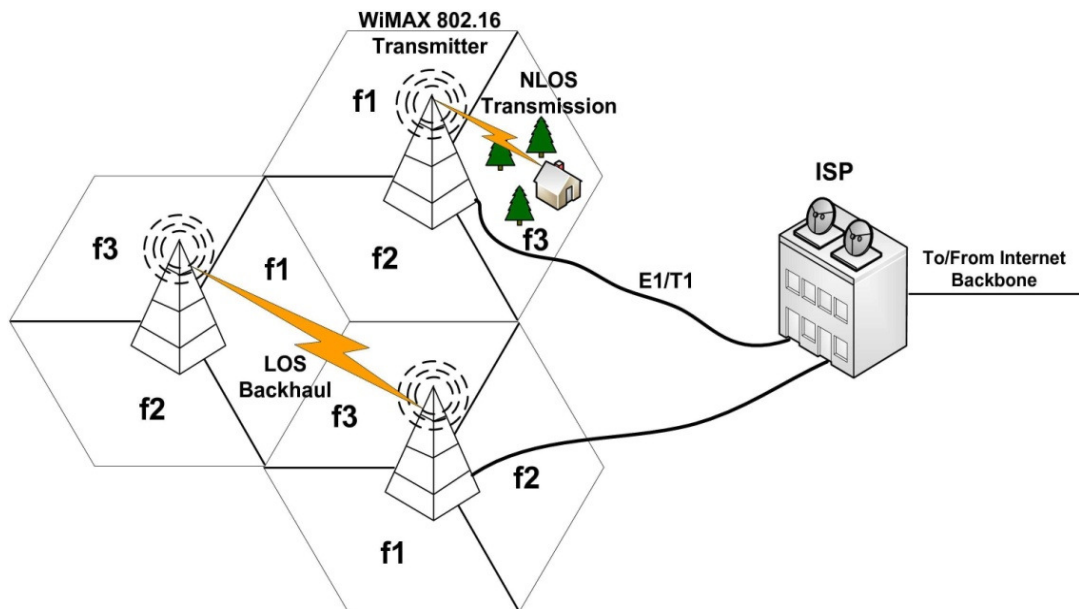
Figure 2-2: WiMAX deployment scenario

As demonstrated in Figure 2-2, each base station is serving a single cell, and is able to transmit at the 2.3GHz, 2.5GHz, 3.5GHz and/or 5.7GHz bands depending on regulatory issues [22, 29]. For Europe, the 3.5GHz licensed band is typically allocated to service providers [22, 30, 31].

To increase the spectral efficiency across a cell, a frequency reuse technique is employed so that each cell is being sectorised and WiMAX base stations accessing the individual sectors with

directional antennas [23]. An illustration of that is shown in Figure 2-2 where a frequency reuse with a factor of 1:3:3 is assumed [23]. However, this approach could impose strong inter-cell interference and as a result interference management should be applied with multi-site processing [32]. Coordination, via direct communication, between the cooperating base stations needs to be established, requiring therefore additional capacity on the backhaul link.

In addition, the WiMAX signals are broadcasted from a base station to all subscribers in a cell or a sector within a radius of typically 3-5 miles [30]. Therefore, due to the inherited point-to-multi-point (P2MP) distribution, TDMA is typically applied in upstream [33] to serve as the required contention control mechanism, similar to TDM-PONs. To reduce the traffic congestion, coverage and throughput due to TDMA, more densely spaced base stations with improved spectral efficiency and QoS could be deployed resulting, however, in increased deployment cost.

Current WiMAX standards include the existing IEEE802.16d [24] and IEEE802.16e [25], providing fixed and mobile broadband wireless operation respectively. The main characteristics of these standards are summarised in Table 2-1. Compared to initial WiMAX standard definitions, IEEE802.16-2001 [34], at the physical layer these standards are operating at 2-11 GHz transmission bands, licensed and license-exempt, driven by the need for non-line-of-sight (NLOS) operation [24, 25]. For efficient multipath propagation mitigation the modulation technique utilised is primarily based on orthogonal frequency division multiplexing (OFDM) where data is carried over closely spaced orthogonal subcarriers, generated by Fast Fourier Transform (FFT), with long symbol duration [23]. Each individual subcarrier is modulated with QPSK, 16-QAM or 64-QAM digital modulation formats [23]. In addition a wide range of guard times, attached to an OFDM symbol, are defined in the WiMAX standards to allow for the necessary trade-off between spectral efficiency and delay spread robustness [24, 25]. The

OFDM is also used by mobile WiMAX as a multiple-access technique (OFDMA), whereby different users can be allocated to different subsets of the OFDM tones [25]. All transmission profiles currently defined by the WiMAX forum [35] specify a minimum 256-subcarrier OFDM out of which 192 are used for user data and the rest as overheads for wireless channel estimation and impairment mitigation due to the channel.

Table 2-1: Fundamental characteristics of key WiMAX standards [23]

	802.16	**802.16d-2004**	**802.16e-2005**
Frequency Band	10GHz-60GHz	2GHz-11GHz	2GHz-6GHz mobile
Application	Fixed LOS	Fixed NLOS	Fixed and mobile NLOS
Architecture	Point-to-multipoint, mesh	Point-to-multipoint, mesh	Point-to-multipoint, mesh
Transmission Scheme	Single carrier	Single carrier, 256 OFDM or 2048 OFDM	Single carrier, 256 OFDM, or scalable OFDM with 128, 512, 1024 or 2048 subcarriers
Gross Data Rate	32Mbps-134Mbps	1Mbps-75Mbps	1Mbps-75Mbps
Multiplexing	Burst TDM/TDMA	Burst TDM/TDMA, OFDMA	Burst TDM/TDMA, OFDMA
Duplexing	TDD and FDD	TDD and FDD	TDD and FDD

2.3 Next Generation Developments

2.3.1 NG-PONs

To provide higher transmission bandwidth alone, in view of the standards and their developments presented before, is not sufficient and should be accompanied by greater coverage and penetration. To that direction next generation PON (NG-PON) studies in network elements and architectures have evolved [2, 4, 18]. One approach would be to further increase the speed and reach/split of the existing PON standards, offering economical bandwidth and service upgrade by merging the access and metropolitan networks to grant cost savings for network operators [7, 20, 36, 37] and subsequently users.

Another approach would be to employ a greater number of wavelengths to rapidly increase the network throughput allowing for multiple media-rich services to be accommodated on a shared access network infrastructure simultaneously [2]. Also, to ensure flexibility and smooth migration, compatibility between TDM and next generation densely penetrated PONs is required [4]. In that direction the ITU-T has recently defined extended bands reserved for extra services to be overlaid via WDM over the current power-splitter infrastructures [38]. Another scenario involving the application of WDM is to assign a single wavelength to each subscriber to provide virtual point to point PON links in the form of a WDM-PON employing an arrayed waveguide grating (AWG) in the distribution point. The obvious merit of the latter, due to the dedicated bandwidth, would be greater security and protocol transparency [4, 39].

Figure 2-3 illustrates the resulting roadmap for NG-PON1 and NG-PON2, where NG-PON1 is viewed as a mid-term upgrade and NG-PON2 as a longer-term solution. The timeline shown reflects the nominal expected period for specification and publication of standards for NG-PON1 and NG-PON2 [2].

24
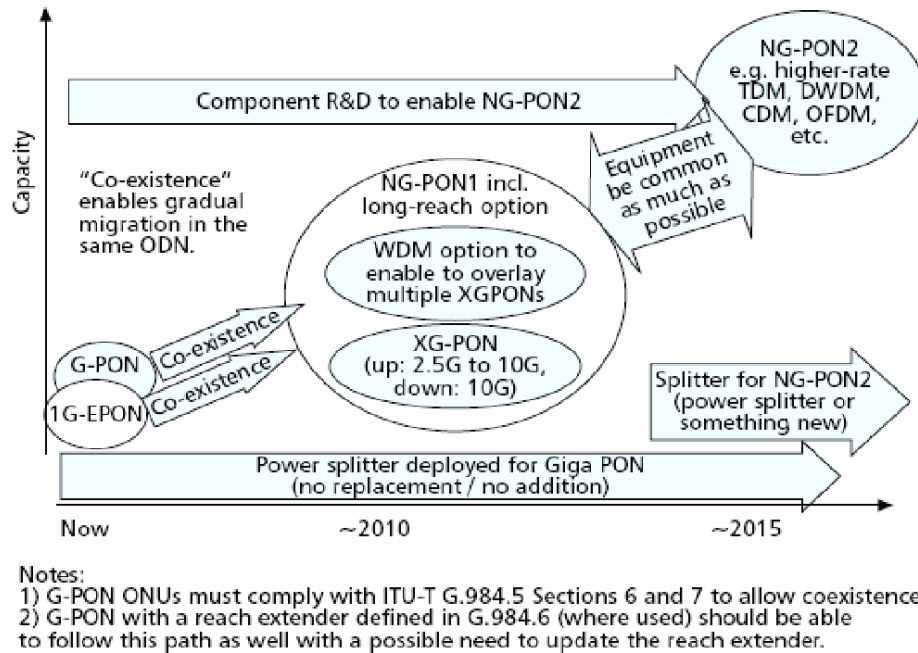
Figure 2-3: NG-PON roadmap [2]

2.3.2 Extended Wavelength Band Overlay over NG splitter-PON

As already mentioned the application of WDM over the existing optical backbone in access networks is believed to deliver ultra high-speed services by enabling service providers to supply dedicated wavelengths straight to homes and businesses [39-43]. In addition, research initiatives in that front have progressively focused on establishing wavelength independent ONUs, also known as a colourless ONU [3, 44, 45].

Currently the chosen infrastructures to demonstrate the application of WDM, distinguish between power-splitter schemes and AWG-based schemes with varying implications between them in view of the MAC layer, network reach, flexibility and complexity. WDM-PONs, typically the terminology is reserved for the AWG-based architectures, on one hand are currently considerably costly to implement, precisely operate and maintain as they require work on the outside plant and disruption on existing services. A more practical approach is to enable multi-wavelength transmission over power splitting PON infrastructures, whereby wavelength selection is done at each ONU by means of an additional optical band-pass filter [3, 46, 47].

25

As a result, several multi-wavelength recommendations have been proposed, concentrating primarily on the architecture level with some initiatives developed recently in the protocol side with the generation of dynamic wavelength allocation algorithms for EPON [47] and GPON [38] relative designs. For reasons of convergence with legacy GPONs and EPONs, new operating wavelengths would have to coexist with those of the legacy networks [2].

An example of an architecture demonstrating multi-wavelength transmission over a splitter-based EPON has been proposed in [48]. Shown also in Figure 2-4, tuneable optical filters are utilised at ONUs to select the desired wavelength, following their broadcasting from the passive splitter. The filters for downstream and feeding light at an ONU are independently tuneable allowing the combination of any downstream wavelength with any upstream wavelength for an ONU. The colourless transmission is achieved by means of the reflective semiconductor amplifiers (RSOAs). However, this approach would require typically dual feeder fibres in order to limit the Rayleigh backscattering effect at the RSOA. Subsequently, a single-port power splitter in the remote node will need to be replaced with dual-port for data transmission and seeding light. In addition, multiple AWGs in the OLT would be needed for downstream and upstream transmission and to provide the seeding light for the RSOA.
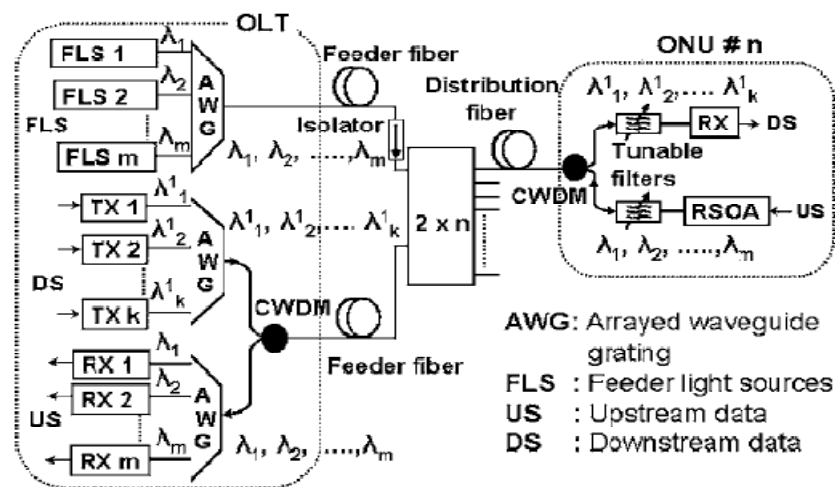
Figure 2-4: Multi-wavelength EPON [48]

26

Alternatively, in support of the GPON standard, enhancements to address the network of the future requirements have been also recently defined by ITU-T [38] by employing extended wavelength band operation. To that extent, multi-wavelength transmission over the currently deployed splitter-based PONs should be demonstrated at the slightest modification in network hardware, supporting e.g. 10G-PON operation on separate wavelengths simultaneously with GPON. To ensure that next generation and traditional ONUs can operate concurrently in the same PON the standard defines the application of wavelength selective filters to be supported by traditional ONUs. As displayed in Figure 2-5 [38], inside the OLT next generation access (NGA) and RF (e.g. video or wireless) related services are multiplexed on different wavelengths and broadcasted to each ONU via passive splitter. Inside the ONU a specific wavelength is selected by wavelength division multiplexer (WDM) filter prior to the signal reception at the Rx. The wideband blocking filter (WBF) could then be used to separate different services supported by specific ONU on the same wavelength (e.g. GPON and video).
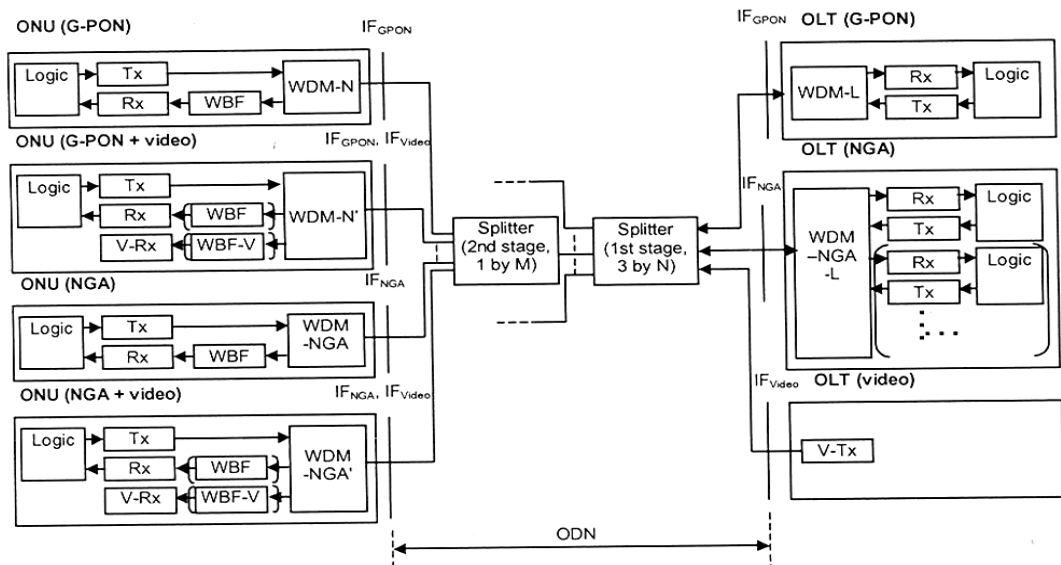
* V-Tx-Video Transmitter, N-splitter size, IF-interface, NGA-Next Generation Access, WBF(V)-Wideband Filter (Video),

Figure 2-5: Enhancement band for gigabit capable optical access networks [38]

2.3.3 Broadband Wireless Standards Enhancements

From the wireless prospective, with the advancement of state-of-the-art signal processing, coding and multiple-input-multiple-output (MIMO) antenna techniques, amendments to the existing standards have been proposed to further extend the coverage and the capacity with enhanced QoS provisioning. Towards this direction, the WiMAX 802.16 working group has started development of the IEEE802.16m standard, promising to deliver twice the performance gain over baseline 802.16d/e standards in various measures such as sector throughput, average user throughput and peak data rates through the use of MIMO technologies [49, 50].

To further improve signal to interference ratios and consequently increase coverage and capacity at the cell edges, the IEEE802.16j task group has also developed amendments to extend the 802.16e to support multihop relay operation [51]. In this scenario a remote base station, typically placed at the cell edge, is used to aid communication from base station to mobile station and vice versa [52].

Additionally, since access to spectrum below 1000 MHz for broadband wireless services would enable more cost-effective deployments, the ultra high frequency (UHF) band from 470 MHz to 862 MHz, often referred to as the 700 MHz band, has been considered as future band of operation for WiMAX service providers [53, 54]. Due to the low path loss, better building penetration and low Doppler shift at these frequency bands further range and capacity enhancements are expected.

2.3.4 Integration of Optical and Wireless Access Networks

Having considered the requirements outlined so far in this thesis and the individual network developments it can be safely concluded that NG access networks would benefit from the integration of PON connections, with wireless terminations. Figure 2-6 [2, 19] portrays a scenario where a PON provides a wireless backhaul of mobile standards, such as WiMAX and

LTE, since it can incorporate many access points efficiently as it can residential FTTH users [19].
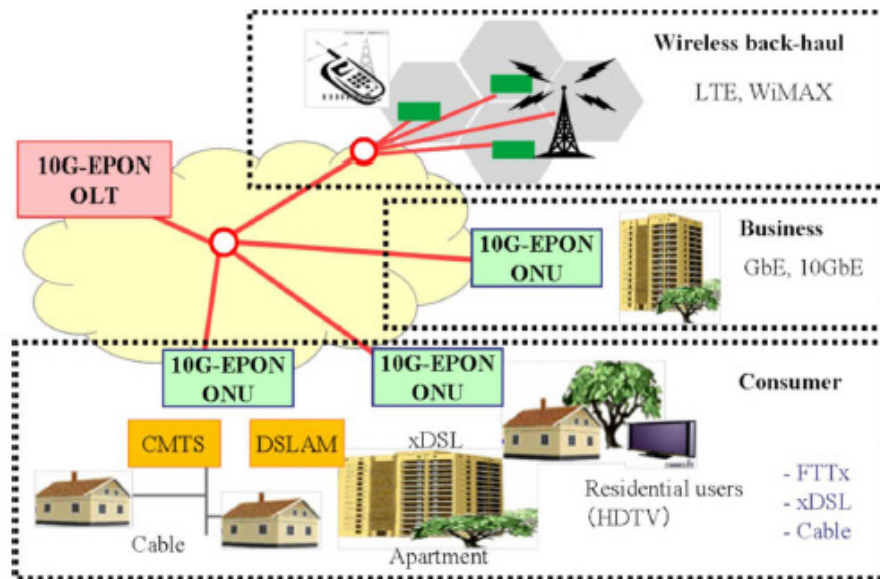
Figure 2-6: NG-PON use cases [2, 19]

A range of possible scenarios, in particular between EPON and WiMAX, are reviewed in [55, 56]. What is common in these architectures is the employment of the complete WiMAX base station functionalities at common ONU/BSs. However, this would require significant modifications at the MAC layers of both networks to achieve fine bandwidth granularity. In addition, the benefits of the optical network as the backbone are not efficiently utilised since all WiMAX modulation is still performed at the ONU/BSs.

Instead, to achieve smaller radio cells, considered as a prerequisite for higher spectral efficiency than the currently standardised and deployed wireless networks, the application of RoF could deliver radio signals through the high-capacity fibre to densely spaced remote BSs [57-60]. Among these initiatives, [61] presents a scheme developed throughout this research programme. Its merits will be discussed and evaluated in detail in following chapters.

In view of RoF application complex equipment and processing is kept at the centralised head-end allowing for easy installation and maintenance of the network. Consequently, low power consumption is achieved due to the passive nature of these base stations (BSs). In addition to the above, due to the signal transparency, a RoF approach could be used to distribute multi-operator and multi-service traffic resulting in high economic savings [62]. Finally, as it will be described in proceeding chapters, RoF networks allow for dynamic resource allocation due to the centralised processing and control. For instance, in view of FDM transmission additional sub-carriers could be dropped to a base station increasing its capacity.

The application of RoF techniques alone would not be sufficient to exploit all benefits of optical backhauling to wireless standards. Although optical fibres, compared to copper and free space media, can provide superior transmission of radio frequency (RF) signals for long distances, their utilisation is however hampered by the limitation in bandwidth of electrical systems. Efficient multiplexing techniques, such as FDM, are therefore required to increase the optical bandwidth utilisation.

The presented challenges have very recently drawn the attention of research consortia worldwide, on establishing the critical aspects associated with the integration and implementation of optical and radio standards, the pros and cons of which will be analysed in the following chapter against the network developed in this work.

2.4 Summary

This chapter offered a revision of PON and WiMAX standards and their benefits in developing current and future access networks. Progressively, to accelerate in terms of bandwidth utilisation, reach and penetration and consequently welcome upcoming bandwidth-demanding fixed and mobile online services at low cost, a number of research initiatives in access networks were presented.

The reported optical solutions focused around three major research directions. Increasing the speed and reach/split of the existing PON standards to distances of at least 100km, employing higher number of wavelengths in PON infrastructures to allow significant increase in network throughput and security and finally to ensure compatibility with next-generation access networks.

From the wireless prospective, enhancements to the existing standards have also been defined to support higher data rates and number of users as well as to exploit transmission diversity through the application of MIMO antennas.

Significantly, the WiMAX potential to inter-operate with xPONs has been reported in the direction of offering sufficient backhaul capacity for high-end wireless services, ensuring network flexibility with efficient network administration and management. In particular, the application of RoF techniques is promoted to deliver broadband WiMAX to remote radio BSs. An architecture based on this principle defines the aim of this research programme and will be presented extensively in the chapters to follow.

References

[1] C.-H. Lee, S.-M. Lee, K.-M. Choi, J.-H. Moon, S.-G. Mun, K.-T. Jeong, J. H. Kim, and B. Kim, "WDM-PON experiences in Korea (Invited)," *J. Opt. Netw.*, vol. 6, pp. 451-464, (2007).

[2] J. i. Kani, F. Bourgart, A. Cui, A. Rafel, M. Campbell, R. Davey, and S. Rodrigues, "Next-generation PON-part I: technology roadmap and general requirements," *IEEE Communications Magazine*, vol. 47, pp. 43-49, (2009).

[3] E. Frank, C. David, H. Onn, K. Glen, L. R. Ding, O. Moshe, and P. Thomas, "An introduction to PON technologies," *IEEE Communication Magazine*, vol. 45, pp. S17-S25, (2007).

[4] F. Effenberger, H. Mukai, P. Soojin, and T. Pfeiffer, "Next-generation PON-part II: candidate systems for next-generation PON," *IEEE Communications Magazine*, vol. 47, pp. 50-57, (2009).

[5] A. Cauvin, A. Tofanelli, and J. Lorentzen, "Common technical specifications of the G-PON system among major worldwide access carriers," *IEEE Communication Magazine*, vol. 44, pp. 34-40, (2006).

[6] J. Halpern and G. Garceau, "Fiber: revolutionizing the Bell's telecom networks," *Bernstein/Telcordia Technologies Study*, (2004).

[7] L. G. Kazovsky, W. T. Shaw, D. Gutierrex, N. Cheng, and S. W. Wong, "Next-Generation Optical Access Networks," *J. Lightw. Technol.*, vol. 25, pp. 3428-3442, (2007).

[8] *Ethernet in the First Mile Task Force*, IEEE 802.3ah, 2004

[9] *Gigabit-capable Passive Optical Networks (GPON): General characteristics*, ITU-T G.984.1, 2003

[10] *Gigabit-capable passive optical networks (GPON): Physical media dependent (PMD) layer specification*, ITU-T G.984.2, 2003

[11] *Gigabit-capable passive optical networks (GPON): transmission convergence layer specification*, ITU-T G.984.3, 2003

[12] G. Kramer and G. Pesavento, "Ethernet Passive Optical Network (EPON): Building a Next-Generation Optical Access Network," *IEEE Communications Magazine*, pp. 66-73, (2002).

[13] D. Gutierrez, K. S. Kim, S. Rotolo, F.-T. An, and L. G. Kazovsky, "FTTH Standards, Deployments and Research Issues (Invited)," presented at Joint International Conference on Information Sciences (JCIS), 2005.

[14] Q. Xing-Zhi, P. Ossieur, J. Bauwelinck, Y. Yi, D. Verhulst, J. Vandewege, B. De Vos, and P. Solina, "Development of GPON upstream physical-media-dependent prototypes," *J. Lightw. Technol.*, vol. 22, pp. 2498-2508, (2004).

[15] M. Hajduczenia, P. R. M. Inacio, H. J. A. Silva, M. M. Freire, and P. P. Monteiro, "10G EPON Standardization in the Scope of IEEE 802.3av Project," presented at National Fiber Optic Engineers Conference, 2008.

[16] *IEEE Standard for Information technology - Telecommunications and information exchange between systems - Local and metropolitan area networks - Specific requirements Part 3: Carrier Sense Multiple Access with Collision Detection (CSMA/CD) Access Method and Physical Layer Specifications Amendment 1: Physical Layer Specifications and Management Parameters for 10 Gb/s Passive Optical Networks*, IEEE Std 802.3-2009 (Amendment to IEEE Std 802.3-2008), 2009

[17] *FSAN NGA* (Online). Available: http://www.fsanweb.org/nga.asp

[18] F. Effenberger, H. Mukai, J. i. Kani, and M. Rasztovits-Wiech, "Next-generation PON-part III: system specifications for XP-PON," *IEEE Communications Magazine*, vol. 47, pp. 58-64, (2009).

[19] K. Tanaka, A. Agata, and Y. Horiuchi, "IEEE 802.3av 10G-EPON Standardization and Its Research and Development Status," *J. Lightw. Technol.*, vol. 28, pp. 651-661, (2010).

[20] R. Davey, J. Kani, F. Bourgart, and K. McCammon, "Options for future optical access networks," *IEEE Communications Magazine*, vol. 44, pp. 50-56, (2006).

[21] *Driving 4G: WiMAX & LTE - White Paper* (Online). Available: www.motorola.com

[22] *Fixed, nomadic, portable and mobile applications for 802.16-2004 and 802.16e WiMAX networks* (Online). Available: www.wimaxforum.org

[23] J. G. Andrews, A. Ghosh, and R. Muhamed, *Fundamentals of WiMAX: Understanding Broadband Wireless Networking*: Prentice Hall, 2007.

[24] "IEEE Standard for Local and Metropolitan Area Networks Part 16: Air Interface for Fixed Broadband Wireless Access Systems," *IEEE Std 802.16-2004 (Revision of IEEE Std 802.16-2001)*, pp. 0_1-857, (2004).

[25] "IEEE Standard for Local and metropolitan area networks Part 16: Air Interface for Fixed and Mobile Broadband Wireless Access Systems Amendment 2: Physical and Medium Access Control Layers for Combined Fixed and Mobile Operation in Licensed Bands and Corrigendum 1," *IEEE Std 802.16e-2005 and IEEE Std 802.16-2004/Cor 1-2005 (Amendment and Corrigendum to IEEE Std 802.16-2004)*, pp. 0_1-822, (2006).

[26] S. Ahson and M. Ilyas, *WiMAX: Standards and Security*: CRC Press, 2008.

[27] *WiMAX backhaul: No longer takes a back seat* (Online). Available: www.ceragon.com

[28] *Carrier Ethernet backhaul strategies for WiMAX* (Online). Available: www.telecomasia.net

[29] *Delivering Cutting Edge WiMAX Services to Small and Medium Size Cities in the US - DigitalBridge Communicaitons Case Studies* (Online). Available: www.wimaxforum.org

[30] *Maximizing Return with WiMAX in a Highly Competitive Market - Danske Telecom Case Studies* (Online). Available: www.wimaxforum.org

[31] *Wireless Broadband in Central and Eastern Europe - WiMAX Telecom Case Studies* (Online). Available: www.wimaxforum.org

[32] M. C. Necker, "Local Interference Coordination in Cellular OFDMA Networks," presented at IEEE 66th Vehicular Technology Conference, VTC-2007 Fall, 2007.

[33] S.-I. Chakchai, R. Jain, and A. K. Tamimi, "Scheduling in IEEE 802.16e mobile WiMAX networks: key issues and a survey," *IEEE Journal on`Selected Areas in Communications,*, vol. 27, pp. 156-171, (2009).

[34] "IEEE Std. 802.16-2001 IEEE Standard for Local and Metropolitan area networks Part 16: Air Interface for Fixed Broadband Wireless Access Systems," *IEEE Std 802.16-2001*, pp. 0_1-322, (2002).

[35] *WiMAX forum* (Online). Available: http://www.wimaxforum.org/home/

[36] G. Talli and P. D. Townsend, "Hybrid DWDM-TDM long-reach PON for next-generation optical access," *J. Lightw. Technol.*, vol. 24, pp. 2827-2834, (2006).

[37] J. A. Lazaro, J. Prat, P. Chanclou, G. M. Tosi Beleffi, A. Teixeira, I. Tomkos, R. Soila, and V. Koratzinos, "Scalable Extended Reach PON," presented at Conference on Optical Fiber communication/National Fiber Optic Engineers Conference, OFC/NFOEC, 2008.

[38] *Enhancement band for gigabit capable optical access networks*, ITU-T G.984.5, 2007

[39] S.-J. Park, C.-H. L. K.-T. Jeong, H.-J. Park, J.-G. Ahn, and K.-H. Song, "Fiber-to-the-Home Services Based on Wavelength-Division-Multiplexing Passive Optical Network (Invited)," *J. Lightw. Technol.*, vol. 22, pp. 2582-2591, (2004).

[40] J.-I. Kani, M. Teshima, K. Akimoto, N. Takachio, H. Suzuki, and K. Iwatsuki, "A WDM-Based Optical Access Network For Wide-Area Gigabit Access Services," *IEEE Optical Communications*, pp. S43-S48, (2003).

[41] S. Dong Jae, J. Dae Kwang, S. Hong Seok, K. Jin Wook, H. Seongtaek, O. Yunje, and C. Shim, "Hybrid WDM/TDM-PON with wavelength-selection-free transmitters," *J. Lightw. Technol.*, vol. 23, pp. 187-195, (2005).

[42] I. Tsalamanis, E. Rochat, S. Walker, M. Parker, and D. Holburn, "Experimental demonstration of cascaded AWG access network featuring bi-directional transmission and polarization multiplexing," *Opt. Express*, vol. 12, pp. 764-769, (2004).

[43] H. Yu-Li, M. S. Rogge, S. Wei-Tao, L. G. Kazovsky, and S. Yamamoto, "SUCCESS-DWA: a highly scalable and cost-effective optical access network," *IEEE Communications Magazine*, vol. 42, pp. S24-S30, (2004).

[44] E. Wong, L. K. Lun, and T. B. Anderson, "Directly Modulated Self-Seeding Reflective Semiconductor Optical Amplifiers as Colorless Transmitters in Wavelength Division Multiplexed Passive Optical Networks," *J. Lightw. Technol.*, vol. 25, pp. 67-74, (2007).

[45] F. Ponzini, F. Cavaliere, G. Berrettini, M. Presi, E. Ciaramella, N. Calabretta, and A. Bogoni, "Evolution Scenario Toward WDM-PON (Invited)," *IEEE/OSA J. of Opt. Comm. Netw.* , vol. 1, pp. C25-C34, (2009).

[46] M. Maier, "WDM Passive Optical Networks and Beyond: the Road Ahead (Invited)," *IEEE/OSA J. Opt. Commun. Netw.*, vol. 1, pp. C1-C16, (2009).

[47] M. P. McGarry, M. Reisslein, and M. Maier, "WDM Ethernet passive optical networks," *IEEE Communications Magazine*, pp. 15-22, (2006).

[48] T. Jayasinghe, C. J. Chae, and R. S. Tucker, "Scalability of RSOA-based multiwavelength Ethernet PON architecture with dual feeder fiber," *J. Opt. Netw.*, vol. 6, pp. 1025-1040 (2007).

[49] L. Qinghua, L. Xintian, Z. Jianzhong, and R. Wonil, "Advancement of MIMO technology in WiMAX: from IEEE 802.16d/e/j to 802.16m," *IEEE Communications Magazine*, pp. 100-107, (2009).

[50] *The Draft IEEE 802.16m System Description Document*, IEEE 802.16m, 2009

[51] *IEEE Standard for Local and metropolitan area networks Part 16: Air Interface for Broadband Wireless Access Systems Amendment 1: Multiple Relay Specification*, IEEE Std 802.16j-2009 (Amendment to IEEE Std 802.16-2009), 2009

[52] S. W. Peters and R. W. Heath, "The Future of WiMAX: Multihop Relaying with IEEE 802.16j," *IEEE Communications Magazine*, vol. 47, pp. 104-111, (2009).

[53] *Airspan 700 MHz WiMAX Solution* (Online). Available: http://www.airspan.com/solutions_700.aspx

[54] *WiMAX Forum Position Paper for WiMAX Technology in the 700 MHz Band* (Online). Available: www.wimaxforum.org

[55] G. Shen, R. S. Tucker, and C.-J. Chae, "Fixed Mobile Convergence Architectures for Broadband Access: Integration of EPON and WiMAX," *IEEE Communications Magazine*, vol. 45, pp. 44-50, (2007).

[56] Y. Kun, O. Shumao, K. Guild, and C. Hsiao-Hwa, "Convergence of ethernet PON and IEEE 802.16 broadband access networks and its QoS-aware dynamic bandwidth allocation scheme," *J. Select. Areas Commun.*, vol. 27, pp. 101-116, (2009).

[57] *Allen Telecom's Radio-over-Fiber Technology Powers Mobile Communications at Sydney 2000 Olympics Fiber Optics Business* (Online). Available: http://findarticles.com/p/articles/mi_m0IGK/is_21_14/ai_73843087

[58] M. Milosavljevic, P. Kourtessis, A. Gliwan, and J. M. Senior, "Advanced PON topologies with wireless connectivity," presented at 11th International Conference on Transparent Optical Networks, ICTON '09. , 2009.

[59] N. Ghazisaidi, M. Maier, and C. Assi, "Fiber-wireless (FiWi) access networks: a survey," *IEEE Communications Magazine*, vol. 47, pp. 160-167, (2009).

[60] J. E. Mitchell, "Radio over fibre networks: Advances and challenges," presented at 35th European Conference on Optical Communication, ECOC, 2009.

[61] M. Milosavljevic, P. Kourtessis, and J. M. Senior, "Wireless-PONs with Extended Wavelength Band Overlay," presented at Access Networks and In-house Communications (ANIC), OSA Technical Digest (CD), (Optical Society of America, 2010), 2010.

[62] C. H. Cox, III, E. I. Ackerman, G. E. Betts, and J. L. Prince, "Limits on the performance of RF-over-fiber links and their impact on device design," *IEEE Transact. Microw. Theo. Techniq.* , vol. 54, pp. 906-920, (2006).

Chapter 3

Optical and Wireless PHY Integration

Contents

This chapter outlines the research initiatives and possible deployment scenarios demonstrating optical/wireless integration. The benefits and potential limitations of applying RoF techniques over such architectures follow in order to establish the key impairments affecting the transmission of radio signals over the optical link. In particular the degradation due to chromatic dispersion on the intensity modulation with direct detection (IM-DD) link in the presence of OFDM propagation is simulated in Virtual Photonic Inc. (VPI). The chapter closes with the description of the VPI/MATLAB co-simulation requirements for the design of WiMAX transceivers.

3.1 Optical/Wireless Research Initiatives

The European FP7 IP project, "architectures for flexible photonic home and access networks" (ALPHA) [1] is set to investigate the architecture and transmission properties associated with the integration of wired and wireless technologies over a converged system infrastructure. The

ALPHA project mainly addresses the challenges of building the future access and all types of in-building networks for home and office environments using primarily the latest physical layer (PHY) dispersion mitigation properties as well as architecture solutions and adequate control and management. The project supports the evolution towards a cognitive network by dynamically utilising the resources of an optical network infrastructure to support a heterogeneous environment of wired and wireless technologies. This is expected to be achieved by means of wireless signal propagation over the manifold of optical fibres (single-, multi-mode and plastic). In particular, ALPHA is intended to transport existing 2G/3G and Beyond 3G (B3G) signals whether they are IP or non-IP-based.

In comparison, the FP7 "fibre optic networks for distributed and extendible heterogeneous radio architectures" (FUTON) [2] project aims at researching, developing and validating a flexible architecture for wireless systems based on the joint processing of the radio signals from distinct remote antenna units and supported by a transparent fibre infrastructure. This allows the development of virtual multiple antenna transmission/reception concepts to achieve broadband wireless transmission, and also inter-cell interference cancellation.

Alternatively to mitigate frequency congestion at the microwave bands, research and development activities have shifted into the millimetre spectrum [3-6]. The RoF transmission in these bands is an ideal technology for home pico-cellular network architectures offering data rates above 1 Gbit/s [6]. The generic architecture and technologies of the optical-wireless home networks is shown in Figure 3-1 [7].
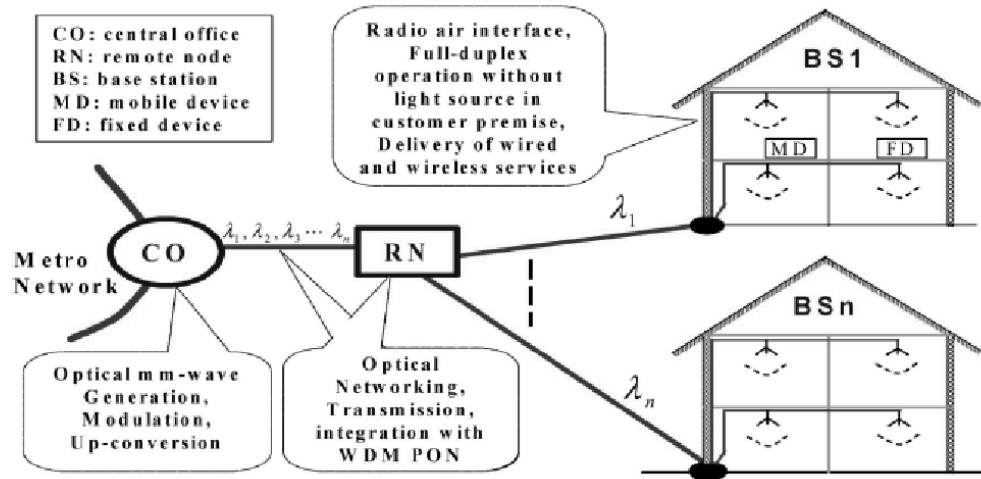
Figure 3-1: Generic architecture for mm-wave transmission [7]

At the central office (CO), the optical mm-wave signals are generated and mixed by using a cost efficient all optical approach. After being transmitted over an optical network they are detected at the home gateway and distributed to each room. The key enabling technologies for optical mm-wave generation and detection are reviewed in [7]. In addition, some studies have considered convergence of WiFi, WiMAX and millimetre wave signals on a common architectural platform based on optical interleaves to separate these frequency bands at the base station with a single light source in the central office [8]. However, this approach could lead to high deployment cost and network complexity as the number of components required is increased exponentially with the number of supported base stations.

Using a similar philosophy, a different research group has been focusing on a network architecture based on a optical frequency multiplication (OFM) technique for mm-waveband up-conversion [9]. This is achieved by periodic filtering and photo-detection of an optical signal whose wavelength is continuously swept by the low-frequency RF signal. The desired signal is selected by the bandpass filter.

Another project targeting mm-waves for delivering Gbit/s services within home networks is the European project, "home gigabit access" (OMEGA) [10]. The UWB, broadcasting by use of visible-light communications (VLC), power-line communications (PLC) or even wireless mesh technologies are investigated.

However, OMEGA does not consider the use of optical infrastructures or provide user mobility and hybrid optical/wireless routing while the remaining in-home network initiatives can find no applications at access and beyond area networks. They also assume the provision of a FTTH access gateway that might not be the case in the majority of deployment scenarios, prohibited by the cost.

In a different direction, there is strong motivation to extend the optical infrastructure with wireless mesh access [11, 12]. Wireless mesh networks (WMN), have individually received research attention in the last few years [13-15]. This trend is driven by the existence of real-world, community-oriented WMNs and also by the ease of deployment and inherent resilience features due to path redundancy. Most approaches are focused on IEEE 802.11-based networks, with intelligence built into mesh nodes so that wise routing decisions can be made. However, there are distinct problems in the operation of WMNs, which mainly stem from the very nature of wireless communication in an unlicensed spectrum. Bandwidth may be scarce and interference may cause significant performance degradation, thus traditional approaches for various network functions cannot readily be applied to WMNs to achieve comparable performance.

Despite these limitations, the "hybrid wireless-optical broadband-access network" (WOBAN) project is set to investigate wireless mesh capabilities over standardised PONs [16]. The wireless part of WOBAN has been gaining recently increasing attention, and early versions are being deployed as municipal access solutions to eliminate the wired drop to every wireless

router at customer premises [16]. The wireless architecture is based on a mesh topology for bidirectional transmission from the OLT to end users via multiple hops. The end terminal mobility can be supported at the IP layer by one of the three dominant approaches developed at the Internet Engineering Task Force (IETF), namely, mobile IP, migrate, and host-identity protocol [16].

Another integrated optical/WMN architecture following a similar approach to WOBAN is the "grid reconfigurable optical and wireless network" (GROW-Net) [17], which also attempts to exploit the cost-effectiveness of wireless mesh networks in urban areas. The initial intention of this project was to define loop-based optical routing strategies for the optical part combined with routing strategies defined for the wireless to potentially exchange some information that will affect the decisions of both networks. However, further evolutions of the architecture eventually led to solutions that are similar to WOBAN based on an optical ring serving as the backbone infrastructure, gathering traffic from the wireless multi-hop network and forwarding it to the central office. The central office is in control of network operation and management.

In view of the mesh topologies utilised, packets in both these schemes need to traverse many nodes before they reach their destination. This would most certainly impose additional delays therefore requiring complex MAC layer designs, applicable to both wired and wireless, parts of the network, in order to compensate for the multiple hops. Also, the network performance largely depends on placement of ONUs in the field [16].

Finally, for the implementation of RoF solutions developments, in terms of bandwidth and carrier frequency of optical components, particularly relevant to generating light and optical modulation, are of special interest. An example of that would be the advances in vertical cavity surface emitting lasers (VCSELs) due to their low bias currents suitable for high bandwidth modulation and operation at longer wavelengths [18, 19]. Recently, low-cost VCSEL arrays

have found application in WDM-PONs where they are typically installed at ONUs for colourless transmission [20, 21] since they are not limited by Rayleigh backscattering and small bandwidth typically encountered with RSOA devices [22]. Significantly, the use of VCSELs has been also proposed in RoF architectures [23, 24].
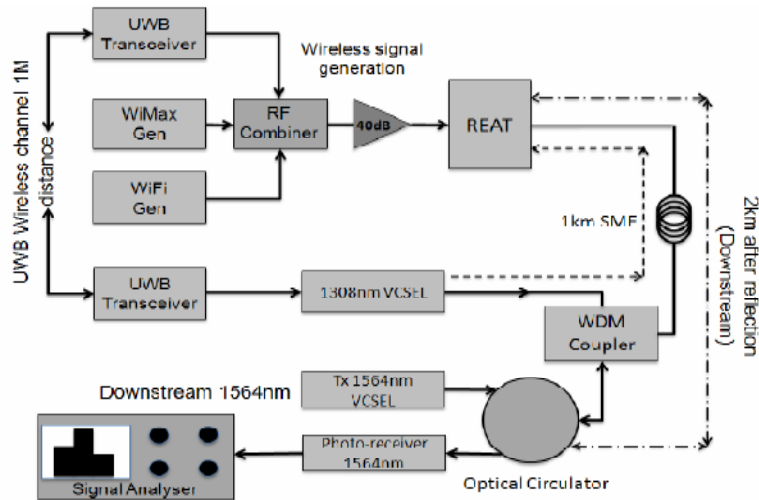
Figure 3-2: Triple-Format radio-over-fiber experimental set-up with long-wavelength VCSEL [24]

As seen in Figure 3-2, successful transmission of UWB, WiFi and WiMAX has been achieved with long wavelength VCSELs in a point-to-point network architecture. A VCSEL bias current of just 7 mA has been demonstrated requiring low cost drive circuits. However, these investigations were performed over short fibre distances that are not common in typical deployment scenarios.

Although several research paths are set to investigate optical/wireless integration scenarios, they collectively do not deploy techniques such as RoF with FDM in a sense of providing bandwidth-on demand and redundancy. As a result they do not investigate extended features of these networks that could be gained by the integration, automatically distinguishing this project from these initiatives.

3.2 Layer-1 Integration

Figure 3-3 represents a common PHY structure widely applicable to all emerging broadband wireless standards including WiMAX and LTE [25]. This illustration could be utilised to demonstrate possible integration points with the xPON.

The WiMAX is widely described in detailed in the remaining chapters of this thesis. The LTE is not consider further apart from only at the very end as part of conclusion as an emerging technology. Nevertheless, it should be mentioned at this point that LTE should also be supported since in comparison to WiMAX, although uses same modulation format downstream, it provides for higher spectral efficiency, lower transmit time interval and it exploits current 3G network infrastructure.

Following the forward error correction (FEC) block, user data is mapped to complex QAM symbols and structured according to the logical mapping mechanisms. Up to this point the packets to be transmitted to the diverse mobile users are still separated. Four possible splitting points (a-d) can be identified. These can vary from transmitting solely the user payload (as it is done today) and perform the complete baseband processing chain within the respective BS (a), up to finalizing the user specific processing within the central office (d) and solely performing framing and multicarrier modulation within the wireless nodes.

Once the user data is mapped to its logical bins the multicarrier frames are assembled. Here the physical assignment of user data is performed in (e). Additionally control signals are generated and added (e.g. maps and preamble for WiMAX, control channels and reference signals for LTE). Once the multicarrier symbols are assembled they are fed to the inverse-FFT (IFFT) and the cyclic prefix (CP) is added. After parallel to serial conversion the baseband processing is completed.
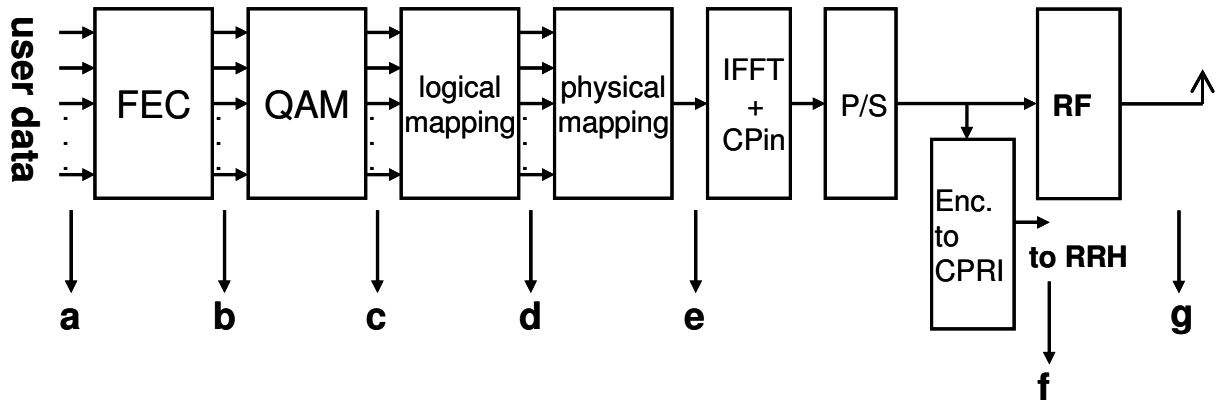
Figure 3-3: PHY structure of emerging broadband wireless networks [25]

In recent years, efforts have been dedicated in defining a standardized format for the connection of remote radio heads to the baseband processing unit, the so-called CPRI specification (Common Public Radio Interface) [26]. CPRI represents a means to transport analogue baseband signals digitally. This would be realised in the figure by utilising reference point (f). Alternatively a RoF approach would exploit connection point (g) where the analogue radio signal gets transmitted via the xPON.

The various alternatives by means of interfacing the wireless and PON architectures would offer the common infrastructure different functionality properties. The more processing functionalities are shifted into the CO for example, the higher the amount of data to be transmitted over the PON. Integration at point (a) would need the minimum amount of resources since only the payload is communicated. In point (b) the packet overhead starts increasing due to the application of forward error correction. If the physical mapping operation at point (e) is fully performed in a centralized manner within the CO the overhead increases as in this case further frame elements such as pilots, reference symbols and frequency guards have to be transmitted via the xPON. Finally, at points (f) and (g) the overhead would be at its maximum as the cyclic prefix consumes resources.

Finally the selection of the interface point would impose significant influence to the PON signal quality. Analogue transport of the radio signals is considered to be more susceptible to distortions of the optical link than digital transmission.

3.3 Deployment Scenarios

Examples of potential deployment scenarios to demonstrate wireless backhauling over optical access networks are outlined below.

One of the options would involve a wireless (WiMAX or LTE) base-station node placed on top of building roofs or facades and sometimes collocated with already installed 3G equipment. The latter can also leverage on the converged infrastructure to get extra or new connectivity with a corresponding remote node controller at the CO, as shown in Figures 3-4 and 3-5.
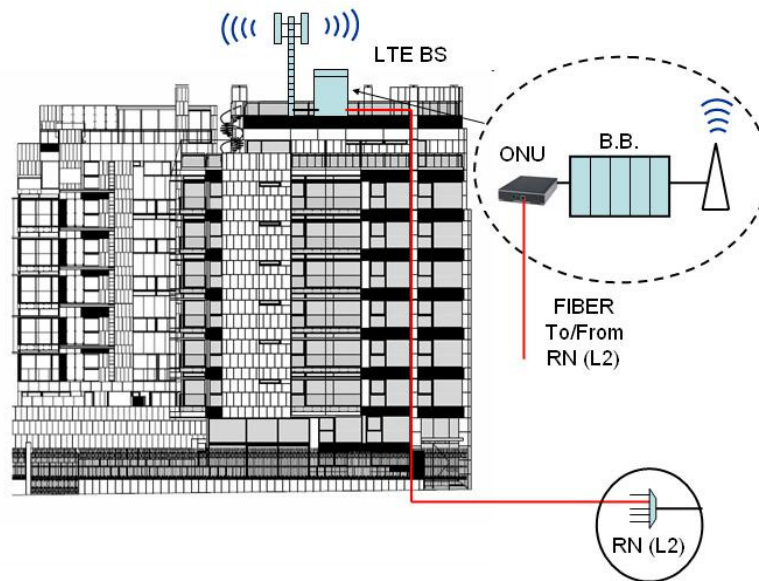
Figure 3-4: Roof-top deployment scenario [25]
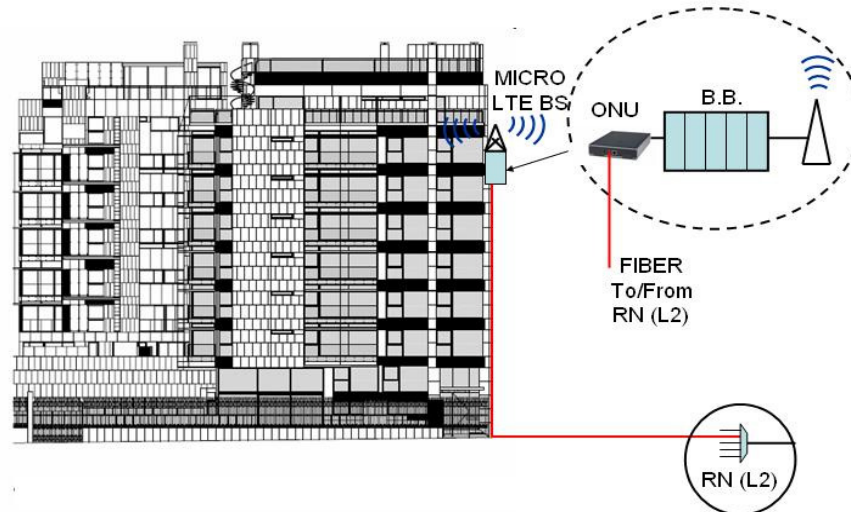
Figure 3-5: Antenna at building facades [25]

Alternatively, a wireless remote head, located on a pole at a building facade or on a roof could

be considered. In that case the remote head would be connected to the mobile station base-band

resources via the PON ONUs, as shown in Figure 3-6.
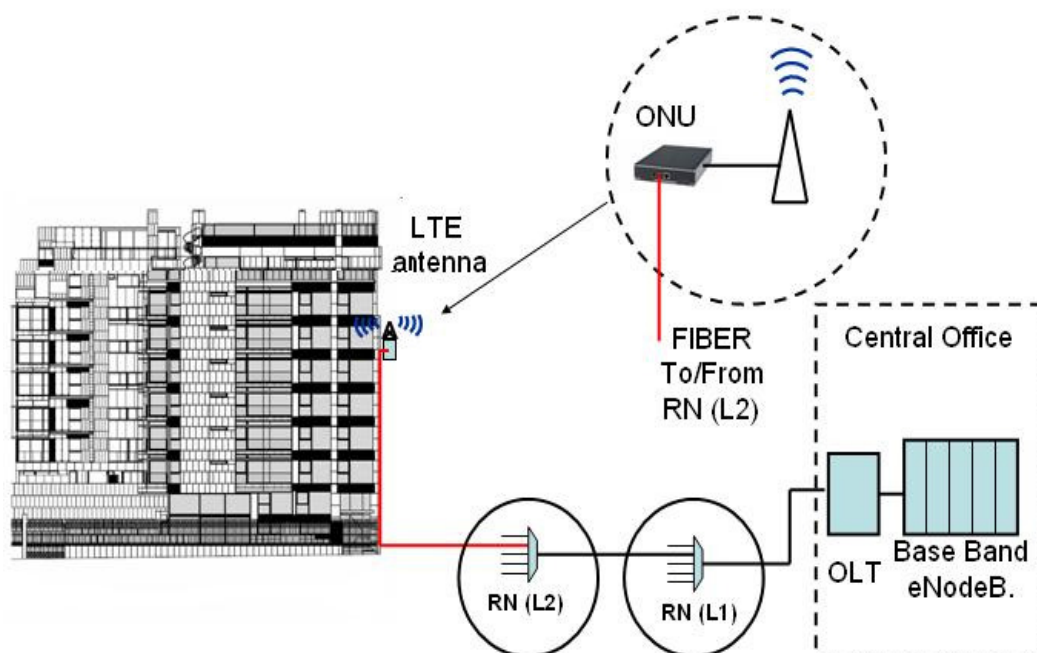
Figure 3-6: Antenna at the pole of a building facade [25]

3.4 Simulation of Radio Signal Transmission over Fibre

RoF signal transport over optical fibre links has been extensively studied in the past as a possible technology for simplifying the architecture of remote BSs [27-29]. While the fibre has enormous bandwidth to support high capacity transmission, current and future wireless applications will still use a wide range of frequencies [27]. This raises more challenges to the implementation of RoF systems in a cost-effective manner since in an analog photonic link the wireless signals experience a number of inevitable signal impairments, especially at higher frequency bands, as illustrated in Figure 3-7 [30, 31].
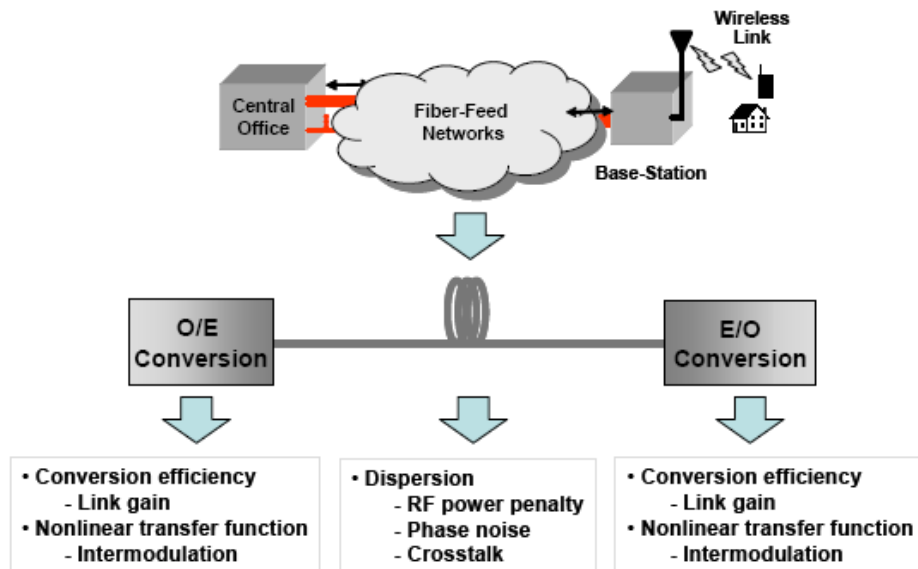
Figure 3-7: Typical impairments with RoF links [30]

These impairments arise as a result of the nonlinear characteristics of the optoelectronic conversion process at the transmitter and receiver which leads to increased inter-modulation distortion and reduced dynamic range. Studies have shown that nonlinearities in the optical front-end limit the overall system dynamic range [27]. To minimize nonlinear distortion arising from optoelectronic conversion, the amplitude of the drive signals has to be greatly reduced which subsequently leads to low conversion efficiency and reduced link gain.

Considering the frequency of the RF signal is fed into the RoF link at the head-end, RoF implementation may be classified into three categories, namely RF-over-fibre, IF-over-fibre, and baseband-over-Fibre [32]. The RF over fibre approach involves the transmission of the actual RF signal over the fibre. However, in case of IF or baseband over fibre the desired microwave signal is generated at the remote antenna units through up-conversion with a local oscillator (LO), which is either provided separately at the remote antenna units, or is transported remotely. Therefore, the complexity of the base station will depend on the transmission method used with the RF over fibre approach providing for the highest simplicity. In that direction, simplicity of implementation is supported in the current network architecture by FDM to reduce component cost and signal processing requirements at remote radio heads.

To generate and transport microwave signals over a fibre, a variety of schemes can be applied. The most popular and cost effective solution is based on IM-DD [32]. In this approach, the intensity of the light is directly modulated with the analog signal, using direct detection at the photo-detector to recover the original signal.

IM could be either performed by directly modulating a laser current or using an external modulator, such as a Mach-Zehnder modulator (MZM), to externally modulate the intensity of a continuous wave laser. The two options are displayed in the Figure 3-8 [32]. After transmission through the fibre and direct detection on a photodiode, the photocurrent is a replica of the modulating RF signal.
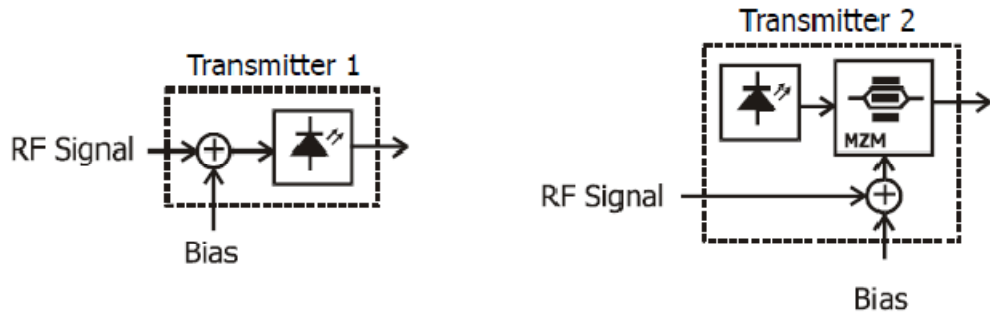
Figure 3-8: Generating RF signal by direct modulation (left) and external modulation (right) [32]

One drawback of the RF and IM-DD techniques is that it is difficult to be utilised for high frequency mm-wave applications due to the fibre chromatic dispersion and limited bandwidth of electrical components. However, the RoF approach described in this thesis is based on transmission of microwave frequencies and is therefore not limited to the aforementioned impairments.

3.4.1 Effects of Fibre Chromatic Dispersion on IM-DD Link

In IM the resulting optical spectrum will consist of two sidebands located at the wireless carrier frequencies on either side of the optical carrier, exhibiting an optical double-sideband (ODSB) modulation format. When the optically modulated signal propagates along a dispersive fibre, its two sidebands will experience a different amount of phase shift relative to the optical carrier. Upon detection at the system receiver, the square-law process generates two beat components at the wireless frequency. To that extent, the received RF power of the wireless signal varies depending on the relative phase difference between the two beat components. This variation is dependent on the fibre dispersion parameter, the transmission distance and also the wireless carrier frequency used [33].

The effect of chromatic dispersion on the analog wireless signal has been demonstrated, using VPI, by the development of a simple P2P system based on external optical modulation, as shown in Figure 3-9. An electrical impulse is used to excite the fibre at all frequencies. The

thermal and shot noise figures of the photo-diode are excluded from this analysis in order to
determine only the effect of the chromatic dispersion.
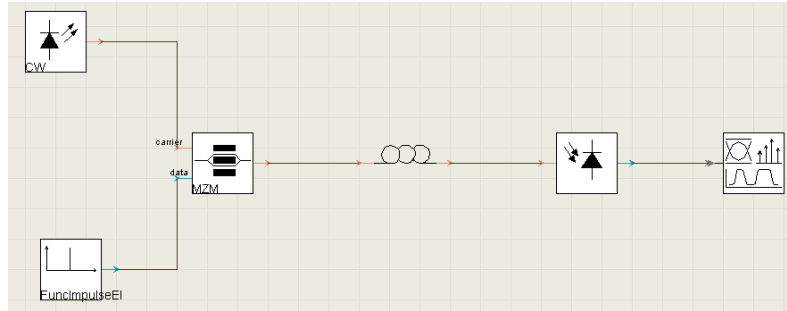
Figure 3-9: A simple point-to-point link for demonstrating fibre chromatic dispersion effects

Table 3-1: Photo-diode parameters in VPI

Parameter	Value	Unit
Responsivity	1	A/W
Photo Diode Model	PIN	/
Dark Current	0	nA
Thermal Noise	0	$pA/(Hz)^{1/2}$
Shot Noise	OFF	/

For transmission, a 20km SSMF reel has been utilised with standard parameters as shown in
Table 3-2.

Table 3-2: Fibre parameters

Parameter	Value	Unit
Length	20	km
Group Refractive Index	1.47	/
Attenuation	0.2	dB/km
Dispersion	16e-6	s/m^2
Dispersion Slope	0.08e3	s/m^3

The obtained transfer function in Figure 3-10, measured at the output of the photodiode,
demonstrates amplitude variations at certain frequencies caused mainly due to the fibre
chromatic dispersion. Based on these primary results it becomes evident that the application of
RoF needs to be carefully designed in order to avoid high attenuations at certain subcarrier

frequencies. The number of subcarriers in the network could thus be limited not only by the

small bandwidth of optical and electrical components but also by the fibre chromatic dispersion.
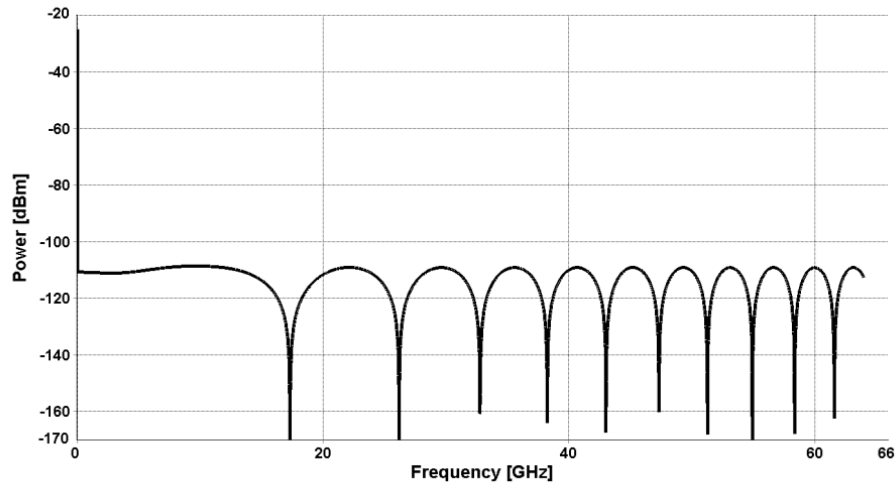
Figure 3-10: Amplitude variations due to fibre chromatic dispersion

3.4.2 OFDM Transmission Evaluation

Having previously established the key characteristics of RoF transmission, it is equally

important to evaluate the impact of optical fibres this time on RF OFDM signals. OFDM

modulation is utilised in all emerging broadband wireless standards [34, 35] and as a result its

performance evaluation in view of its compatibility with optical transmission links in

architectures enabling wireless/optical integration is paramount. In that direction, for the

OFDM, error vector magnitude (EVM) is one of the most important test parameter to ensure the

transmitter ability to produce more power and yet maintain signal quality.
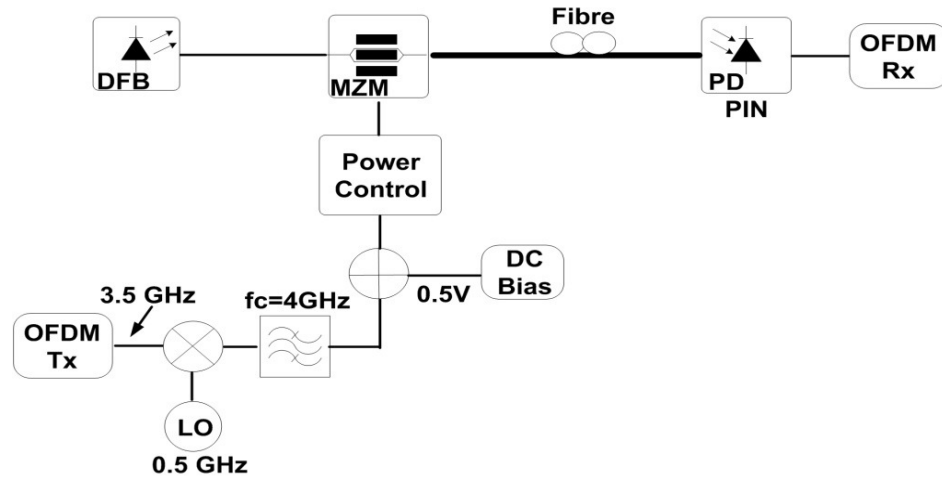
Figure 3-11: OFDM transmission investigation setup

Figure 3-11 displays a point-to-point RoF link devised in VPI, demonstrating external optical modulation of an FDM multiplexed, OFDM channel, to estimate the EVM of the received signal after transmission over various lengths of the optical fibre.

The OFDM transmitter comprises of 64 subcarriers with 16-QAM modulation each, at a 3.5 GHz carrier. This carrier is up-converted to 4 GHz and filtered in order to avoid unwanted sidebands. The resulting signal is then fed, via a power control unit, to a MZM RF input biased at its quadrature point. The power control circuit of Figure 3-11 is utilised to adjust the input RF power inside the MZM.

The second MZM arm was fed by a 1550nm optical carrier at 0 dBm output power ending up supplying the SSMF with -6 dBm. The modulated output is then transmitted over various lengths of the fibre before being received by a PIN photo-detector and demodulated in the OFDM receiver. The receiver parameters comply with the transmitter parameters to achieve accurate demodulation.

Figure 3-12 presents the obtained EVM figures at the OFDM receiver with respect to the MZM RF drive power for varying fibre lengths. The relative constellation root-mean-square error, or EVM, is calculated at the receiver as proposed in [35],

$$EVM = \sqrt{\frac{\sum_{i=1}^{Ns}\left(I_{Tx_i} - I_{Rx_i}\right)^2 + \left(Q_{Tx_i} - Q_{Rx_i}\right)^2}{\sum_{i=1}^{Ns}\left(I_{Tx_i}^2 + Q_{Tx_i}^2\right)}} \tag{3.1}$$

where I_{Tx_i} and I_{Rx_i} are the transmitted and receiver I components of the complex symbols respectively. The same notation applies for the Q_{Tx_i} and Q_{Rx_i} components.
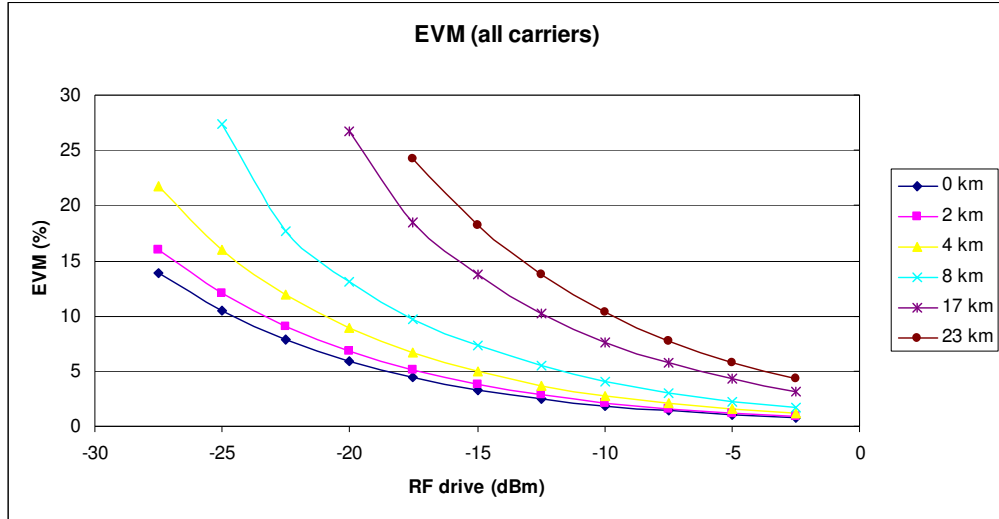
Figure 3-12: EVM against RF drive power for different fiber lengths

As expected, the EVM characteristics increase with the optical link noise for low RF drive powers (i.e. for power levels in the range of -27 dBm the EVM is 14%). With the power levels in the range of 2.5 dBm the EVM below 5% is observed. Further degradation of the system performance can also be seen for increasing fibre lengths due to chromatic dispersion. Taking into consideration the stringent requirements, as they are dictated by emerging broadband wireless standards, EVM figures in the range of 2-5% [34, 35] will be typically required at antenna inputs. Therefore, RF drive power inside the optical modulator and fibre link lengths are important factors in designing a RoF transmission link for these wireless signals.

Finally, the obtained constellation diagrams at -3 dBm RF drive power for back-to-back and 23 km fibre transmission links are shown in Figure 3-13.
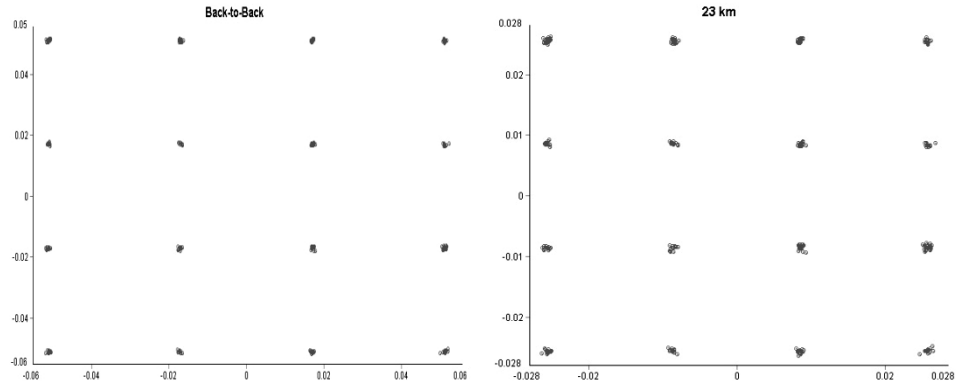
Figure 3-13: Constellation diagram of all carriers, 16-QAM

The pilot tones were not considered by the OFDM transmitter therefore only data points are visible on the constellation. It can be seen that while the EVM for the 23km fibre link is higher, resulting unavoidably to more points received in error, the constellation is still recoverable due to the relatively high, -3dBm RF drive power. In real systems, however, high RF drive powers would be required in order to increase the conversion efficiency resulting in greater non-linear effects and consequently more symbols in error.

3.5 VPI/MATLAB Co-Simulation Requirements

The industrial standard VPI simulation platform enables modelling of a wide range of optical communication networks and photonic devices [36]. However, following the emergence of wireless standards and the need to integrate those with optical networks, co-simulation capabilities between VPI and the well established software platforms for wireless simulations, such as MATLAB, are required. To that extent, this section attempts to present the VPI co-simulation capabilities with MATLAB and layout the principles, to be employed in proceeding chapters for the implementation of the wireless/optical architecture models.

The general concept allowing the synergy between VPI and alternative simulators is shown in Figure 3-14. The co-simulation (CoSim) interface block is used to pass parameters to be executed at the target application. For each simulation run, the input and parameter data are

stored in the target environment (i.e. MATLAB) via galaxy ports (e.g. CoSimInputOpt) and then a specified function is executed. The expected output data are then collected and fed back to VPI.
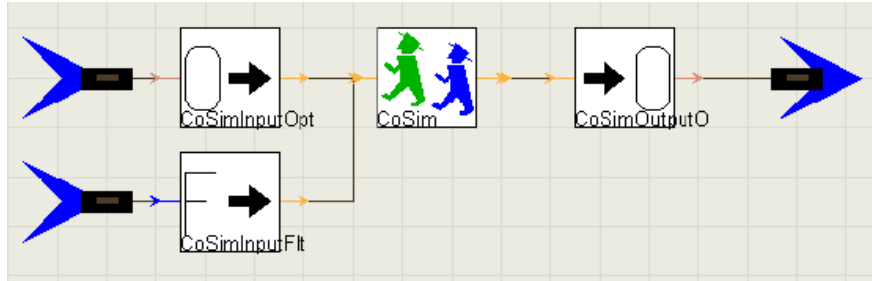
Figure 3-14: Co-simulation interface in VPI

3.6 WiMAX Signal Generation and Detection

To perform an interoperable model and evaluate its preliminary performance, a IEEE802.16d WiMAX OFDM transceiver model was built in MATLAB and applied at the VPI CoSim interface. Figure 3-15 portrays at block diagram the transmitter and receiver, demonstrating clearly the interworking functionalities of the distinct modelling platforms. The performance of WiMAX channels was modelled with no channel coding applied in order to present a worst case scenario.
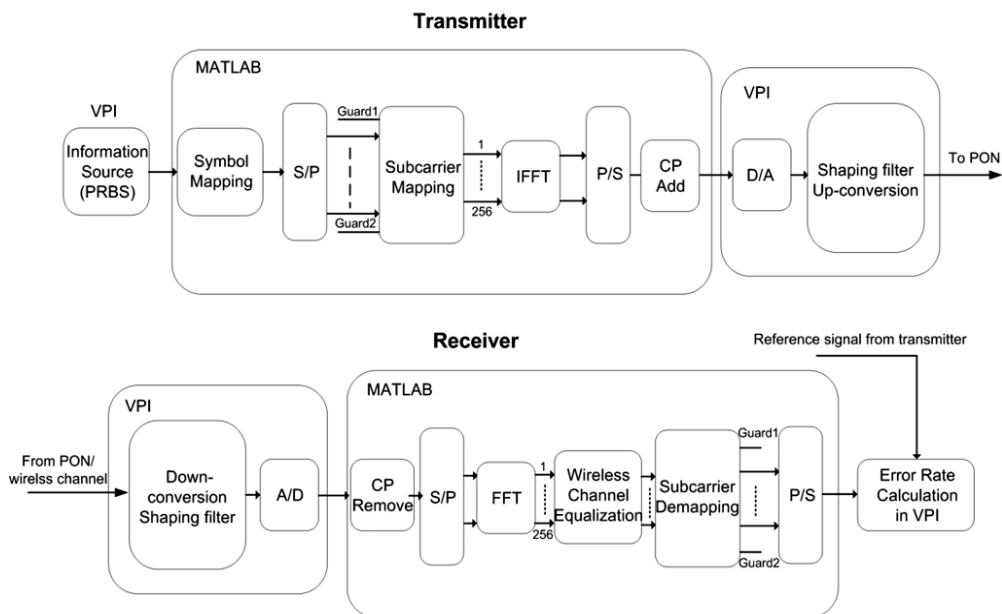
Figure 3-15: General description of inter-software functionalities for WiMAX transceivers

At the transmitter, following the symbol formation and serial to parallel conversion in MATLAB, the subcarrier mapping block could be used to insert guard carriers for a brick-wall spectrum shape [35].

The resulting frequency domain signal was subsequently transformed to the time domain using the 256 point IFFT prior to parallel to serial conversion and cyclic prefix addition. The quantisation process and signal shaping are performed in VPI.

At the other end, the WiMAX receiver performs the inverse functions to those of the transmitter. The 14 bits digital to analog (D/A) and analog to digital (A/D) converters at the transmitter and receiver respectively were used to minimise quantisation noise [35]. The cyclic prefix removal, FFT and wireless channel equalisation at the receiver are performed in MATLAB while VPI is used for estimating the symbol error rate (SER) and EVMs.

Critically, estimating the SER of the electrical mQAM signal in RoF systems raises additional issues compared to classical systems where only additive white Gaussian noise (AWGN) influences signal quality [37]. The probability density function (PDF) of the received I and Q signals does not always follow a Gaussian distribution. It was shown that this PDF is Gaussian when electrical or optical noise (ASE) is the main impairment [37]. On the other side, when composite triple beat (CTB) also called third-order inter-modulation distortions (IMD3) occurs, this PDF tends to an Exponential distribution. More generally, the PDF lies between a Gaussian and an Exponential distribution, making the SER more complicated to estimate. In addition to the above, nonlinear distortions can be amplitude-dependent so that the distribution statistics (e.g. the variance) may be different for each symbol [37].

To account for these characteristics, the SER estimation is based on an independent approximation of the left and right tails of the signal's PDF, corresponding to each mQAM symbol [38].

A central symmetry property of the constellation diagram, in specific the statistical equivalence of the symbols, such as (I=x,Q=y), (I=-x,Q=-y), (I=x,Q=-y) and (I=y,Q=x), is used to improve the data statistics [38, 39]. This is realised by reporting all symbols into a single quadrant ((I,Q}>0), and performing the SER analysis on this quadrant only.

Significantly, the constellation mapping for mQAM symbols is based on Gray coding therefore the bit error rate (BER) can be easily calculated from the obtained SER by [39]:

$$BER = \frac{SER}{BitsPerSymbol} \tag{3.2}$$

That way, demodulation of complex symbols is not required in order to estimate the BER. Detailed implementation of the WiMAX transceivers as they have been devised using the VPI/MATLAB co-simulator is presented in chapter 4.

3.7 Summary

This chapter introduced highly referenced optical/wireless integration scenarios as they have emerged from research initiatives worldwide, followed by the review of possible deployments infrastructures. Although the integrated architectural platforms have been employed mainly for short range in-home networks (OMEGA, FUTON, OFM techniques, etc.) with only a few deployments targeting to connect transparently remote base stations in a point-to-point metro/access configuration, it was established that they have not fully concentrated on developing access networks, deploying emerging wireless broadband standards, such as WiMAX, over standardised point-to-multipoint xPONs aiming to further increase the reach and capacity of both networks.

To define the initial concepts of a wireless backhauling and primarily at this stage the properties of its transmission links, it was concluded that RoF reduces unnecessary overheads, typically presented in alternative signalling formats such as digital. As a result the specifications of RoF signal generation and demonstrated link impairments by means of VPI simulations are delivered.

Successively preliminary results were drawn with reference to fibre chromatic dispersion and OFDM signal quality estimation in terms of EVM plots. Simulation results have confirmed that due to optical double sideband modulation amplitude deeps could occur at certain frequencies of the fibre transfer function. Therefore, careful consideration is required in subcarrier selection when FDM is applied. Also, due to inherent optical nonlinearities and link noise it was suggested that in the presence of OFDM transmission the optical modulator drive powers must be carefully selected to meet the stringent requirements at the remote bases stations.

Finally, VPI/MATLAB co-simulation requirements for WiMAX signal detection and generation are presented where wireless digital signal processing will be performed exclusively

by MATLAB. Detailed network models to be utilised throughout this work are presented in the

following chapter.

References

[1] *Architectures for Flexible Photonic Home and Access Networks (ALPHA)* (Online). Available: http://www.ict-alpha.eu

[2] *Fibre-Optic Networks for Distributed Extendible Heterogeneous Radio Architectures and Service Provisioning (FUTON)* (Online). Available: http://www.ict-futon.eu

[3] J. E. Mitchell, "Radio over fibre networks: Advances and challenges," presented at 35th European Conference on Optical Communication, ECOC, 2009.

[4] F. Lecoche, E. Tanguy, B. Charbonnier, H. Li, F. van Dijk, A. Enard, F. Blache, M. Goix, and F. Mallecot, "Transmission Quality Measurement of Two Types of 60 GHz Millimeter-Wave Generation and Distribution Systems," *J. Lightw. Technol.*, vol. 27, pp. 5469-5474, (2009).

[5] C. Bock, T. Quinlan, M. P. Thakur, and S. D. Walker, "Integrated Optical Wireless Access: Advanced topologies for future access networks," presented at ICTON '09. 11th International Conference on Transparent Optical Networks, 2009.

[6] M. C. R. Medeiros, R. Avo, P. Laurencio, I. Darwazeh, J. E. Mitchell, P. M. N. Monteiro, and H. J. A. da Silva, "Convergence of optical and millimeter-wave broadband wireless access networks," presented at 11th International Conference on Transparent Optical Networks, ICTON, 2009.

[7] J. Zhensheng, Y. Jianjun, G. Ellinas, and G. K. Chang, "Key Enabling Technologies for Optical-Wireless Networks: Optical Millimeter-Wave Generation, Wavelength Reuse, and Architecture," *J. Lightw. Technol.*, vol. 25, pp. 3452-3471, (2007).

[8] Z. Jia, J. Yu, Y.-T. Hsueh, H.-C. Chien, A. Chowdhury, and G.-K. Chang, "Wireless high-definition services over optical fiber networks," *J. Opt. Netw.*, vol. 8, pp. 235-243, (2009).

[9] M. G. Larrode, A. M. J. Koonen, J. J. V. Olmos, and A. Ng'Oma, "Bidirectional radio-over-fiber link employing optical frequency multiplication," *Photon. Technol. Lett.*, vol. 18, pp. 241-243, (2006).

[10] *Home Gigabit Access (OMEGA)* (Online). Available: http://www.ict-omega.eu

[11] N. Ghazisaidi, M. Maier, and C. Assi, "Fiber-wireless (FiWi) access networks: a survey," *IEEE Communications Magazine*, vol. 47, pp. 160-167, (2009).

[12] S. Wei-Tao, W. Shing-Wa, C. Ning, K. Balasubramanian, Z. Xiaoqing, M. Maier, and L. G. Kazovsky, "Hybrid Architecture and Integrated Routing in a Scalable Optical-Wireless Access Network," *J. Lightw. Technol.*, vol. 25, pp. 3443-3451, (2007).

[13] *Enhanced, Ubiquitous, and Dependable Broadband Access using MESH Networks (EU-MESH)* (Online). Available: http://www.eu-mesh.eu

[14] *Carrier Grade Mesh Networks (CARMEN)* (Online). Available: http://www.ict-carmen.eu

[15] *An All-wireless Mobile Network Architecture (WIP)* (Online). Available: http://www.ist-wip.org

[16] S. Sarkar, S. Dixit, and B. Mukherjee, "Hybrid Wireless-Optical Broadband-Access Network (WOBAN): A Review of Relevant Challenges," *J. Lightw. Technol.*, vol. 25, pp. 3329-3340, (2007).

[17] *Grid Reconfigurable Optical and Wireless Network (GROW-NET)* (Online). Available: http://wdm.stanford.edu/grownet/grownet.htm

[18] E. Kapon, S. A., I. V., M. A., C. A., and S. G., "Recent Developments in Long Wavelength VCSELs Based on Localized Wafer Fusion," presented at 11th International Conference on Transparent Optical Networks, ICTON, 2009.

[19] A. Hayat, A. Bacou, A. Rissons, J. C. Mollier, V. Iakovlev, A. Sirbu, and E. Kapon, "Long Wavelength VCSEL-by-VCSEL Optical Injection Locking," *IEEE Transact. Microw. Theo. Techniq.* , vol. 57, pp. 1850-1858, (2009).

[20] W. Hofmann, E. Wong, G. Bohm, M. Ortsiefer, N. H. Zhu, and M. C. Amann, "1.55-um VCSEL Arrays for High-Bandwidth WDM-PONs," *Photon. Technol. Lett.*, vol. 20, pp. 291-293, (2008).

[21] L. Xu, H. K. Tsang, W. Hofmann, and M. C. Amann, "10-Gb/s colorless re-modulation of signal from 1550nm vertical cavity surface emitting laser array in WDM PON," presented at European Conference on Lasers and Electro-Optics 2009 and the European Quantum Electronics Conference. CLEO Europe 2009.

[22] C. Keun Yeong, L. Yong Jik, H. Y. Choi, A. Murakami, A. Agata, Y. Takushima, and Y. C. Chung, "Effects of Reflection in RSOA-Based WDM PON Utilizing Remodulation Technique," *J. Lightw. Technol.*, vol. 27, pp. 1286-1295, (2009).

[23] M. Bakaul, N. Nadarajah, A. Nirmalathas, and E. Wong, "Internetworking VCSEL-Based Hybrid Base Station Towards Simultaneous Wireless and Wired Transport for Converged Access Network," *Photon. Technol. Lett.*, vol. 20, pp. 569-571, (2008).

[24] T. Manoj, Q. Terence, B. A. Siti, H. David, W. Stuart, S. David, B. Anna, and M. Dave, "Triple-Format, UWB-WiFi-WiMax, Radio-over-Fiber Co-Existence Demonstration Featuring Low-Cost 1308/1564nm VCSELs and a Reflective Electro-Absorption Transceiver," presented at Optical Fiber Communication Conference, 2009.

[25] *ACCORDANCE: Deliverable 2.1 (D2.1)* (Online). Available: http://ict-accordance.eu

[26] *Common Public Radio Interface (CPRI); Specificaiton v4.1*, http://www.cpri.info, 2009

[27] C. Lim, A. Nirmalathas, M. Bakaul, P. Gamage, K.-L. Lee, Y. Yang, D. Novak, and R. Waterhouse, "Fiber-Wireless Networks and Subsystem Technologies," *J. Lightw. Technol.*, vol. 28, pp. 390-405, (2010).

[28] P. H. Gomes, N. L. S. da Fonseca, and O. C. Branquinho, "Analysis of performance degradation in Radio-over-Fiber systems based on IEEE 802.16 protocol," presented at IEEE Latin-American Conference on Communications, LATINCOM '09. , 2009.

[29] J. E. Mitchell, "Techniques for Radio over Fiber Networks," presented at 19th Annual Meeting of the IEEE Lasers and Electro-Optics Society, LEOS 2006. , 2006.

[30] L. Christina, N. Ampalavanapillai, Y. Yang, Dalma N, and W. Rod, "Radio-over-fiber systems," presented at Communications and Photonics Conference and Exhibition (ACP), Asia, 2009.

[31] T. Kurniawan, A. Nirmalathas, C. Lim, D. Novak, and R. Waterhouse, "Performance analysis of optimized millimeter-wave fiber radio links," *IEEE Transact. Microw. Theo. Techniq.*, vol. 54, pp. 921-928, (2006).

[32] A. Ng'oma, A. M. J. Koonen, I. T. Monroy, H. P. A. Boom, and G. D. Khoe, "Using optical frequency multiplication to deliver a 17 GHz 64 QAM modulated signal to a simplified radio access unit fed by multimode fiber," presented at Optical Fiber Communication Conference OFC/NFOEC, 2005.

[33] C. H. Cox, III, E. I. Ackerman, G. E. Betts, and J. L. Prince, "Limits on the performance of RF-over-fiber links and their impact on device design," *IEEE Transact. Microw. Theo. Techniq.* , vol. 54, pp. 906-920, (2006).

[34] *Technica Specification Group Services and Systems Aspects, Service Aspects: Services and Services Capabilities*, 3GPP TS 22.105 V 6.2.0, 2003

[35] "IEEE Standard for Local and metropolitan area networks Part 16: Air Interface for Fixed and Mobile Broadband Wireless Access Systems Amendment 2: Physical and Medium Access Control Layers for Combined Fixed and Mobile Operation in Licensed Bands and Corrigendum 1," *IEEE Std 802.16e-2005 and IEEE Std 802.16-2004/Cor 1-2005 (Amendment and Corrigendum to IEEE Std 802.16-2004)*, pp. 0_1-822, (2006).

[36] *VPI photonics Inc.* (Online). Available: http://www.vpiphotonics.com

[37] H. Louchet, K. Kuzmin, and A. Richter, "Efficient BER Estimation for Electrical QAM Signal in Radio-Over-Fiber Transmission," *Photon. Technol. Lett.*, vol. 20, pp. 144-146, (2008).

[38] *VPI reference manual (VCSEL operation)* (Online). Available: http://www.vpiphotonics.com

[39] J. G. Proakis, *Digital Communications*, Fourth ed, 2001.

Chapter 4

FDM Simulation Platform with Wireless Compatibility

Contents

A converged passive optical network architecture supporting standard WiMAX OFDM transceivers for transmission to and from remote ONU/BSs has been reported using VPI/MATLAB modelling. Significantly, transparent communication of five WiMAX FDM subcarriers is performed featuring external versus direct modulation evaluation measurements to estimate the maximum number of subcarriers to be supported in a FDM window.

4.1 Principle of RoF Approach in the Integrated Architecture

The cost-effectiveness and scalability of RoF techniques [1], to supply fixed to mobile convergence by means of FDM constitute powerful properties in enhancing broadband wireless networks and TDM-PON operation [2, 3]. Although extensive proposals of hybrid optical/wireless architectures have been investigated, as presented in previous chapters, the

application of WiMAX over legacy PONs have not been collectively examined, by means of enhancing their operation features with respect to aggregate capacities, reach and number of supported users. Figure 4-1 demonstrates an architecture accounting for these features. Even though the figure in particular portrays a basic overview of the architecture, for the benefit of building an argument in this chapter, its enhancements and corresponding modes of operation fully embrace the properties outlined above supported by scalability and dynamicity.
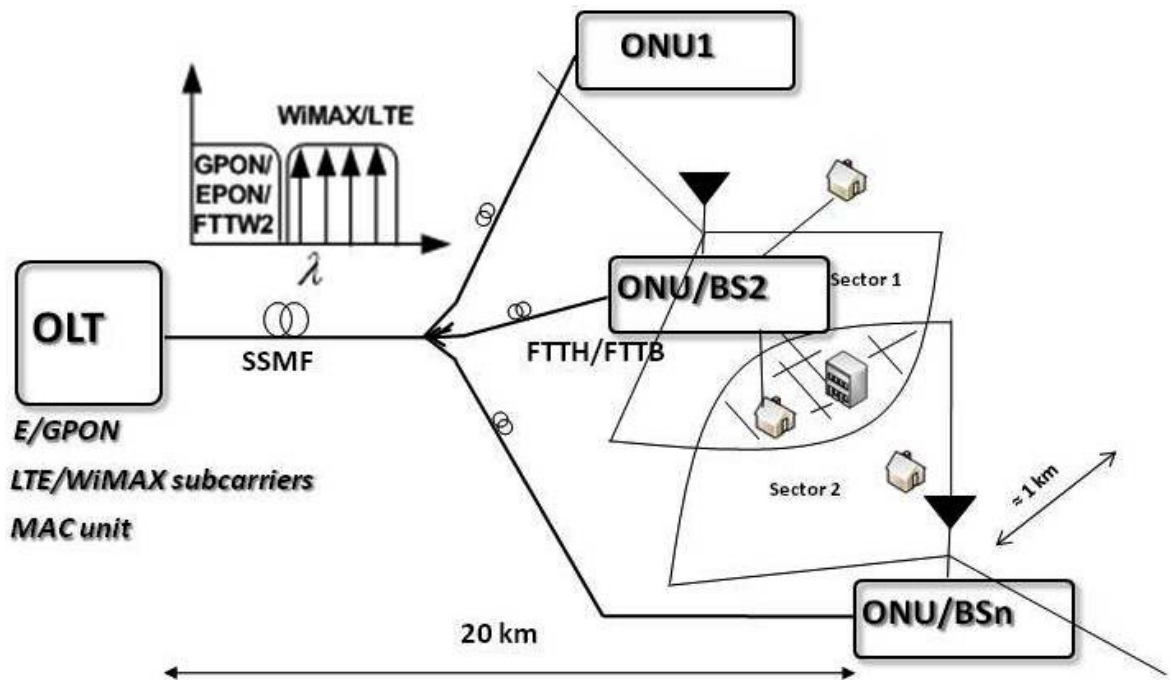
Figure 4-1: FDM approach for the proposed optical/wireless integration

The topology consists of one OLT located at the CO and several ONU/BSs located either at the user premises or at remote antenna posts which will be used for providing connectivity to mobile terminals. One single feeder optical fibre from the OLT is used to carry all upstream and downstream signals up to a passive splitter which broadcasts them to multiple network segments.

Inside the OLT, multiple RF broadband wireless channels are frequency multiplexed in a given spectral window, avoiding interference with legacy PONs in downstream. The combined

spectrum is then modulated onto an optical carrier and broadcasted to each remote ONU/BS. This approach provides for transparency to any wireless signal formats as radio frequency sub-carriers are transmitted over the optical fibre completely independent to xPON functionalities. The remote base station solutions are therefore simplified since all the wireless processing and subcarrier allocation are performed centrally at the OLT. Consequently, densely populated base stations could be deployed providing for high spectral efficiency across an area as well as increased frequency reuse pattern.

To that extent, the OLT manages the assignment of traffic to a large number of sub-carriers which travel all along the optical distribution network (ODN), to be de-multiplexed only at the user side and vice versa. Therefore, the CO can generally be thought of as a PON OLT but combining the additional functionalities of a wireless base transceiver station (BTS).

In addition, upstream transmission could be either based on a TDMA approach, as in standard xPONs and shown in the current architecture, or dedicated wavelengths could be assigned to each ONU/BS to avoid optical beat interference and further reduce deployment cost as sub-carrier multiplexing is not required.

Finally, since RoF could impose various impairments on the standard wireless signal formats further investigations would be required to examine the efficiency of the network with regards to signal routing.

4.2 WiMAX Specifications and Requirements

To support mobility, the air interface management must adequately be able to react quickly to changing signal conditions and it also must hand over a connection between base stations when the user is moving. For battery-driven devices, the air interface had to be optimized to be as power-efficient as possible during times when no data is being transferred. To that extent, the WiMAX air interface was enhanced to allow higher transmission speeds. Significantly, as mentioned in the previous chapter, the signal transmission is based on OFDM technology [4-6] making the network robust to high delay spreads of the wireless channel.

WiMAX can be implemented as fixed or mobile scenario. Regarding mobile WiMAX the standard supports FDM and TDM multiplexing scheme, although initial deployments will only make use of the TDM option [6]. The table below includes relevant physical parameters of mobile WiMAX. Various channel bandwidths are supported depending on the regulatory issues for certain deployment scenarios as detailed in chapter 2.

Table 4-1: Mobile WiMAX parameters [7, 8]

Parameter	Value
Chanel Bandwidth	1.25 MHz, 2.5 MHz, 5 MHz, 10 MHz, 20 MHz.
FFT size	Typical: 1024
Number of Antennas	Tx: 1, 2, 4 Rx: 1, 2, 4
Multiple Access Technology	DL: OFDMA UL: OFDMA
Modulation Schemes	QPSK, 16QAM, 64QAM
Maximum BS output power	Not standardised. According to local regulations. Assumptions: 5MHz: 43 dBm 10 MHz: 46 dBm 20 MHz: 49 dBm
Maximum EVM	64QAM: < -30 dB

In addition, Figure 4-2 shows the structure of a WiMAX frame (TDM) in more detail. In general this WiMAX TDM frame has duration of 5 ms. The downlink sub-frame starts with the preamble. It helps the mobile users to identify the cell and to roughly synchronize to the frame timing [6]. Then the frame control elements are placed (FCH, downlink MAP and uplink MAP). The FCH is the first element to be decoded by a mobile. It carries the length of and the coding scheme used by the MAPs. They contain information elements regarding the placement of the user data, the modulation and coding schemes and the zone switches. The FCH and the MAPs are to be decoded by all users. The first zone within the downlink sub-frames must be in partially used subcarrier (PUSC) mode [6]. The rest of the sub-frame is dedicated to the transport of the user data.

71
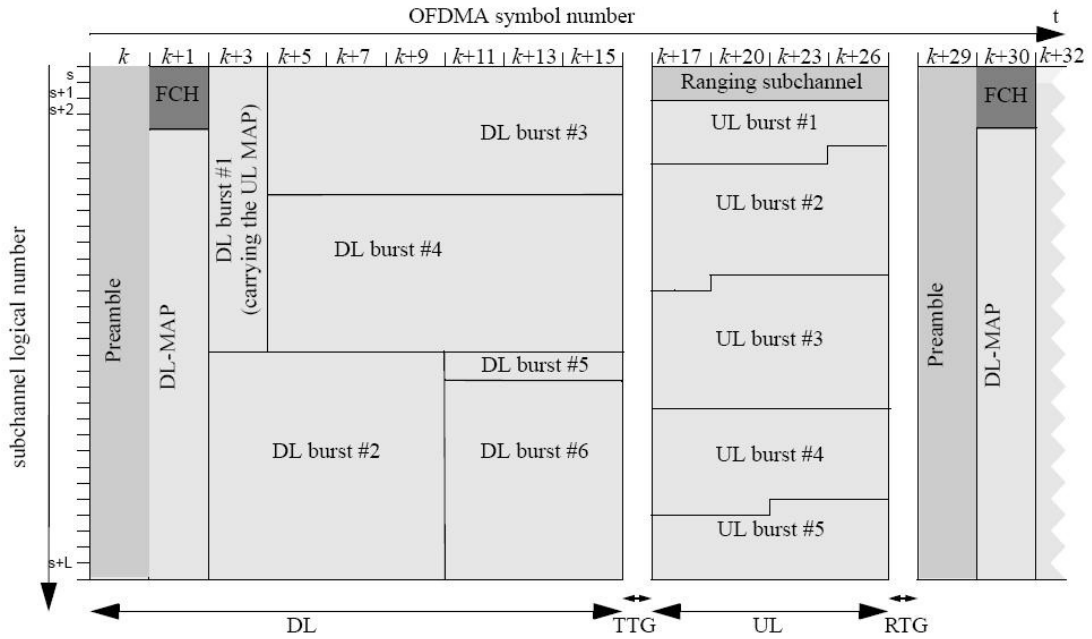
Figure 4-2: Example of a mobile WiMAX OFDMA frame [6]

In downlink QPSK, 16QAM and 64 QAM can be used (as shown in Table 4-1), in uplink only

QPSK and 16QAM are available to modulate the subcarriers. For the sake of channel estimation

and synchronization, pilots are placed regularly within the sub-frames (the actual placements

depend on the applied allocation scheme [6]). To ensure multipath robustness a CP is added to

every OFDM symbol.

The main PHY difference between the mobile and fixed WiMAX standards is that in the latter

the subcarrier spacing is fixed and is typically 256. Also, mobile WiMAX data transmissions to

individual users can be multiplexed in both time and frequency, due to the much higher number

of available sub-channels. For this reason, this form of data transmission is referred to as

OFDMA.

Taking into account all of the above and due to the high resemblance among the modulation

techniques used in both IEEE802.16d [4] and IEEE802.16e [6] standards, the feasibility

investigations to be conducted will be based on fixed WiMAX. This would be sufficient to

demonstrate optical network transparency to wireless signals delivered to remote base station antennas and wireless users bidirectionally.

4.3 VPI/MATLAB Elements for the WiMAX Transceiver

To initially establish accurate WiMAX signal routing over the xPON, the OFDM transmitter and receiver are devised in VPI in co-simulation with MATLAB utilising the functional blocks outlined in the previous chapter.

Figure 4-3 displays the OFDM transmitter with the pseudo random binary sequence (PRBS) fed from VPI to the input MATLAB interface (i.e. OFDM coding block).
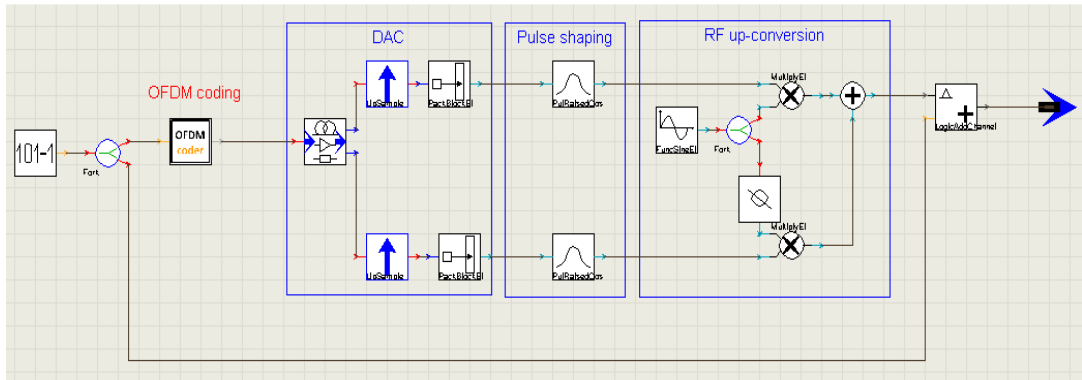
Figure 4-3: VPI/MATLAB components of the OFDM transmitter

Inside the OFDM coder, symbol mapping, IFFT and cyclic prefix are performed using MATLAB and the resulting output is passed to VPI for further processing (i.e. SER and EVM estimation). The MATLAB interface configuration is given in Figure 4-4.
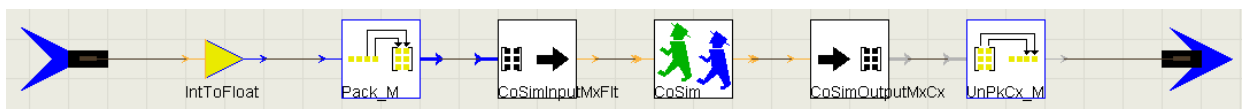
Figure 4-4: MATLAB interface for OFDM transmitter

In order to transfer the correct number of samples to the CoSim interface the PRBS sequence from VPI is initially packed into a matrix form containing Nbits=BitRate x TimeWindow number of samples, where the TimeWindow parameter represents the duration of simulation [9]. Consequently, the total number of symbols simulated (i.e. Nsymbols=N/BitsPerSymbol) is determined by this parameter.

The input bit stream is then passed to MATLAB and symbol mapping is performed by the ***cod*** function described in Appendix A. The Appendix A provides detail simulation coding and corresponding functions for the OFDM transmitter and receiver.

Furthermore, this is followed with the conversion of frequency domain symbols to time domain by performing 256 point IFFT. The 1/4 cyclic prefix, using matrix concatenation, is also added.

Once all symbols have been formed, the output matrix variable is passed to the VPI for digital to analog conversion and signal shaping. The digital to analog conversion is achieved by initially normalising the symbol amplitudes, followed by quantisation as shown in Figure 4-5 [9]. The maximum number of quantisation levels considered in the simulations, as stated before, is 14 [4].
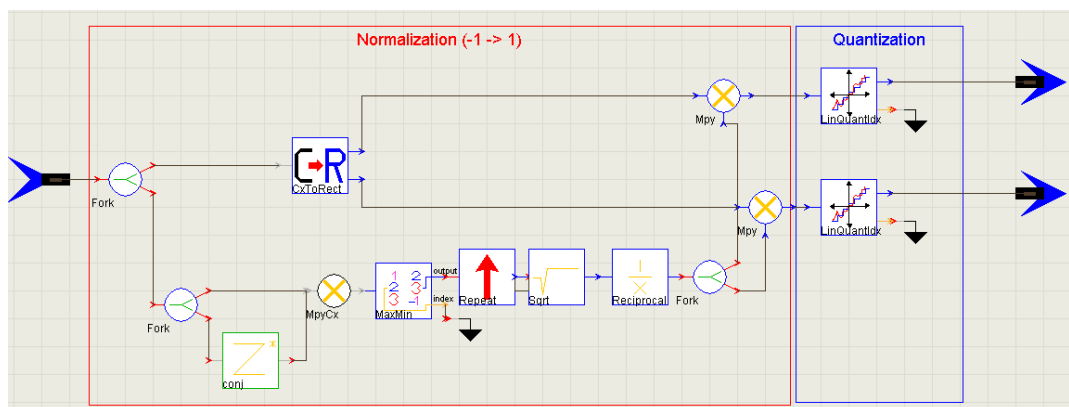
Figure 4-5: Quantisation process

Finally, square root-raised-cosine filters with a roll of factor of 0.25 [4], shown previously in Figure 4-3, were used for the I and Q channels to shape the signals and minimise inter symbol interference (ISI) prior to RF up-conversion. The bandwidth of these filters is equivalent to the OFDM symbol duration defined as its bit rate divided by the number of bits per symbol.

For OFDM reception, the incoming signal is first down-converted and subsequently applied to an ISI shaping filter, using the same parameters with the one used at the transmitter. The receiver design is shown in Figure 4-6.
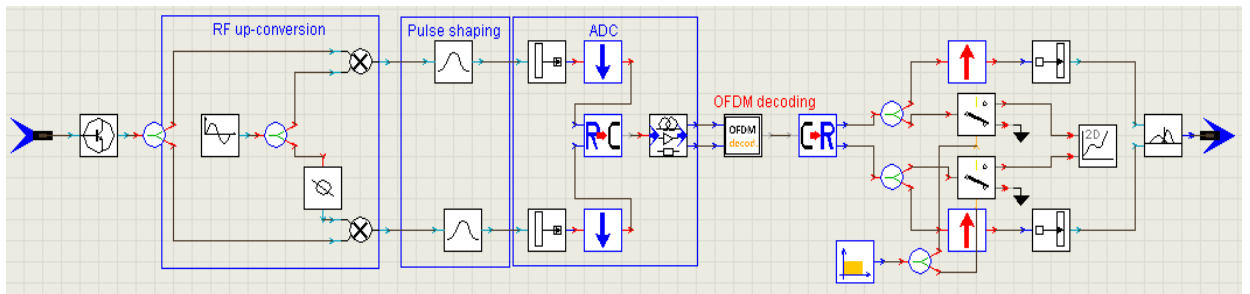
Figure 4-6: OFDM receiver VPI/MATLAB components

The resulting I and Q channels are then quantised and passed to a MATLAB simulator for further processing using the CoSim interface described in Figure 4-7.
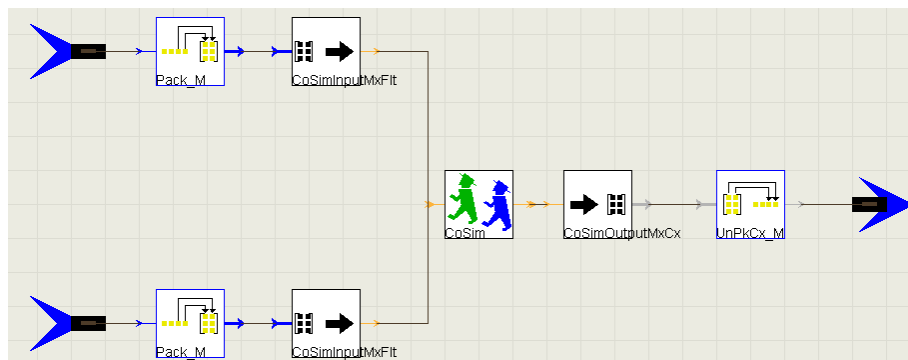
Figure 4-7: MATLAB interface for OFDM receiver

The CoSim interface in the receiver operates in a similar manner to the transmitter interface, except this time the I and Q channels are fed separately to MATLAB with the input matrix size equal to the total number of symbols as defined in eq. 4.1.

$$TotalNumSymbols = \frac{BitRate \times TimeWindow}{BitsPerSymbol} \tag{4.1}$$

The transmission evaluation of the OFDM symbols over the multi-path channel is then performed using the MATLAB function described in Appendix A. The application of ISI, to model the effect of different cycle prefixes, is achieved by introducing random OFDM symbols (*SymbolTx = [NextSymbol NextSymbol Frame])* to the transmitted symbols before filtering.

Finally, to obtain the original QAM symbols, FFT processing and cyclic removal are then performed by what is identified as the *receiver* function. This also includes the *equalization* function used to compensate for multi-path channel distortion of the resulting QAM symbols prior to EVM and SER estimations performed in VPI.

4.3.1 High Power Amplifier (HPA)

Equally important, the additive distortion of the high power amplifier (HPA) on the transmitted WiMAX signals had to be precisely modelled in VPI for accurate network operation. This is displayed in Figure 4-8.

A limiter block is used for representing nonlinear transfer function characteristics exhibiting amplitude clipping and consequently distorting transmitted signal to noise ratio. This is then filtered to avoid excessive leakage of unwanted components to adjacent channels. The required transmitted EVM, as defined by the standard [4], could be adjusted based on setting the maximum and minimum amplitudes of the limiter block.

Figure 4-8: High power amplifier (HPA) modelling

To that extent, limiter amplitudes of 0.68V and -0.68V were required to achieve -31dB EVM figures, the maximum allowed for 64-QAM modulation in WiMAX [4]. This estimation is performed based on back-to-back transmission of the OFDM signal in the absence of the wireless channel. The obtained spectrum at the output of the amplifier is shown in Figure 4-9 clearly demonstrating the HPA signal distortion corresponding to a maximum achievable SNR of 31 dB [2].
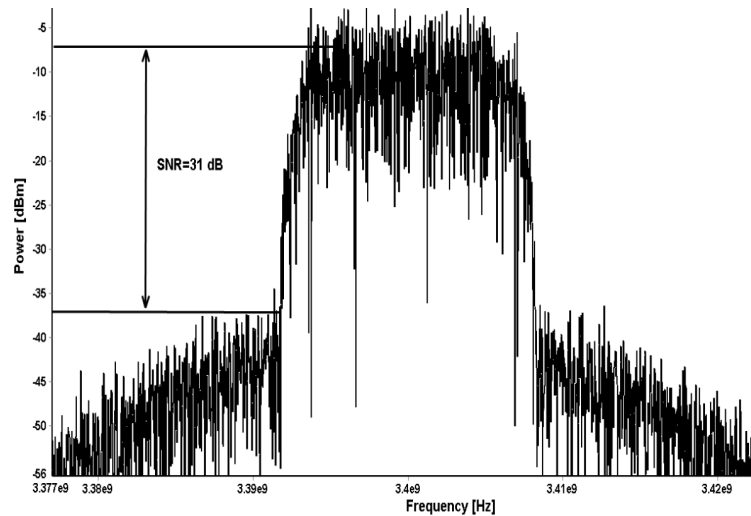
Figure 4-9: Output spectrum from HPA

4.4 Wireless Channel Modelling

Accurate implementation of the wireless channel is fundamental in evaluating wireless propagation. Parameters that affect signal transmission across the air are typically the path loss and multipath delay spread. Therefore, the model must be carefully designed to account for these parameters if it was to implement realistic network scenarios. There are various established models for evaluating the performance of wireless channels for fixed application, each designed for different scenarios and operational frequencies.

The most widely used sub-urban model for signal strength prediction and simulation in macro-cellular environments is the Hata-Okumura model [10]. This model applies only to frequencies

between 500 – 1500 MHz with possible extension up to 2 GHz [10]. However, 4G wireless networks are expected to operate in frequency ranges above 2 GHz. For application over urban environments the Cost 231 Walfish-Ikegami (W-I) model [11, 12] could have been alternatively considered but is also limited to maximum frequencies of 1.9 GHz.

To that effect, an empirical based path loss model has been utilized that in view of appropriate frequency correction factors has successfully addressed the baud requirements of the intended specification channels [13]. The model parameters, presented in Appendix B, have been extensively used to calculate the appropriate wireless channel path losses of the simulation models presented particularly in chapter 6.

In addition to path loss, wireless channels display multipath delay and fading profiles due to signal scattering. As a result, a complementary model had to be implemented. This is described in the following section and has been widely used for emulating the wireless channel in fixed radio applications, such as in IEEE802.16d.

4.4.1 Stanford University Interim (SUI) Channels for WiMAX

A set of 6 typical channels was selected for the three terrain types that are typical at continental USA [14]. These models can be used for simulations, design, development and testing of technologies suitable for fixed broadband wireless applications as considered in this project.

The typical SUI1-6 channel characteristics are summarized in the following tables. The distinctive A, B and C terrain type coefficient values used in path loss calculations are given in Appendix B.

Table 4-2: SUI channels with different terrain types [14]

Terrain Type	SUI channels
C	SUI-1, SUI-2
B	SUI-3, SUI-4
A	SUI-5, SUI-6

Table 4-3: SUI channels delay spread definitions [14]

Doppler	Low Delay Spread	Moderate Delay Spread	High Delay Spread
Low	SUI-3		SUI-5
High		SUI-4	SUI-6

As already mentioned six SUI channels are defined to represent closely practical implementations with the specifications given below [14]:

- Cells are < 10 km in radius, variety of terrain and tree density types

- BTS antenna beamwidth: 120°

- Receive Antenna Beamwidth: omnidirectional (360°) and 30°. For a 30° antenna beamwidth, two times smaller RMS delay spread is used when compared to an omnidirectional antenna RMS delay spread. Consequently, the 2nd tap power is attenuated by additional 6 dB and the 3rd tap power is attenuated by extra 12 dB (effect of antenna pattern and delays remain the same). For the omnidirectional receive antenna case, the tap delays and powers are consistent with the COST 207 delay profile models [18].

4.4.2 MATLAB Modelling

In order to establish accurate signal routing to and from an end user over combined optical and wireless channel links, a moderate delay spread SUI-4 model is sufficiently employed. Higher delay spread channels, such as SUI-6, could also be considered however, due to the exclusion of

any wireless channel coding, to represent the worst case scenario, more errors would be expected limiting the accurate estimation of the system performance. The maximum of three paths were included where a K of zero for all paths demonstrates non-line-of-sight wireless link between the transmitter and the receiver. Finally, the channel imposes maximum delay and attenuation of 4 µs and 20 dB respectively on the received signal (zeros for the Tap 1 represent that no additional penalties to the original propagation delay and attenuation of this path are introduced).

Table 4-4: Standardised SUI-4 multipath channel parameters for IEEE802.16d [14]

SUI-4 Channel Model			
	Tap 1	**Tap 2**	**Tap 3**
Delay (µs)	0	1.5	4
Power (dB) for 30º ant.	0	-10	-20
K factor for 30º ant.	0	0	0

The complete simulation code for the wireless channel, developed in MATLAB, is as described in Appendix A. The *channelSUI* function generates the output channel coefficients according to the specified bandwidth, cyclic prefix and SUI type.

The OFDM symbol duration is initially calculated as given in [4]. The symbol duration is used for variance calculations by the *CIRpowers* function that calculates variance for each path of the channel.

Finally, once the variance for each path has been calculated the *genh* function is then used to generate the Rayleigh channel coefficients according to the specific SUI type. This is achieved by utilising the Jakes Model [15] to add sinusoids for generating the fading coefficients.

4.5 FDM Subcarrier Spacing Evaluation

Taking into consideration the developed models, in order to exhibit the network feasibility, and constitute the FDM architecture as a viable solution for the transparent transmission of WiMAX over PONs, transmission measurements were initially focused in downstream. Since IMDs, resulting from nonlinearities in the optical link, could degrade the performance of FDM subcarriers, the application of direct and external laser modulation was first examined. Simple frequency up and down-conversion of the WiMAX channels and their transmission over the fibre was evaluated. In upstream, TDMA operation is assumed (as detailed in chapter 5) therefore not requiring the application of FDM.

Five distinct WiMAX channels at 3.5 GHz are generated in the OLT, with frequency reuse of one for each base station, and shifted to address five ONU/BSs. The spacing of the five FDM subcarriers is varied in order to measure IMDs at an ONU/BS. To avoid the interference with G/EPON baseband spectrum the first subcarrier in the FDM window was set at 4 GHz.

The IEEE802.16d WiMAX channels, modelled in MATLAB, comprised of 64-QAM, 256-OFDM modulation with maximum data rate of 70 Mbit/s per channel and relative constellation error (RCE) of -38 dB [4].

The combined FDM subcarriers were initially used to directly modulate commercially available distributed feedback (DFB) lasers at 1490 nm [16] and then applied over an AWG, supplying the fibre with +3 dBm power [16]. To implement an alternative scenario MZM was used to modulate the distributed feedback (DFB) lasers externally, with the FDM subcarriers applied at the modulator's RF input. The laser output power was set to account for various optical component losses, resulting in +3 dBm power launched into the fibre.

At each ONU/BS, the received optical signal is detected by an avalanche photodetector (APD) followed by RF subcarrier down-conversion to result to the transmitted WiMAX channels. To account for 1:16 splitter losses, a 14 dB optical attenuator is used after the fibre.

Performance evaluation measures included EVM estimations at each ONU/BS1 remote antenna input as well as spurious free dynamic range (SFDR) graphs for various FDM subcarriers spacings. The 3rd order IMD products for direct and external modulation are modelled by either increasing the modulation index of the DFB laser or the modulation power inside the MZM RF input respectively.

4.5.1 EVM and SFDR with DML

As shown in Figure 4-10 (left), direct modulation of the five frequency shifted WiMAX channels, has produced an EVM versus laser modulation index figure higher than -31 dB, as required by the WiMAX standard for 64-QAM modulation [4]. This characteristic was drawn for various subcarrier spacing including 50, 100 and 300 MHz. In particularly the -31 dB EVM has been achieve at modulation indexes in the range of 0.8-0.9 for all subcarrier spacing.
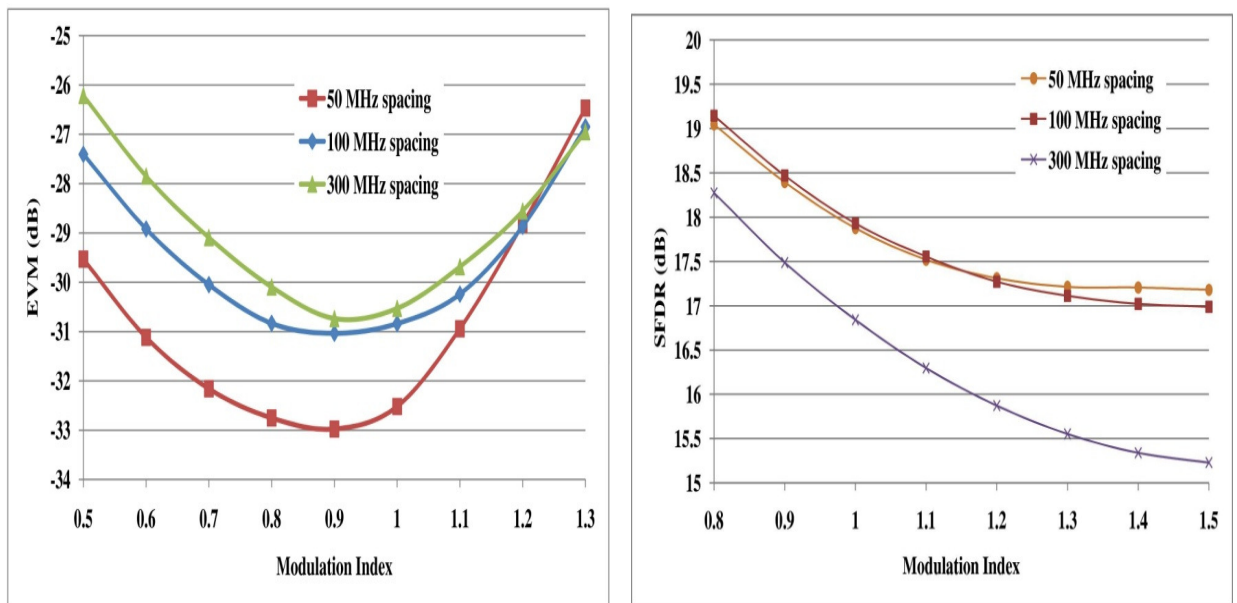
Figure 4-10: EVM (left) and SFDR (right) estimation for DML

In addition, the SFDR plot has displayed maximum dynamic range of 19 dB, with respect to the central FDM subcarrier at 3.5 GHz, for 50 MHz and 100 MHz subcarrier spacing at 0.8 modulation index, as shown in Figure 4-10 (right). As the channel spacing is increased from 100 MHz to 300 MHz, the SFDR is reduced as expected due to the higher level of 3rd order IMD products, interacting with the desired channels. However, even at the highest assumed channel spacing of 300 MHz, an EVM of -31 dB could still be achieved. Since direct modulation (DML) could limit the maximum number of allowed FDM subcarriers, due to SFDR, a chirpless option, produced by externally modulating the DFB lasers, was also investigated.

4.5.2 EVM and SFDR with MZM

To determine compliance with the WiMAX standard requirements at an ONU/BS1 antenna input, EVM characteristics as a function of the MZM RF drive power in the OLT was measured for four different subcarriers spacings. This time higher spacing of 50, 200, 500 MHz and 1GHz was considered, allowing for increased modulation bandwidths, as the MZM is expected to provide for higher dynamic range. To that extent, obtained EVM figures, shown in Figure 4-11 (left), have displayed EVMs greater than -38 dB for all subcarrier spacings at +6 dBm RF drive power into the MZM.
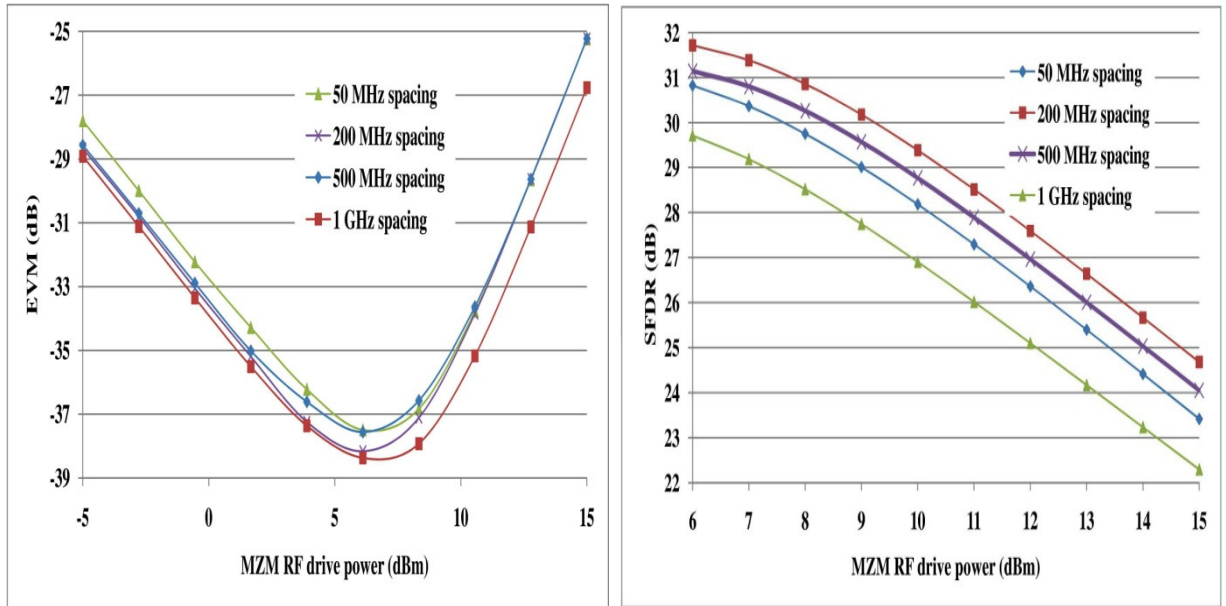
Figure 4-11: EVM (left) and SFDR (right) estimation for MZM

The obtained SFDR figure at these conditions is shown in Figure 4-11 (right). A value higher than 30 dB has been demonstrated compared to a maximum of 19 dB recorded with DML. This is expected since the MZM is biased at the quadrature point of the modulator's optical power versus voltage transfer function, cancelling all even-order distortion products [17]. As the RF drive power is increased, the power of IMD products becomes significant, reducing the network dynamic range. Significantly, the RF subcarriers from the OLT can occupy much wider bandwidth therefore enhancing the network scalability compared to DML. The MZM modulator in the OLT is typically shared by a large number of users minimizing the overall component cost.

4.6 Summary

This chapter presented an integrated access network architecture based on RoF to demonstrate interoperability among TDM-PON infrastructures and WiMAX signal propagation through the application of FDM.

To that extent, VPI/MATLAB building blocks for the WiMAX OFDM transceivers are established. Typical fixed WiMAX parameters in MATLAB are assumed generating an OFDM output that is fed to a VPI platform prior to transmission over the PON. For wireless transmission, a SUI wireless channel model is presented, evaluating practical multi-path radio signal transmission followed by BER estimation for various cycle prefixes.

This chapter went on assembling the VPI and MATLAB blocks to model a hybrid wireless/optical network. The optical network transparency to WiMAX channels has been demonstrated through the obtained EVM characteristics, reporting figures higher than -31 dB for 64-QAM FDM WiMAX channels for various subcarrier spacings at both direct and external laser modulation. The physical layer simulation test-bed consisted of five up-converted WiMAX channels transmitted downstream over 20km of optical fibre.

Finally, it has been shown that even at the maximum considered 1 GHz channel spacing, in the presence of external modulation, transparent WiMAX transmission could still be achieved. The equivalent figure with DML was 300 MHz spacing confirming the expected superiority of external modulation schemes. Also, a higher dynamic range of 30 dB has been measured in view of external modulation in relation to 19 dB obtained with DML allowing for increased modulation bandwidths. Taking into consideration that the MZM modulator is based in the OLT and shared by large number of users, it can also comply with the network cost requirements.

References

[1] C. Lim, A. Nirmalathas, M. Bakaul, P. Gamage, K.-L. Lee, Y. Yang, D. Novak, and R. Waterhouse, "Fiber-Wireless Networks and Subsystem Technologies," *J. Lightw. Technol.*, vol. 28, pp. 390-405, (2010).

[2] H. Kim, J. H. Cho, S. Kim, K. U. Song, H. Lee, J. Lee, B. Kim, Y. Oh, J. Lee, and S. Hwang, "Radio-Over-Fiber System for TDD-Based OFDMA Wireless Communication Systems," *J. Lightw. Technol.*, vol. 25, pp. 3419-3427, (2007).

[3] C. Bock, T. Quinlan, M. P. Thakur, and S. D. Walker, "Integrated Optical Wireless Access: Advanced topologies for future access networks," presented at ICTON '09. 11th International Conference on Transparent Optical Networks, 2009.

[4] "IEEE Standard for Local and Metropolitan Area Networks Part 16: Air Interface for Fixed Broadband Wireless Access Systems," *IEEE Std 802.16-2004 (Revision of IEEE Std 802.16-2001)*, pp. 0_1-857, (2004).

[5] *Technica Specification Group Services and Systems Aspects, Service Aspects: Services and Services Capabilities*, 3GPP TS 22.105 V 6.2.0, 2003

[6] "IEEE Standard for Local and metropolitan area networks Part 16: Air Interface for Fixed and Mobile Broadband Wireless Access Systems Amendment 2: Physical and Medium Access Control Layers for Combined Fixed and Mobile Operation in Licensed Bands and Corrigendum 1," *IEEE Std 802.16e-2005 and IEEE Std 802.16-2004/Cor 1-2005 (Amendment and Corrigendum to IEEE Std 802.16-2004)*, pp. 0_1-822, (2006).

[7] *WiMAX forum* (Online). Available: http://www.wimaxforum.org/home/

[8] *Fibre-Optic Networks for Distributed Extendible Heterogeneous Radio Architectures and Service Provisioning (FUTON)* (Online). Available: http://www.ict-futon.eu

[9] *VPI reference manual (VCSEL operation)* (Online). Available: http://www.vpiphotonics.com

[10] *Urban transmission loss models for mobile radio in the 900- and 1800- MHz bands (Revision 2)*, COST 231 TD (90) 119 Rev 2, 1991

[11] M. S. Smith and C. Tappenden, "Additional enhancements to interim channel models for G2 MMDS fixed wireless applications," in *IEEE 802.16.3c-00/53*.

[12] M. S. Smith and J. E. J. Dalley, "A new methodology for deriving path loss models from cellular drive test data," presented at Proceedings of AP2000 Conference, 2000.

[13] V. Erceg, L. J. Greenstein, S. Y. Tjandra, S. R. Parkoff, A. Gupta, B. Kulic, A. A. Julius, and R. Bianchi, "An empirically based path loss model for wireless channels in suburban environments," *J. Select. Areas Commun.*, vol. 17, pp. 1205-1211, (1999).

[14] *IEEE 802.16 Broadband Wireless Access Working Group* (Online). Available: http://ieee802.org/16

[15] J. G. Proakis, *Digital Communications*, Fourth ed, 2001.

[16] *Gigabit-capable passive optical networks (G-PON): Physical Media Dependent (PMD) layer specification*, ITU-T G.984.2:, 2003

[17] C. H. Cox, III, E. I. Ackerman, G. E. Betts, and J. L. Prince, "Limits on the performance of RF-over-fiber links and their impact on device design," *IEEE Transact. Microw. Theo. Techniq.* , vol. 54, pp. 906-920, (2006).

Chapter 5

Interoperability of xPON and WiMAX

Contents

This chapter evaluates the routing performance of the proposed network by means of WiMAX channel transmission over a PON infrastructure. To that extent, centralised WiMAX, utilising FDM to address multiple ONU/BSs, is displayed. Subsequently, network transmission performance figures are presented at the ONU/BS antennas and at radio receivers mainly in terms of EVMs and bit error rates (BERs) respectively.

5.1 Simulated RoF Access Network Architecture

The focus of the work conducted in this chapter is to capture the merits of PONs and wireless interoperability in a new access network architecture [1] in terms of efficient bandwidth on-demand provisioning and simple radio base stations. This is achieved by the application of centralised control in the OLT and time division multiplexing for upstream transmission enabling efficient dynamic bandwidth allocation for wireless users on a single wavelength as well as minimised optical beat interference at the optical receiver. Hence the network is able to

manage resources across multiple ONU/BSs from the OLT according to traffic penetration and

requirement in bandwidth. This chapter presents a complete transparent optical/wireless access

network architecture based on RoF and FDM.
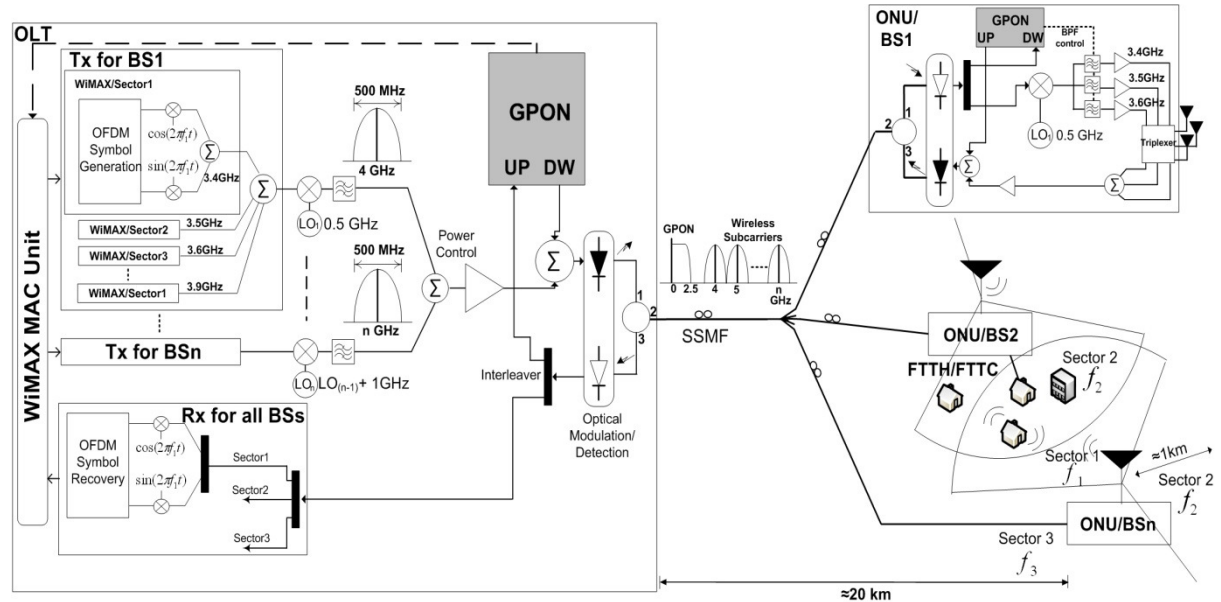
Figure 5-1: WiMAX over xPON architectural platform

The network architecture, depicted in Figure 5-1 [1], consists of a standard GPON with novel

wireless-enabled OLT and ONUs. As outlined in the previous chapter, the ONU/BSs are

relatively simple in their design since they are only responsible for down-conversion and

filtering of the received downstream radio channels. Each WiMAX transmitter at the OLT is

serving a single radio cell at an ONU/BS that is divided into small parts called sectors,

operating on the same or different frequencies, in order to make the cell more efficient in terms

of reduced co-channel interference and increased capacity. In some current deployment

scenarios all sectors are operating on the same frequency to reduce the cost of BSs, however in

the novel proposed architecture frequency reuse patterns of higher order could be considered

due to the deployment cost reduction enabled by the centralised processing in the OLT.

A different RF subcarrier was dedicated to each ONU/BS in downstream to enable concurrent transmission of multiple WiMAX channels to each ONU antenna. Within the OLT, standard microwave OFDM WiMAX symbols [2], generated by Transmitter (Tx) for BS_n, for different sectors in each ONU/BS were up-converted to the predetermined RF subcarriers spectrum before they were combined with the packets for wired users and subsequently modulated onto the optical carrier for 20 km fibre downstream transmission.

Figure 5-2 illustrates how this technique addresses each individual ONU/BS. The microwave RF wireless channels are shifted in frequency using a predetermined LO and BPFs in the OLT prior to being combined and modulated onto an optical carrier. At an ONU/BS a single LO is only required operating on the same frequency for the specific ONU/BS to downshift the WiMAX channels. Multiple band pass filters (BPFs) are needed to select each channel prior to transmission over the air. This approach would significantly simplify the BS design, compared to traditional base-band or IF FDM over fibre approaches [3]. This is expected since only a single LO and multiple electrical filters required. The LO leakage and higher order IMDs of the non-linear mixer inside the OLT and ONU/BSs will not degrade the system performance since in the deployed scenario the unwanted products fall outside the band of interest and are filtered by the BPF.
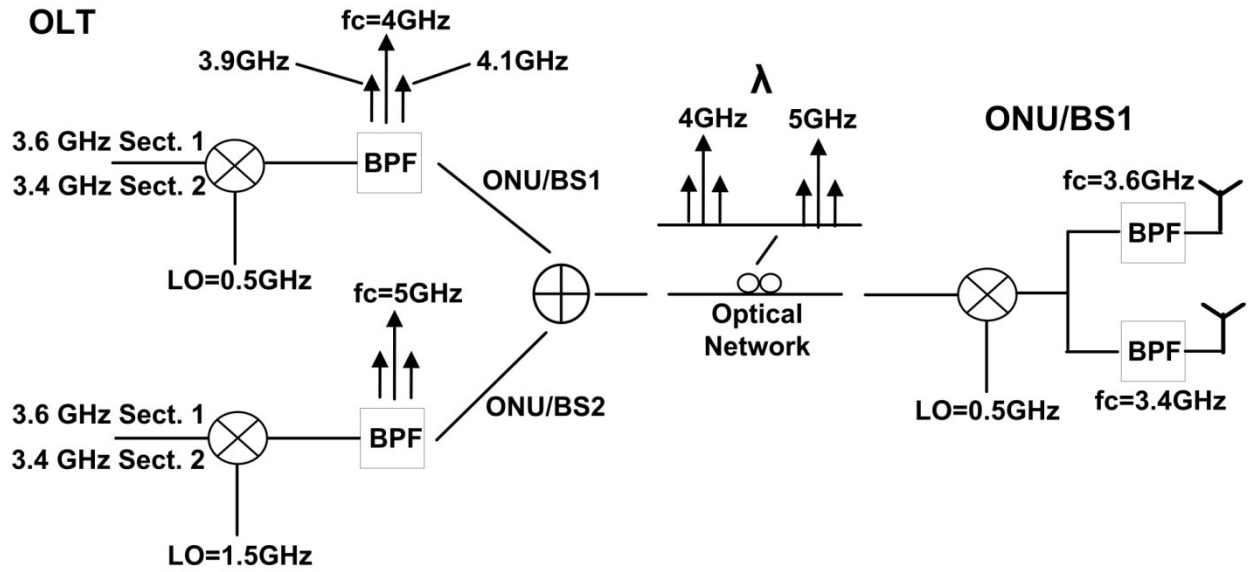
Figure 5-2: FDM approach in the proposed architecture

To ensure minimum interference with the GPON baseband spectrum, individual RF subcarriers centred at 4 GHz and above, are utilised as indicated in Figure 5-1. A 1 GHz spacing between the centre RF subcarriers was considered in order to reduce the electrical filter design complexity in the OLT and consequently minimise the possible subcarrier interference due to inter-modulation products created by an optical modulator [4]. Significantly, in case the total bandwidth demand across a wireless cell cannot be met by a given ONU/BS, an additional channel can then be provided to a sector in downstream, e.g. 3.9 GHz for Sector 1 of Tx for BS1as shown in Figure 5-1, still on a single wavelength. A 500 MHz wide BPF was designed to accommodate the transmission of all required channels. The bandwidth of the filter can be varied depending on the maximum number of supported ONU/BSs. The total number of different WiMAX channels needed from the OLT was determined by a frequency reuse plan for a designed deployment scenario. According to this, three radio sectors per antenna, each operating at different frequencies, 1:3:3 reuse factor, requiring a minimum of three WiMAX channels per ONU/BS antenna plus additional channels for on-demand bandwidth provisioning were designed. After the up-converted WiMAX channels were combined with the GPON user

data [5], they were then broadcasted to all ONU/BSs on the same optical carrier in downstream. In practical deployment scenarios these WiMAX channels could be leased to a single or multiple operators by means of dedicated ONU/BSs.

At an ONU/BS, shown in Figure 5-1, the combined signals were initially demultiplexed into two components: a baseband GPON signal and the up-converted WiMAX channels. The baseband signal is sequentially forwarded to the GPON downlink (DW) port for further processing while the microwave channels were down-converted by a mixer using the same LO frequency as in the OLT. The BPFs select the required WiMAX channel prior to signal transmission for wireless users across a sector. In order to support additional channel drop to a sector, either tuneable or an array of BPFs should be used. Based on information in the OLT downstream frame, the centre frequency of the filters can be controlled by a system-on-chip platform already available in a GPON processing module. In addition, to reduce the count of BPFs required in an ONU/BS, a single filter can be potentially shared by multiple WiMAX channels by assigning different transmission time-slots for each filter managed from the GPON processor.

The key feature of the proposed architecture is the centralised control and management, compared to the distributed approach in a traditional WiMAX deployment, allowing for the creation of overlapping cells, e.g. between Sector 2 and Sector 1 of ONU/BS2 and ONU/BSn respectively in Figure 5-1, operating at different frequency channels. Further analysis on this concept will be included in chapter 6. As a result, users that are in the overlapping regions can have simultaneous wireless support from multiple ONU/BSs, thus increasing the capacity of the WiMAX network and providing redundancy in case of fibre failure between a distribution node and an ONU due to established alternative routes for signal transmission. Since different ONU/BSs are operating on different radio channels no interference would be expected between

overlapping wireless users and thus maintaining their network capacity. Additionally, in case of fibre failure between a distribution node and an ONU only a single wireless channel could be available in an overlapping region resulting in lower data rate availability per user. This has been accounted for in the proposed architecture by the capability of utilising additional wireless channels to failing ONU/BSs. It is also important to mention, however, that the two overlapping cells could operate on the same frequency with the application of spatial multiplexing, controlled from the OLT, currently defined as a prerequisite in next generation wireless standards [6].

Another significant characteristic of the architecture due to the centralised control mechanism and the application of FDM is the efficiency by which multiple channels are allocated per wireless sector, allowing for on-demand bandwidth allocation across a sector. In contrast in traditional WiMAX deployment the base stations are independent and dynamic bandwidth allocation cannot be efficiently provided.

An additional feature of the architecture lies in the upstream where wired and wireless users share a single optical carrier in the time domain resulting in optical signals from all ONU/BSs arriving at different times at the OLT. The overall network upstream transmission would be governed by TDMA to conform to the GPON standard, defining each ONU transmission window to approximately 150 µs [7]. These transmission window slots would be used by the WiMAX MAC unit in the OLT to schedule the transmitting upstream wireless channels, interleaved inside each WiMAX uplink map. Due to the synchronization of the former with the latter no buffering would be introduced in the ONU or OLT. In addition, since encapsulation of WiMAX packets into GPON frames is avoided no modifications in the WiMAX frame format would be required. Therefore, the overall network delay and throughput performance will conform to the GPON delay and throughput figures and will depend on the TDMA-PON

upstream polling cycles [8, 9]. Based on this approach the optical beat interference at the OLT receiver is minimised while a single photoreceiver and WiMAX demodulator is only needed reducing the overall design complexity of the OLT. Also, enabled by the use of time division multiplexing, upconversion to a RF subcarrier is not required, decreasing the BPF and mixer count at each ONU/BS as well as avoiding the generation of additional inter-modulation products at high frequencies due to laser chirp [10]. Wireless users from all sectors communicate directly to registered ONU/BSs via a microwave link that performs amplification of the received radio channels and transmit it together with GPON packets in assigned time-slots back to the OLT. Interference with the GPON spectrum is avoided since the WiMAX radio channels occupy the spectrum above 2.5 GHz. However, the application of TDMA in upstream could result in reduced throughput across a wireless sector therefore a multi-wavelength approach, is also implemented, as will be demonstrated in chapter 6, allowing for dedicated connection to each ONU/BS.

The maximum bandwidth distributed by an ONU/BS is determined by frequency regulation issues specified for a particular deployment scenario. However, as proposed wireless base stations are controlled centrally, small densely spaced cells can be provided supporting wide channel bandwidth with a maximum of 70 Mbit/s aggregate data capacity per channel downstream which is compatible with the WiMAX standard [2]. For higher data rate wireless service provisioning including HDTV and VoD, additional channels can be delivered efficiently to a sector to increase the cell capacity. It is anticipated that up to 50 users per ONU/BS radio sector can be supported, which is consistent with the recent research trend for future network capacity demand [11]. Finally, to further improve the spectrum efficiency and the maximum bandwidth supported across radio cells, smart antennas such as MIMO [12] or adaptive beam-forming techniques [13] could also be used at the ONU/BSs.

5.2 VPI Optical Network Elements

The physical layer network model and individual elements were devised using the VPI physical layer simulation platform enriched with MATLAB functionalities. Subsequently, the functional optical blocks and design parameters for the OLT, outside plant and ONU/BSs, as well as their corresponding modules are described, and successively evaluated independently and in the network as a whole. The WiMAX transmitters and receivers as well as multipath channels are implemented with MATLAB as described in chapter 4.

5.2.1 Optical Line Terminal

The OLT block diagram, shown in Figure 5-3 (left), is displayed in conjunction with its corresponding VPI model shown in Figure 5-3 (right). In downstream, analog modulation is realised by externally modulating a DFB laser module, by means of a standard MZM with WiMAX pass-band signals applied at the MZM's RF input. The low pass filter (LPF) before the MZM is utilised to model the bandwidth constrains associated with the modulator that are not accounted for in the standard VPI module. The RF power to the input of the MZM is controlled by the power control circuit by adjusting the gain of the electrical amplifier based on the specified modulation power. The output port of the MZM is connected to a 3-port optical circulator to allow bidirectional transmission prior to transmitting the signal over the fibre.

The circulator output upstream is directly applied to an APD following the electrical BPF to select the desired channel for the OFDM receiver. Consequently, the error-vector magnitudes and symbol error rates of the OFDM receiver are applied at the corresponding inputs of an XY-plot module y-axis, to display SER and EVM performance characteristics.
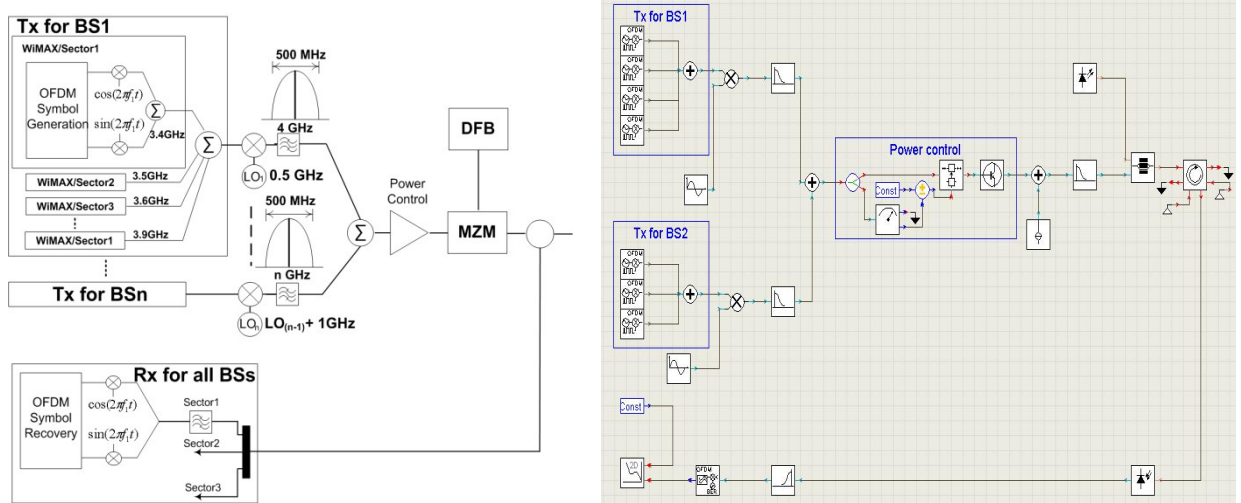
Figure 5-3: Optical line terminal modelling

The VPI Table 5-1 includes the modelling parameters of the externally modulated DFB laser module designed to operate for the wireless communication. As denoted in the table, the DFB laser emission parameters correspond to the emission frequency (wavelength), average emitted power level in milli-Watt units and the laser typical linewidth of 10 MHz [14]. The model accounts for temperature sensitivity of the laser as well as a side mode suppression ratio of 45 dB and relative intensity noise of -150 dB/Hz.

Table 5-1: CW laser modelling parameters

Parameter	Value	Unit
Emission Frequency	2.9979e8/1490e-9	Hz
Average Power	7	mW
Side Mode Separation	150	GHz
Side Mode Suppression Ration	45	dB
LineWidth	10	MHz
RIN	-150	dB/Hz

The MZM parameters are presented in Table 5-2 displaying an extinction ratio (ER) of 20 dB and a symmetry factor of -0.176, corresponding to an alpha factor of 0.7 to match typical specification of a commercially-available device [15].

Table 5-2: MZM modelling parameters

Parameter	Value	Unit
Extinction	20	dB
Symmetry Factor	-0.176	/
Chirp Sign	Positive	/

The VPI Table 5-3 includes the two modelling parameters used in the 3-port optical circulator. The insertion loss of the module is set to a typical 1 dB for clock-wise direction and rejection loss of typical 40 dB in the anti clock-wise direction [16], to prevent leakage of the transmitter downstream signal into the receiver path.

Table 5-3: Optical circulator modelling parameters

Parameter	Value	Unit
Insertion Loss	1	dB
Rejection	40	dB

Finally, Table 5-4 includes the modelling parameters of the optical receiver RX1, employing an APD. Initially, the responsivity and avalanche multiplication parameters were set according to a commercially-available JDSU ERM577 receiver [17]. To consider the worst case, the detector avalanche multiplication was set to 4. It is worth mentioning that the application of a PIN could also be considered, with bandwidths higher than 10 GHz, as it was experimentally demonstrated in Chapter 7.

Table 5-4: Optical receiver modelling parameters

Parameter	Value	Unit
Responsivity	0.7	A/W
Photo Diode Model	APD	/
Dark Current	10	nA
Avalanche Multiplication	4	/
Thermal Noise	10	$pA/(Hz)^{1/2}$
Shot Noise	ON	/

5.2.2 Optical Network Unit/Base Station

The ONU/BS diagram and the corresponding VPI model are specified in Figure 5-4. The design

consists of an APD and optical circulator of the same specification to their OLT counterparts.

The DFB parameters, based on a commercially available device [18] are given in Table 5-5.

Various parameters such as the carrier and photon lifetimes, laser chip length and differential

gain, to mention a few, can be adjusted until a fit is obtained [19, 20] with the performance

specified in the data sheet. The model does not take into account thermal effects, carrier leakage

and spatial-hole burning which are not considered limiting factor in RoF direct laser modulation

[21].
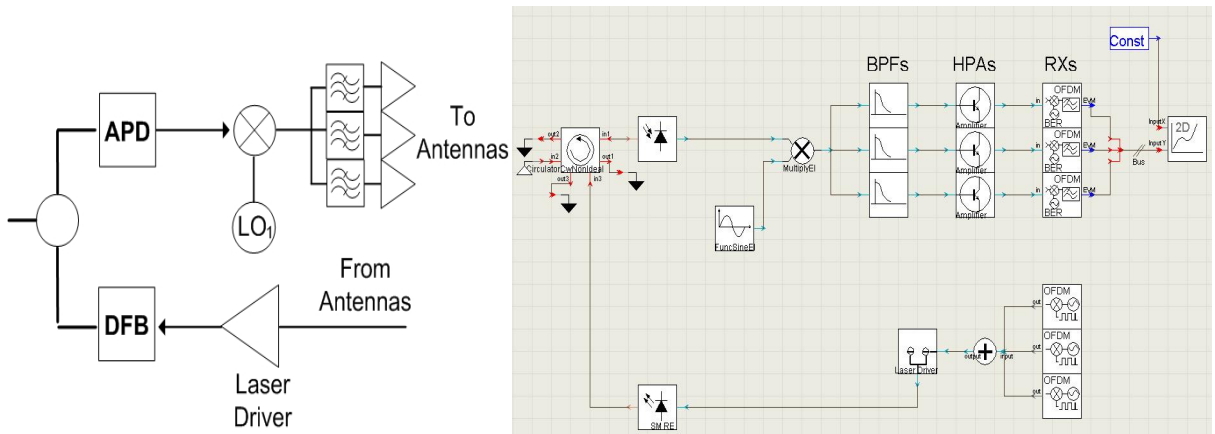
Figure 5-4: Optical network unit/base station modeling

Table 5-5: DFB laser parameters in the ONU/BS

Parameter	Value	Unit
Emission Frequency	2.9979e8/1310e-9	Hz
Average Power	3	mW
Laser Chip Length	100e-6	m
Active Region Width	3e-6	m
Photon Lifetime	3	ps
Carrier Lifetime	2.1	ps
Differential Refractive Index	-1.63e-26	m^3
LineWidth Enhancement Factor	3	/

The laser driver circuit, with the parameters given in Table 5-6, is utilised to bias the laser to produce the required power as well as to set the correct amplitude of the input signal avoiding clipping at the laser output.

Table 5-6: Laser driver parameters

Parameter	Value	Unit
Drive Amplitude	800e-6	V
Bias	21e-3	V

The electrical BPFs, before the HPAs, are used to select the desired channel prior to transmission over the air. The local oscillator is running in synchronism with the OLT oscillator for the specific ONU/BS.

The ONU/BS will be modified at a later stage to include VCSEL array and tuneable optical BPF operation for enhanced network dynamicity by the use of multiple wavelengths. This topology will be investigated in the following chapter. In contrast, the ONU/BS design presented here is adequate for establishing and evaluating transparent WiMAX transmission over legacy TDM PONs.

5.2.3 Optical Outside Plant Simulation

The outside plant consists mainly of a passive splitter and a SSMF as in typical PON deployments. The passive splitter is modelled with the variable optical attenuator to account for various split losses while the 20 km SSMF is modelled using a standard universal fibre VPI module, featuring bidirectional signal flow, nonlinearities, various dispersion effects and loss figures [22].

The VPI Table 5-7 includes the modelling parameters for the 20 km SSMF. A standard chromatic dispersion parameter was utilised to represent a typical fibre. Since, the optical power

99

within the 20 km fibre is expected to be moderate, Rayleigh and Brillouin backscattering and non-linearity effects are disabled to considerably save in simulation time.

Table 5-7: 20 km SSMF parameters

Parameter	Value	Unit
Length	20	km
Group Refractive Index	1.47	/
Attenuation	0.2	dB/km
Dispersion	16e-6	s/m^2
Dispersion Slope	0.08e3	s/m^3
Rayleigh, Brillouin	Disabled	/

5.3 Network Modelling and Simulation Results

In order to demonstrate the capability of the new architecture to transparently transmit IEEE802.16d WiMAX channels successfully over combined xPON and radio-cell links a physical layer simulation platform was devised as shown in Figure 5-5. In particular the model was used to demonstrate WiMAX transmission over multiple subcarriers to ONU/BSs on a single wavelength and to wireless users bi-directionally. In downstream the performance of five WiMAX channels was evaluated with no channel coding applied in order to present a worst case scenario.
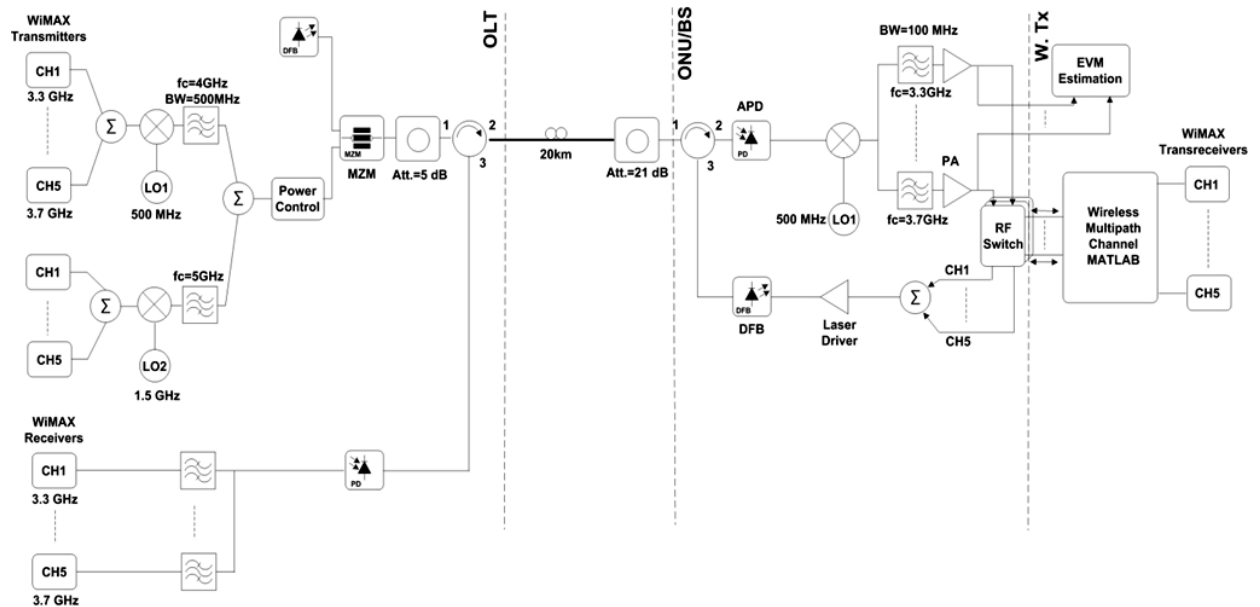
Figure 5-5: WiMAX over GPON physical layer simulation test-bed

The WiMAX OFDM transmitters have 20 MHz bandwidth with 64-QAM per OFDM subcarrier modulation. The OFDM is implemented by a 256-point IFFT, and 64 samples cyclic prefix corresponding to maximum attainable data rate across a cell of 50 Mbit/s [2]. Detailed implementation of the WiMAX transmitters and receivers has been described in chapter 4.

Five downstream WiMAX channels from 3.3-3.7 GHz, with 100 MHz spacing, were up-converted in the OLT using a 500 MHz LO before being applied to a Gaussian BPF with a 4

GHz centre frequency and 500 MHz bandwidth. The bandwidth of the filter allows for the five 100 MHz spaced WiMAX channels to be transmitted simultaneously to a single ONU/BS. Furthermore, an additional subcarrier at 5 GHz was added to simulate potential crosstalk between the two neighbouring subcarriers.

The externally modulated DFB in the OLT operated at +5 dBm output power at 1490 nm [23], to account for the MZM's typical loss of 5 dB alongside additional losses occurred throughout the transmission link and network elements. After transmission over the 20 km SSMF the APD in the ONU/BS was preceded by a fixed attenuator to model the loss of a 1:16 splitter.

To observe the worst case scenario in the presence of inter-modulation products, a maximum RF drive-power of +20 dBm was considered into the RF input of the MZM. The detected WiMAX channels at the APD output are shown in Figure 5-6 with a resolution bandwidth of 1 MHz. It should be noted that the MZM produced second order inter-modulation products that could potentially limit the transmission bandwidth and degrade the BER performance. The fibre non-linear effects, such as self-phase modulation (SPM) and cross-phase modulation (XPM), do not limit the network performance due to the low power levels launched into the fibre as well as due to the short transmission distances used [24].

It has been suggested that octave wide RF subcarriers will cause inter-modulation products to appear outside the desired bandwidth of transmission, particularly in direct laser modulation where a laser is driven in the linear region of its transfer function curve only to avoid the modulation clipping [24]. This would, however, limit the maximum number of allowed RF subcarriers, as investigated in chapter 3. An external modulator, on the other hand, can operate in the nonlinear region and therefore be able to control the amplitude of unwanted inter-modulation products.
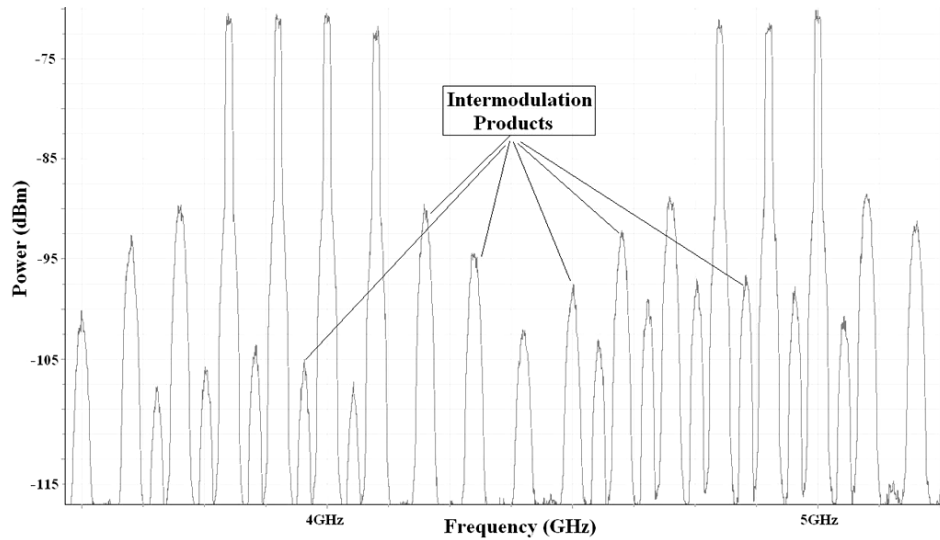
Figure 5-6: Inter-modulation products due to high RF power inside the MZM

The EVMs for the five WiMAX channels, as a function of the RF drive power into the MZM, were plotted to indicate if the maximum allowable RF drive power into the MZM comply with the WiMAX transmitter requirements. This was achieved by scanning the RF drive power for each channel from -5 dBm to +20 dBm while keeping the received optical power at the APD fixed. The average simulated EVM values of all channels are shown in Figure 5-7. It should be commented that for low input power levels into the MZM the performance is limited by thermal and shot noise of the photo-detector, while for high power levels, nonlinear distortions of the MZM increase EVMs. For the 64-QAM WiMAX OFDM transmitter an EVM of -31 dB was obtained, matching closely the performance figure of the WiMAX standard [2], suggesting acceptable performance for wireless users. According to Figure 5-7, EVMs of -31 dB were recorded at the ONU/BS antenna for all wireless channels with RF drive powers between +7.5 dBm and +9 dBm. For lower modulation levels, e.g. 16-QAM, higher EVM values can be tolerated allowing for greater RF drive power levels into the MZM thus further minimising inter-modulation products at the photo-receiver.

103
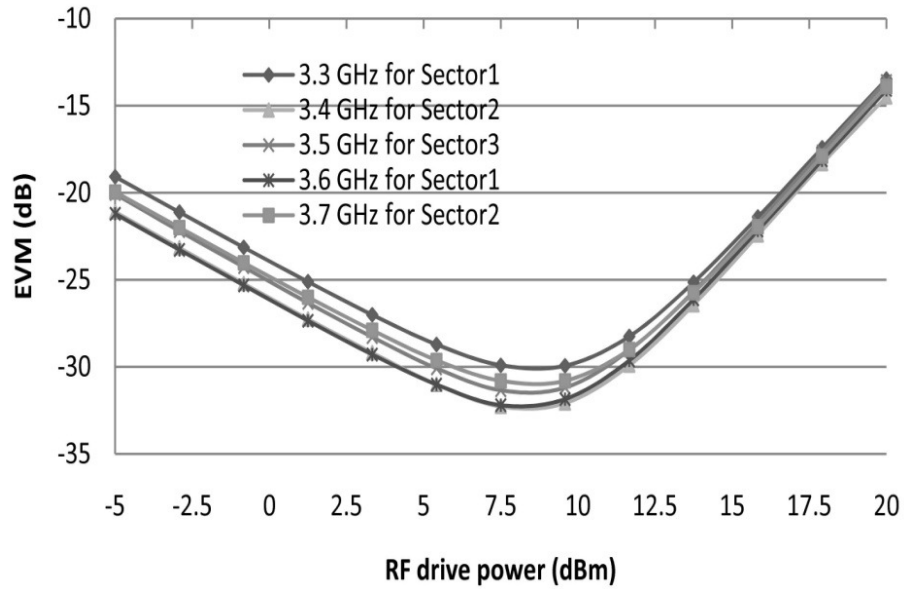
Figure 5-7: EVM versus RF drive power for downstream WiMAX channels

In upstream, the same WiMAX channels were utilised to assess the BER performance at the OLT after transmission over the wireless channel and GPON links. Each upstream WiMAX channel comprises 16-QAM, 256-OFDM occupying 10 MHz bandwidth with the same number of guard carriers and cyclic prefix size as in downstream, corresponding to maximum attainable data rates of 40 Mbit/s [2]. Subsequent to signal reception at the ONU/BS, direct laser modulation with a constant output power level of +5 dBm prior to transmission over a 20 km SSMF was utilised to comply with current GPON deployments [23].

According to the recorded laser transfer function, displayed in Figure 5-8 (left), a +5 dBm laser power is achieved with the bias current of 21mA [18]. The relative intensity noise (RIN) of the laser for WiMAX channels around 3.5 GHz, given in Figure 5-8 (right), is -130 dB.
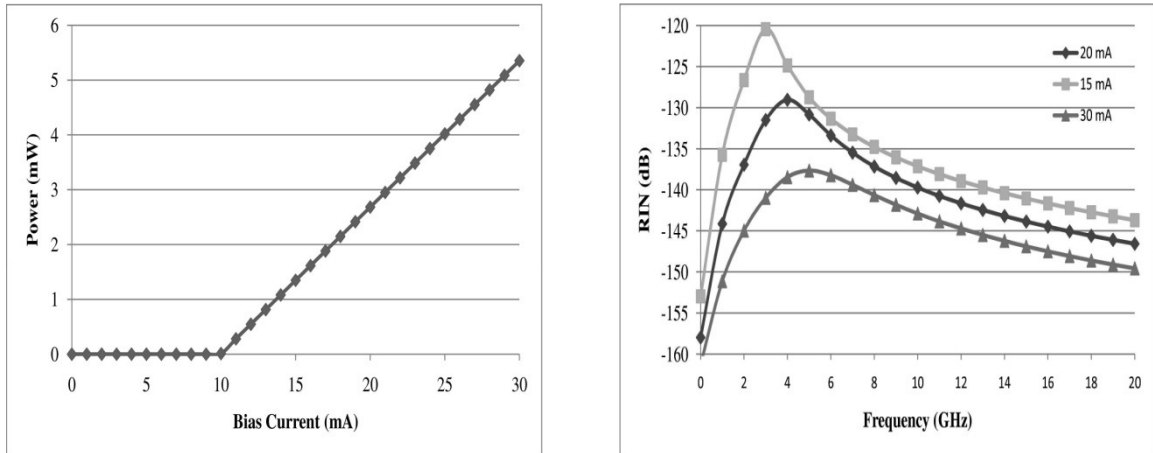
Figure 5-8: DFB bias current versus power (left) and RIN versus frequency (right)

After the circulator, the received signals in the OLT were converted to the electrical domain by APDs before their symbol detection in WiMAX receivers. In a similar manner to downstream, to determine the operating range of the direct modulated laser for optimum performance, the laser drive amplitude against EVM at the OLT was measured and displayed in Figure 5-9. This applied to upstream channels transmitted over the GPON only. EVMs below -27 dB were obtained for all wireless channels at drive currents in the range of 2.4-2.6 mA, matching closely the performance figures specified in the standard with 16-QAM modulation [2]. These figures confirm transparent transmission of WiMAX channels also in the upstream, without the need for complex dispersion compensation mechanisms.
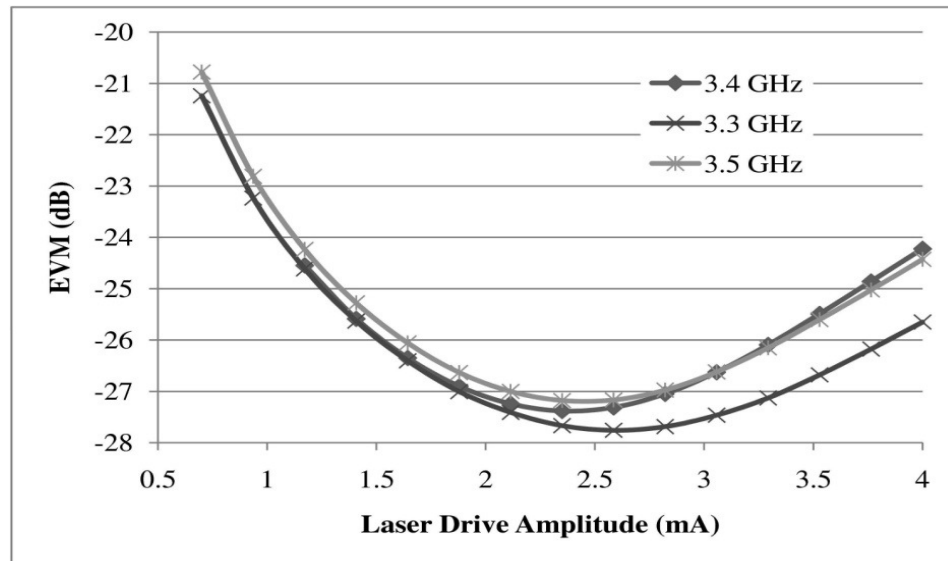
Figure 5-9: EVM versus laser drive amplitude in upstream

5.4 Transmission evaluation

Before transmission of the signal over a wireless channel, following the down-conversion in the ONU/BS, the system must provide sufficient received power to ensure that the minimum SNR is met at all times. Since the power level of the detected subcarriers after the APD is low, high gain power amplifiers are required prior to transmission over the wireless channel. A modified empirically based path loss model, accepted by the IEEE802.16 working group and expanded to cover higher frequencies [25], can then be used to predict coverage of the wireless network based on power budget analysis parameters as it will be extensively discussed in chapter 6. With typical parameters of WiMAX compliant equipment, 300m - 1km coverage for each sector is expected.

Furthermore, in order to consider multipath propagation, the standard SUI4 channel profile with a moderate delay spread, shown in chapter 4 and modelled in MATLAB with a single-input-single-output antenna configuration, was utilised since it provided a satisfactory representation of the macro-cellular environments [26]. Finally, the RF switches after the amplifiers, which are

shown in Figure 5-5, act as multiplexers or de-multiplexers to enable bidirectional wireless transmission.

Three un-coded WiMAX carriers were therefore transmitted across the SUI-4 channel assuming perfect channel knowledge at the receiver. To perform BER evaluations on the received wireless signals a combination of Gaussian and exponential distributions was used since the WiMAX carriers are affected by additive white Gaussian noise and multipath propagation as well as by non-linear effects on the optical link [27]. Bit error rate plots, assuming Gray constellation coding [2], for all three WiMAX channels each employing 50 Mbit/s data transmission with 64-QAM OFDM modulation, are shown in Figure 5-10.
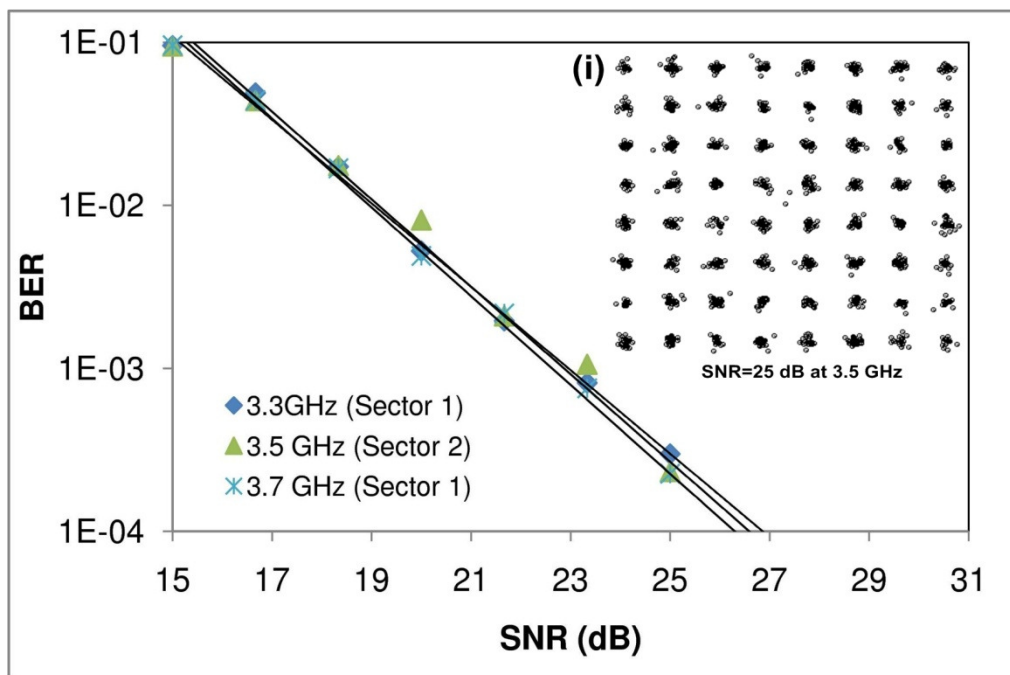
Figure 5-10: BER versus SNR for downstream WiMAX signals over faded SUI-4

Based on field trial measurements to support services such as IPTV [28], online gaming and video streaming and specified by the ITU recommendation and 3GPP technical specifications [29, 30], BERs of 1E-4 are considered acceptable for error free transmission. The proposed architecture has displayed BER figures of 1E-4 at an SNR requirement of around 26 dB for all

carriers obtained by varying the signal-to-noise ratio of the wireless channel with -30 dBm fixed received power at the APD [31]. The application of wireless channel coding techniques, such as convolution or turbo codes, is expected to reduce the recorded worst-case SNRs further.

Significantly the demonstrated 50 Mbit/s aggregate downstream capacity per WiMAX channel could be achieved at aggregate transmission links extended to more than 20 km as opposed to a limited 3-4 km with a standard macro-cellular WiMAX deployment. Alternatively each subscriber could benefit from higher bandwidth achieved in the presence of smaller concentration of wireless users per radio cell, enabled due to the lower cost per base station and as a result smaller cell size. In addition, in case the bandwidth requirement of users in a cell or sector exceeds the aggregate capacity, additional wireless channels, as previously described, could be successfully deployed from the OLT to enable on-demand bandwidth provisioning. GPON redundancy in case of a fibre failure could also be supported by, instead of using the additional carriers to increase capacity of individual users in a cell, to employ them as alternative connections to another ONU/BS in its vicinity.

The constellation diagram, shown in Figure 5-10 as inset (i), represents the obtained 64-QAM data points at the 3.5 GHz WiMAX receiver employed also to define the EVM of Figure 5-7. It is important to mention that this constellation is obtained prior to amplitude and phase equalisation demonstrating that in downstream optical fibre link introduce insignificant distortions.

For upstream transmission with direct laser modulation, BER responses of the three WiMAX channels, displayed in Figure 5-11, demonstrate power penalty of 3 dB at a BER of 1E-4 between the 3.3 GHz and 3.7 GHz channels. As already stated the SNR is expected to improve with appropriate wireless channel coding or with lower dispersion fibre and reduced laser chirp. The obtained 16-QAM constellation diagram, shown as an inset in Figure 5-11, demonstrates

the phase rotation due to the direct laser modulation. Therefore, an equalisation is required in order to compensate for this rotation. This is performed by multiplying the received symbols with the following factor:

$$C = \frac{1}{Ns} \sum_{k=1}^{Ns} \frac{I_{Tx_k} + iQ_{Tx_k}}{I_{Rx_k} + iQ_{Rx_k}} \tag{5.1}$$

where Ns is the total number of symbols and $I_{Tx} + Q_{Tx}$ and $I_{Rx} + iQ_{Rx}$ are transmitted and received complex symbols respectively.
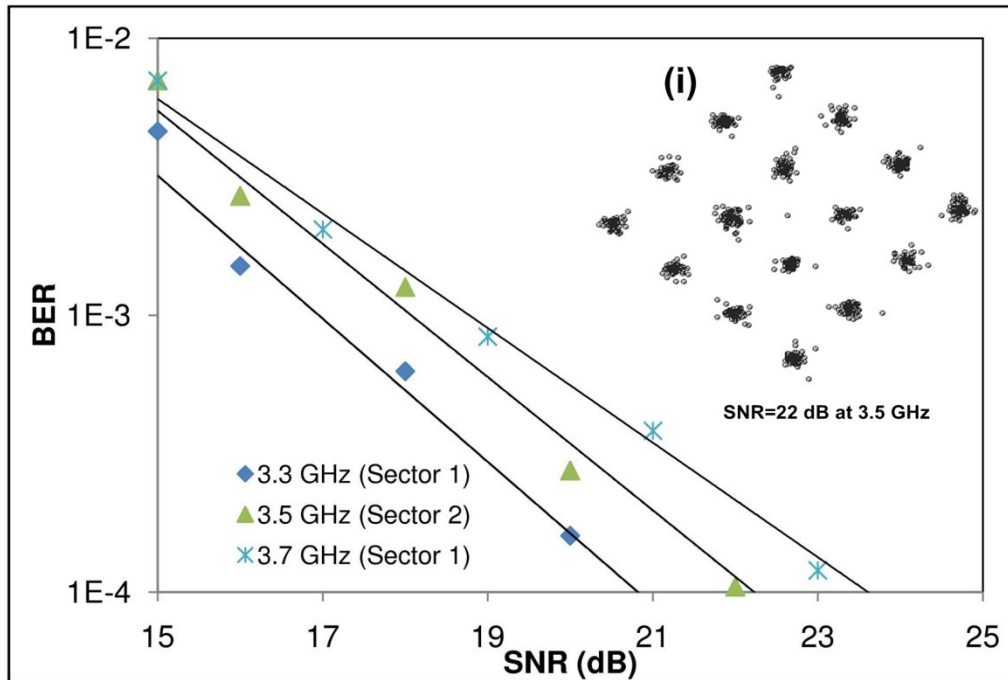
Figure 5-11: BER versus SNR for upstream WiMAX signals over faded SUI-4

Further SNR improvements can be expected at the presence of transmission diversity by multiple antenna elements at the ONU/BS and/or subscriber stations. Finally, wireless devices can exploit the benefits of cognitive radio technology as well by utilising dynamic spectrum access across radio cells and consequently increase the network capacity [32].

5.5 Summary

The innovative broadband access network architecture described in this chapter exploits the merits of standard GPON and WiMAX technologies to capture the best attributes of each, in facilitating high quality of service (QoS) in wire-line networks and ubiquitous connection together with the low deployment cost and mobility of wireless networks.

The maximum EVMs of -30 dB in downstream and -24 dB in upstream were demonstrated for all channels to comply with typical WiMAX transceivers. BER transmission characteristics against SNR from the physical layer simulation test-bed showed 1E-4 error rates for 50 Mbit/s and 15 Mbit/s data capacity per channel in downstream and upstream respectively over the GPON and wireless cells. The recorded SNR values are expected to improve in the application of wireless channel coding in order to comply with the WiMAX standard transceivers. The obtained data rates and error free transmission demonstrate the capability of the architecture to deliver services such as IPTV, online gaming and video streaming not cost effective with the current WiMAX deployment. In addition further analysis showed the potential for dynamic resource allocation per ONU/BS cell providing an additional channel for wireless transmission and thus improved capacity for even higher bandwidth services.

In downstream, the WiMAX channels were transmitted on RF subcarriers for each ONU/BS in order to avoid the interference with the baseband GPON transmission and to utilise the optical fibre efficiently. The time sharing of the optical carrier between wireless and wired signals in upstream could minimise the optical beat interference at the OLT photoreceiver without the need for additional wavelengths and RF upconversion at an ONU/BS. However, TDMA in upstream could result in reduced throughput across a wireless sector and as a result a multi-wavelength approach allowing for dedicated connection to each ONU/BS, as will be demonstrated in the following chapters, is promoted for the proposed network architecture.

References

[1] M. Milosavljevic, Y. Shachaf, P. Kourtessis, and J. M. Senior, "Interoperability of GPON and WiMAX for network capacity enhancement and resilience," *J. Opt. Netw.*, vol. 8, pp. 285-294, (2009).

[2] "IEEE Standard for Local and Metropolitan Area Networks Part 16: Air Interface for Fixed Broadband Wireless Access Systems," *IEEE Std 802.16-2004 (Revision of IEEE Std 802.16-2001)*, pp. 0_1-857, (2004).

[3] K. Kyoungsoo, L. Jaehoon, and J. Jichai, "Performance Limitations of Subcarrier Multiplexed WDM Signal Transmissions Using QAM Modulation," *J. Lightw. Technol.*, vol. 27, pp. 4105-4111, (2009).

[4] H. Ronqquinq, A. Benyuan, H. Renxiang, C. T. Allen, K. R. Demarest, and D. Richards, "Subcarrier multiplexing for high speed optical transmission," *J. Lightw. Technol.*, vol. 20, pp. 417-427, (2002).

[5] Z. Jia, J. Yu, A. Chowdhury, G. Ellinas, and G. K. Chang, "Simultaneous Generation and Delivery of Independent Wired and Wireless Services in Radio-over-Fiber Systems Using a Single Modulator," presented at Proceedings of European Conference and Exhibition on Optical Communication, 2007.

[6] *IEEE 802.16 Task Group m (TGm)* (Online). Available: http://www.ieee802.org/16/tgm/

[7] *Gigabit-capable Passive Optical Networks (G-PON): Transmission convergence layer specification*, ITU-T G.984.3, 2004

[8] C.-H. Chang, N. M. Alvarez, P. Kourtessis, and J. M. Senior, "Dynamic Bandwidth assignment for Multi-service access in GPON," presented at Proceedings of European Conference on Networks and Optical Communication, 2007.

[9] C. Ching-Hung, N. M. Alvarez, P. Kourtessis, R. M. Lorenzo, and J. M. Senior, "Full-Service MAC Protocol for Metro-Reach GPONs," *J. Lightw. Technol.*, vol. 28, pp. 1016-1022, (2010).

[10] M. Sauer, K. Kojucharow, H. Kaluzni, and M. Otto, "Impact of laser chirp on carrier and IMD power in electro-optical upconverted millimetre-wave fibre optic links," *Electr. Lett.*, vol. 35, pp. 834-836, (1999).

[11] M. Hajduczenia, P. R. M. Inacio, H. J. A. Silva, M. M. Freire, and P. P. Monteiro, "10G EPON Standardization in the Scope of IEEE 802.3av Project," presented at National Fiber Optic Engineers Conference, 2008.

[12] A. J. Paulraj, D. A. Gore, R. U. Nabar, and H. Bolcskei, "An Overview of MIMO Communications – A Key to Gigabit Wireless," presented at Proceedings of IEEE 2004.

[13] A. Alexiou and M. Haardt, "Smart antenna technologies for future wireless systems: trends and challenges," *IEEE Communication Magazine*, vol. 42, pp. 90-97, (2004).

[14] M. Milosavljevic, M. P. Thakur, P. Kourtessis, J. E. Mitchell, and J. M. Senior, "A Multi-Wavelength Access Network featuring WiMAX Transmission over GPON Links," presented at Proceedings of European Conference on Networks and Optical Communication (ECOC), 2010.

[15] M. Milosavljevic, P. Kourtessis, and J. M. Senior, "Wireless-PONs with Extended Wavelength Band Overlay," presented at Access Networks and In-house Communications (ANIC), OSA Technical Digest (CD), (Optical Society of America, 2010), 2010.

[16] *Aeroflex Test Solutions* (Online). Available: http://www.aeroflex.com/

[17] *JDSU*   (Online).   Available: http://www.jdsu.com/products/optical-communications/products/detectors-receivers.html

[18] *FITEL Global site-Products* (Online). Available: http://www.furukawa.co.jp/fitel/eng/active/pdf/Cooled/ODC-3S002E_FRL1xDDRx-A31_E.pdf

[19] M. Ahmed, M. Yamada, and M. Saito, "Numerical modeling of intensity and phase noise in semiconductor lasers," *IEEE J. Quantum Electron.*, vol. QE-37, pp. 1600-1610, (2001).

[20] C. J.C. and S. R. C., "Extraction of DFB laser rate equation parameters for system simulation purposes," *J. Lightw. Technol.*, vol. 15, pp. 852-860, (1997).

[21] D. Wake, A. Nkansah, N. Gomes, G. de Valicourt, R. Brenot, M. Violas, Z. Liu, F. Ferreira, and S. Pato, "A Comparison of Radio Over Fiber Link Types for the Support of Wideband Radio Channels," *J. Lightw. Technol.*, vol. 28, pp. 2416 - 2422, (2010).

[22] *VPI photonics Inc.* (Online). Available: http://www.vpiphotonics.com

[23] *Gigabit-capable passive optical networks (GPON): Physical media dependent (PMD) layer specification*, ITU-T G.984.2, 2003

[24] X. Zhaowen, W. Yang Jing, Z. Wen-De, C. Tee Hiang, M. Attygalle, C. Xiaofei, Y. Yong-Kee, W. Yixin, and L. Chao, "Characteristics of Subcarrier Modulation and Its Application in WDM-PONs," *J. Lightw. Technol.*, vol. 27, pp. 2069-2076, (2009).

[25] V. Erceg, L. J. Greenstein, S. Y. Tjandra, S. R. Parkoff, A. Gupta, B. Kulic, A. A. Julius, and R. Bianchi, "An empirically based path loss model for wireless channels in suburban environments," *J. Select. Areas Commun.*, vol. 17, pp. 1205-1211, (1999).

[26] *IEEE 802.16 Broadband Wireless Access Working Group* (Online). Available: http://ieee802.org/16

[27] H. Louchet, K. Kuzmin, and A. Richter, "Efficient BER Estimation for Electrical QAM Signal in Radio-Over-Fiber Transmission," *Photon. Technol. Lett.*, vol. 20, pp. 144-146, (2008).

[28] K. N. Skalman, H. E. Sandstrom, and M. Gidlund, "Techno-Economical Study for Open Horizontal IPTV in the Access and Home Networks – from a Swedish Perspective," presented at Proceedings of European Conference on Networks and Optical Communication, 2008.

[29] *One-way transmission time*, ITU-T G.114, 2003

[30] *Technica Specification Group Services and Systems Aspects, Service Aspects: Services and Services Capabilities*, 3GPP TS 22.105 V 6.2.0, 2003

[31] *Gigabit-capable passive optical networks (G-PON): Physical Media Dependent (PMD) layer specification*, ITU-T G.984.2:, 2003

[32] I. F. Akyildiz, W. Y. Lee, M. C. Vuran, and S. Mohanty, "A Survey on Spectrum Management in Cognitive Radio Networks," *IEEE Communication Magazine*, vol. 46, pp. 40-48, (2008).

Chapter 6

Multi-Wavelength WiMAX-PONs with Overlapping Cells

Contents

This chapter presents the application of extended wavelength band overlay over a splitter, wireless-enabled PON to demonstrate enhanced scalability and dynamicity in comparison to the architecture presented in the previous chapter. The overlapping cell concept is investigated that in parallel with the wavelength band overlay is expected to provide increased wireless spectral efficiency and resilience. The application of RoF is still in the focus by means of accessing each remote ONU/BS sharing a given wavelength by FDM. To demonstrate the network scalability, multiple FDM windows were routed over multiple wavelengths, with the slightest modification in network hardware. EVM figures at selected remote base stations antenna inputs and BER characteristics for users in the overlapping sectors have been recorded.

6.1 Extended wavelength band overlay over wireless-enabled PON

The WiMAX-GPON architecture [1-3] presented in the previous chapter, utilised a single wavelength to address multiple ONU/BSs bidirectionally based on FDM. In that architecture, the ONU/BSs received in upstream time-interleaved WiMAX channels, avoiding at the optical receiver in the OLT any potential optical beat interference. To that extent, each wireless subscriber station transmits its signal in predetermined time slots dictated centrally from the OLT. This could however result in restricting the bandwidth utilisation efficiency for the wireless users. Also, a single wavelength approach could impose high dispersion penalties across the fibre as the number of frequency subcarriers in the FDM window is increased, to address larger number of ONU/BSs. As a result, increased network penetration would require sophisticated, high bandwidth optical and electrical components.

The application of extended wavelength band overlay [3, 4] reduces optical beat interference in upstream while allowing for low component cost with high scalability and dynamicity. This has been achieved in the current architecture over a typical splitter PON, requiring the slightest modification in network hardware. Subsequently, each ONU/BS's allocated FDM subcarrier downstream could be dynamically multiplexed on different wavelengths. The low-cost long-wavelength VCSEL arrays [5] and tuneable optical band-pass filters (BPF) [6, 7] are universally employed in the ONUs to demonstrate colourless wireless-PONs with no requirement of wavelength-specific optical sources.

In addition, the network resilience is demonstrated through the drop of multiple wavelengths, to users terminated to ONU/BSs exhibiting overlapping cells to potentially double their spectrum efficiency. These extended features of the wireless network, compared to traditional deployments, are justified through the significant reduction in the WiMAX base station deployment cost by the application of the proposed RoF transmission.

116

6.2 Network architecture design

The revised network architecture is shown in Figure 6-1. The OLT and ONU/BSs are modified

to accommodate multi-wavelength transmission over a passive splitter in the remote node. Any

wavelength in the selected operating spectrum could be partially or exclusively assigned to

different ONU/BSs, providing in the latter service levels similar to WDM-PONs without

requiring any modifications in the ODN. Therefore, this approach will provide smooth

migration path from TDM-PONs to WDM-PONs.

For simplicity, the centre frequency of the tuneable optical filters in ONU/BSs can be adjusted

from the OLT by means of a controller circuit. Unused AWG input ports, as shown in Figure 6-

1, could be exploited to assign a unique wavelength to each ONU/BS or to support multiple

wireless-enabled PONs from a single OLT, considered as a prerequisite for NG-PONs [8].
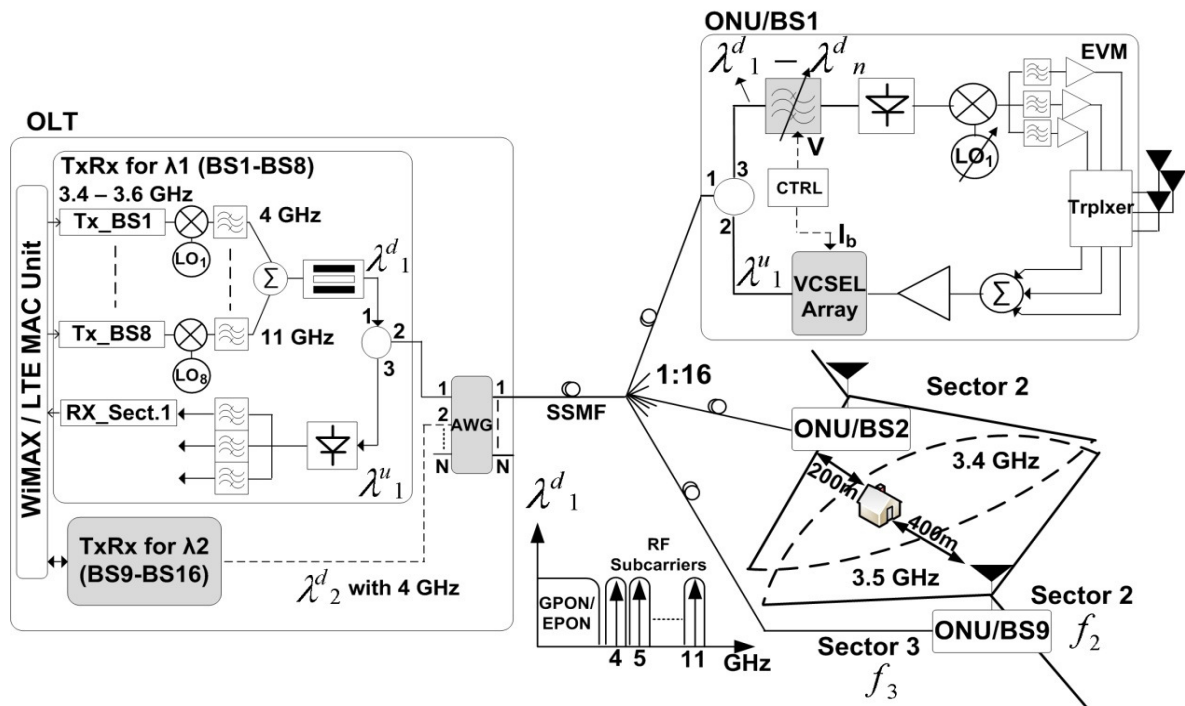
Figure 6-1: Multi-wavelength WiMAX-PON

On each wavelength, multiple microwave WiMAX channels are arranged in a FDM window to

address individual ONU/BSs. The same FDM window could be carried on multiple

wavelengths relaxing significantly the bandwidth requirements of the optical and electrical devices in the network. In addition, the maximum radio frequency on a single wavelength is relatively low therefore no dispersion compensation is required.

Figure 6-1 displays the formation of overlapping cells/sectors, e.g. between ONU/BS2 and ONU/BS9, operating as expected at different frequency channels. Since different ONU/BSs are operating on different radio channels no interference would be expected between overlapping wireless users and thus maintaining their network capacity. The transmission distances formed between ONU/BSs in Figure 6-1, allow for higher spectral efficiency compared to traditional WiMAX deployment while could be potentially extended with the application of relay techniques [9].

The use of low-cost long-wavelength VCSEL arrays [5, 10] at ONU/BSs demonstrate colorless terminations upstream with simple coupling optics. In contrast to RSOAs [11], VCSEL arrays do not require wavelengths to be used in upstream to have been first transmitted simultaneously with downstream data. Although RSOAs could be possibly investigated [11], interference among multiple delayed versions of the upstream signal generated due to Rayleigh backscattering could potentially degrade performance. Following the use of VCSEL arrays, upstream wavelength selection can be managed by a means similar to tuning the ONU/BS filters. TDMA, where each ONU/BS is transmitting at specific time slot on a single wavelength, could still be applied upstream [12].

6.3 Modified Network Models

Similar to the previous chapter, a physical layer simulation test-bed was implemented using VPI, enriched in functionalities with MATLAB programming, to build an integrated simulation platform for the transmission of frequency shifted wireless channels over a multi-wavelength GPON with overlapping cells. Performance evaluation measures included EVM estimations at the remote antenna inputs for two base stations, and measurements of the WiMAX received power at the radio receiver in downstream and ONU/BS in upstream versus recorded BERs for various transmission distances of the proposed micro-cellular overlapping links.

6.3.1 WiMAX Power Budget Analysis

As described in chapter 4, the WiMAX transceivers are modeled to include the effect of wireless channel path loss based on data sheet parameters used in practical deployment scenarios. The power budget parameters of the implemented links for the transmission across the air are given in Table 6-1. The effective isotropic radiated power (EIRP), which is given by the maximum power from the power amplifier plus the antenna gain taking into consideration cable losses, is 40 dBm and 35 dBm for downstream and upstream respectively. The wireless channel propagation losses are varied between 100-120 dB to estimate the maximum transmission distance with respect to the calculated receiver sensitivity as it will be analysed in following sections.

Table 6-1: Modeling parameters for practical wireless signals

IEEE 802.16d WiMAX [13]			
Transmitters DW/UP		**Receivers DW/UP**	
Modulation	64- / 16-QAM	SS_antenna gain	17 dB
Channel Bandwidth	20 / 10 MHz	SS_cable loss	1 dB
RCE	39 / 25 dB	Noise figure	4 dB
Power at amplifier output	25 / 20 dBm	Noise in BW	-100.1 / -104 dBm
BS_antenna gain	17 dB	SS noise floor	-96.1 / -100 dBm
BS_cable loss	2 dB	SNR_required	24.4 / 18.2 dB
BS_antenna height	30 m	Rx sensitivity for BER=1E-6	-71.7 / -81.8 dBm
EIRP	40 / 35 dBm	Shadow margin	8 dB
Propagation Loss with Cat. B [14]	100-120 dB		

6.3.2 OLT

Specified by the OLT model in Figure 6-1, MZM were used to externally modulate commercially available DFB laser sources, having parameters as detailed in previous chapters, with WiMAX channels applied at modulator's RF input. The DFBs output powers were set to account for various optical component losses, as shown in Table 6-2, producing the maximum lunched power of +3.2 dBm into the fiber [15].

Table 6-2: Modeling parameters for practical optical network

ITUT G.984.2 GPON [15]					
OLT		**RN**		**ONU**	
Laser Tx Power	+8.5 dBm	SSMF Loss (20km)	4 dB	Received Power DW	-17.8 dBm
MZM Loss	3 dB	Splitter Loss (1:16)	14 dB	VCSEL Power UP	+1.2 dBm
Circulator Loss	1 dB	Optical Filter Loss at ONU/BS	3 dB		
AWG Loss	1.3 dB				
Launch power DW	+ 3.2 dBm				
Received Power UP	-19.1 dBm				

The three 70 Mbit/s downstream IEEE802.16d channels for three sectors are modeled in MATLAB [12]. Subsequently, they are generated individually by Tx_BS1 and Tx_BS9, ranging from 3.4 to 3.6 GHz, with 100 MHz spacing. The spectral profile of the WiMAX

transmitters, given in Figure 6-2 (right), clearly satisfies the spectral mask specification of the standard to prevent excessive energy leakage outside the desired channel bandwidth [16]. Similar results for the spectral mask were obtained for the 10 MHz upstream transmitter.
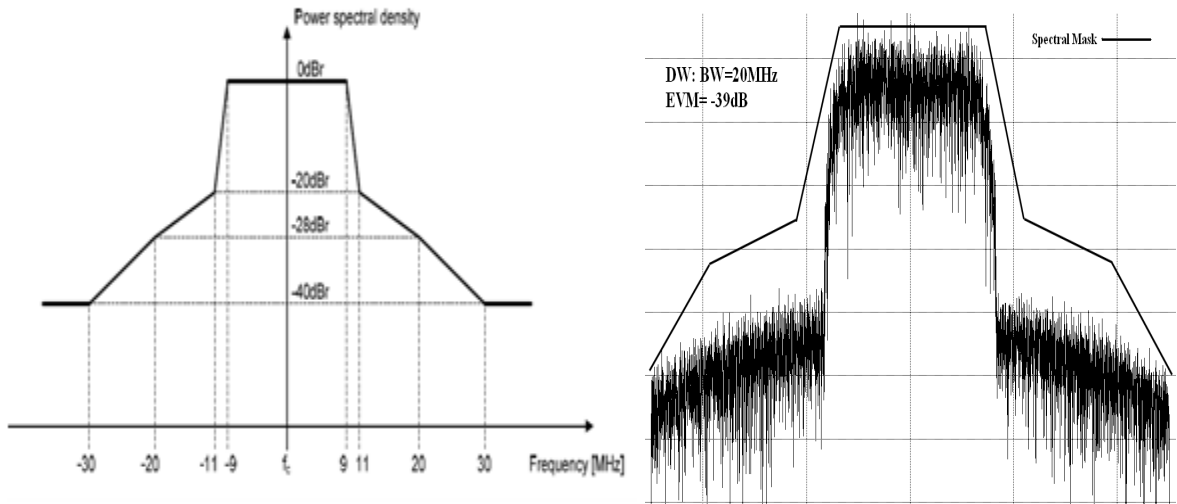
Figure 6-2: Required WiMAX spectral mask (left) [16] in comparison to modeled (right)

Consequently, the WiMAX channel transmitter relative constellation error, imposed by the non-linear high power amplifiers, is -39 dB, a figure higher than the minimum required by the standard for 64-QAM modulation [13]. This has been achieved due to the small RF powers utilised to drive the MZM.

As shown in Figure 6-1, the WiMAX channels are then frequency shifted around the same 4 GHz RF subcarrier using a 500 MHz local oscillator. The same RF spectrum was modulated on two wavelengths to demonstrate the network scalability in terms of it being able to support increased number of base stations as well as to provide for low-component costs due to the reduced FDM bandwidth now required at each wavelength.

Subsequently, signals from both transmitters are modulated on λ^d_1=1553.33 nm and λ^d_2=1554.13 nm and after applied over the corresponding circulators for bidirectional

transmission, the modulated wavelengths are multiplexed at the commercially available AWG [17] and broadcasted to each ONU/BSs of the corresponding PON through 20km of SSMF.

Figure 6-3 shows the resulting optical spectrum at the AWG output clearly demonstrating two FDM windows modulated on each optical carrier using ODSB modulation. Single sideband (SSB) modulation could also be considered for longer fibres to reduce chromatic dispersion on the received channels. However, it typically requires additional optical band pass filters at the output of the optical modulator to select one band, increasing the cost of the system.
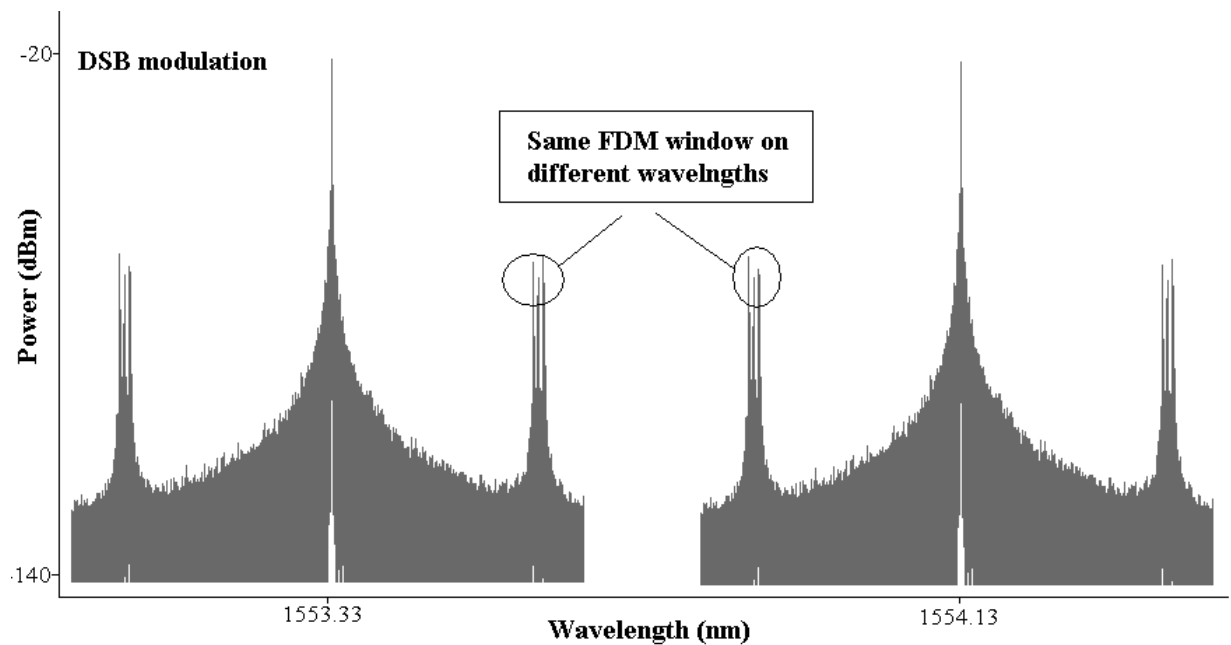
Figure 6-3: Transmitted optical spectrum observed at the output of the AWG

The 5×5 Gaussian dense AWG [17] with 100 GHz channel spacing, displayed in Figure 6-4, comprises two identical standard Gaussian AWG modules employed to accommodate the two waveguide transmitted modes, the transverse electric (TE) and transverse magnetic (TM). The odd number of AWG input/output ports was considered for simplicity since the same performance is expected for any port sizes. As displayed in the figure, each of the five input ports of the model is applied at a polarisation beam splitter (PBS), where its x and y coordinated outputs are applied at the corresponding TE and TM mode AWGs. Subsequently, the outputs of

the two AWGs are combined using polarisation beam combiners (PBCs) and applied at each of

the corresponding output ports of the model providing realistic performance.
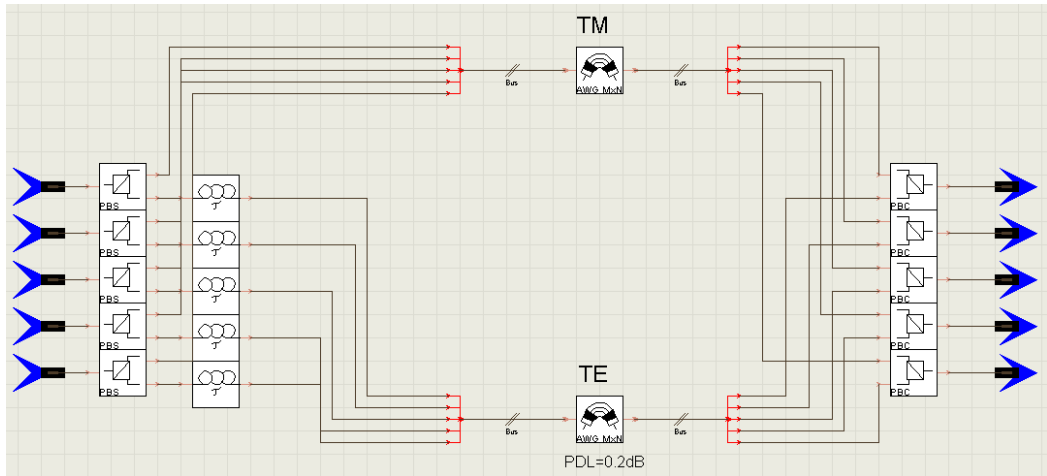
Figure 6-4: AWG modeling in VPI

The VPI Table 6-3 includes the design parameters for the TM mode only. The central

wavelength is set to 1553.33 nm with 3.5 dB insertion loss [17]. Similar parameters are

considered for the TE mode at an additional 0.2 dB polarisation depended loss added to the

inherited insertion loss [17]. The adjacent channel crosstalk was set to 26 dB matching closely

the performance figure of the data sheet model [17].

Table 6-3: AWG parameters

Parameter	Value	Unit
Number of Ports	5	/
Channel Centre Frequency	193	THz
I/O Channel Spacing	100	GHz
Passband Type	Gaussian	/
Bandwidth_3dB	50	GHz
Adjacent Crosstalk	26	dB
Non-Adjacent Crosstalk	35	dB
Insertion Loss	3.5	dB
Loss Uniformity	1.5	dB

Finally, the modelled Gaussian AWG offers compliance with commercialised dense AWGs

[17], while provides the most effective means of evaluating the performance of the modelled

device against the recorded data sheet figures [17]. To that extent, the obtained transmission spectra is shown in Figure 6-5, confirming comparable AWG passband characteristics with [17]. The polarisation mode delay was set to 0.5 ps.
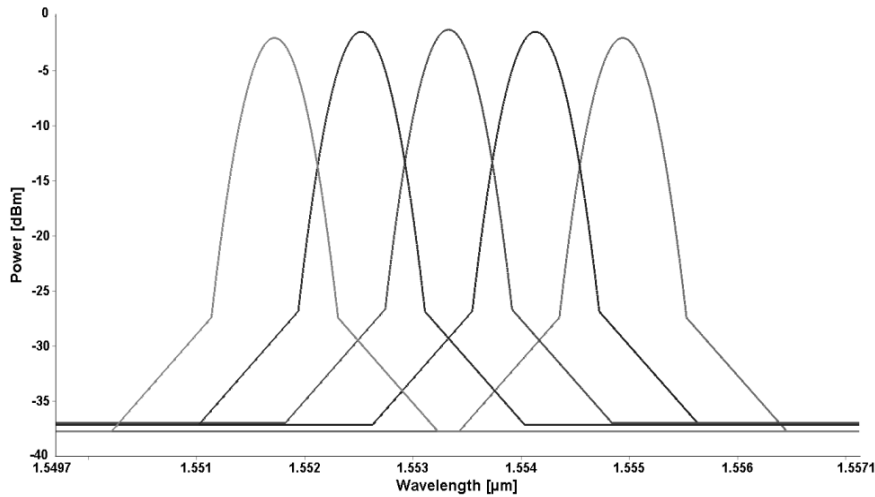
Figure 6-5: 5×5 Gaussian response of dense AWG modeling

6.3.3 ONU/BS

Each ONU/BS, shown in Figure 6-6, incorporates a tunable optical band-pass filter with 50 GHz bandwidth to select each received wavelength which is then detected by an APD followed by RF subcarrier down-conversion to result to the downstream transmitted WiMAX channels.

The resulting channels for each sector are then electrically filtered with a 100 MHz BPF, amplified by a non-linear high gain amplifier and transmitted over AWGN, multi-path SUI-4 wireless channels [18]. For the faded wireless path the cyclic prefix of 1/4 is included to reduce inter-symbol interference. The subscriber receiver is allocated in the overlapping region between two base stations as shown in Figure 6-1.
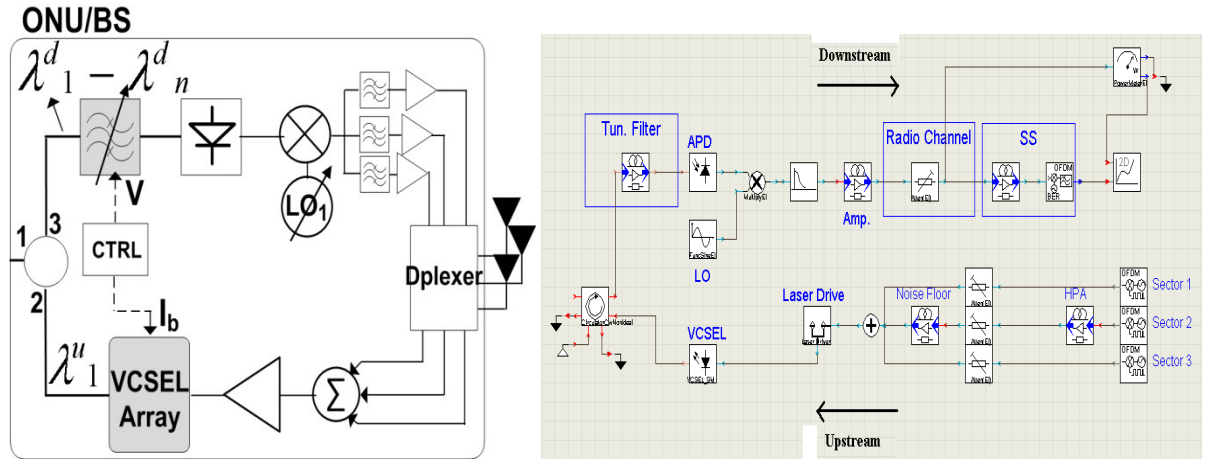
Figure 6-6: Modified ONU/BS to account for multi-wavelength transmission

The two upstream WiMAX channels at 3.4 GHz and 3.5 GHz originating at the overlapping sector are received by ONU/BS2 and ONU/BS9 respectively and are directly modulated in a 6 mW biased, +1.2 dBm [5] VCSEL array each at λ^u_1=1553.33 nm and λ^u_1=1554.13 nm respectively. The VCSEL parameters are given in Table 6-3. A threshold current of 0.75mA and 1.5 mW thermal rollover power are specified according to the model in [5]. The laser is assumed to be operated at the ambient temperatures for which the bias current versus output power (L-I) characteristics are given in Figure 6-5 (left). Other physical parameters of the laser such as the core radius, active region thickness, and spontaneous recombination rate are adjusted to comply with a typical device data sheet. To that extent, the obtained transfer function of the laser is given in Figure 6-7 (right).

Table 6-4: VCSEL parameters

Parameter	Value	Unit
Emission Frequency	2.9979e8/1553.33e-9	Hz
Average Power	1.5	mW
Core Radius	4.5e-6	m
Active Region Thickness	0.03e-6	m
Spontaneous Recombination Rate	1e-4	/
Carrier Lifetime	5	ps
LineWidth Enhancement Factor	4	/
Threshold Current	0.75	mA
Thermal Rollover Power	1.5	mW
Thermal Rollover Current	8	mA
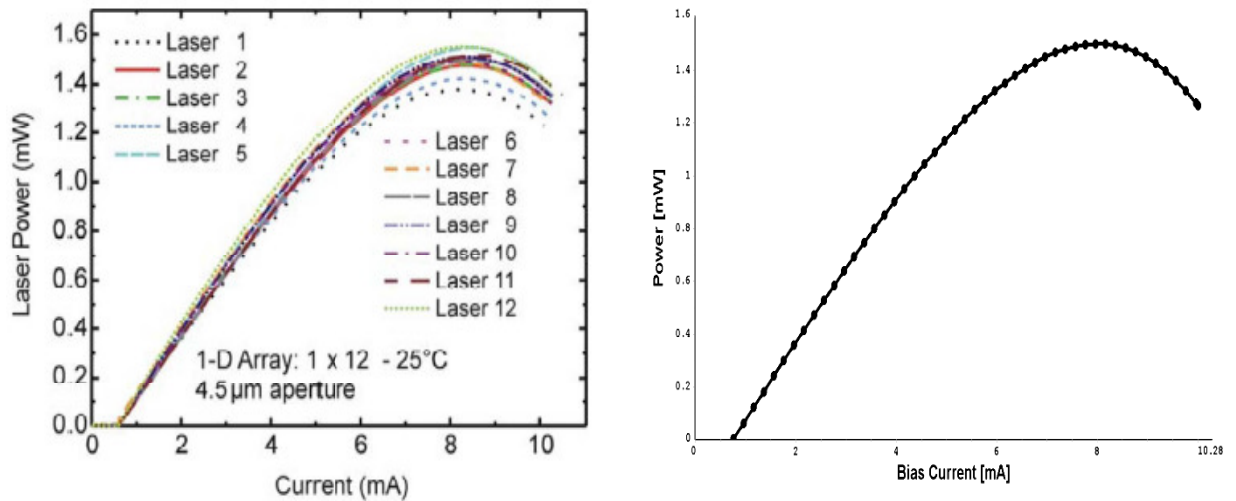
Figure 6-7: VCSEL array - practical (left) [5] and modeled (right)

As it could be observed from the figure the same performance was obtained with the practical device in terms of L-I curve. As expected, the power level after a certain bias current, known as the thermal roll over current, starts to drop due to the thermal behavior of the laser [19].

Finally, the upstream WiMAX channels utilise 16-QAM, 256-OFDM modulation with maximum data rate of 40 Mbit/s. The small-signal-gain amplifier in both ONU/BSs is utilized to drive the VCSEL laser array. Consequently, due to its grooming property, the same

126

input/output (I/O) port of the AWG as in downstream will be used before the signal is routed

through the corresponding circulator to the destination receivers (Rx_Sect.X) in the OLT.

6.3.4 WiMAX Receiver

In order to include the realistic limitations, such as path loss, expected in the wireless receivers

due to signal transmission over the air, the models needed to be modified to include typical

noise figures encountered in practical devices. Therefore, for the downstream WiMAX receiver,

the noise in considered 20 MHz bandwidth is given by [20]:

$$\text{Noise Power} = 10\log(kTB) \tag{6.1}$$

where kT is the thermal noise of the receiver, typically -174 dBm and B is the WiMAX

bandwidth.

The total noise in the given bandwidth is thus equal to -100.1 dBm which in association with

the receiver noise figure of 4 dB, results to a noise floor of -96.1 dBm. According to the

WiMAX standard for 64-QAM modulation the minimum received SNR should be 24.4 dB [13].

The downstream receiver sensitivity is then -71.7 dBm which with the effective isotropic power

of +40 dBm, as specified in Table 6-1, allows for a maximum attenuation of 111.7 dB across

the wireless channel.

Similar calculations have been performed for the upstream WiMAX receivers in the OLT

giving a sensitivity figure of -81.8 dBm and a maximum allowable attenuation of 135 dB. The

higher attenuation values allowed in upstream are due to the fact that 16-QAM modulation

mapping has been utilized for the upstream transmitter.

Figure 6-8 demonstrates the VPI model at the wireless receiver utilized to set the constant noise

floor. Essentially, the white noise source is initially band pass filtered, according to the

transmission bandwidth, producing the required output noise power [20]. The transmission

bandwidth is considered as the WiMAX signal width applied in the model for transmission over the converged network. The resulting output noise is added to the input signal setting the noise floor.
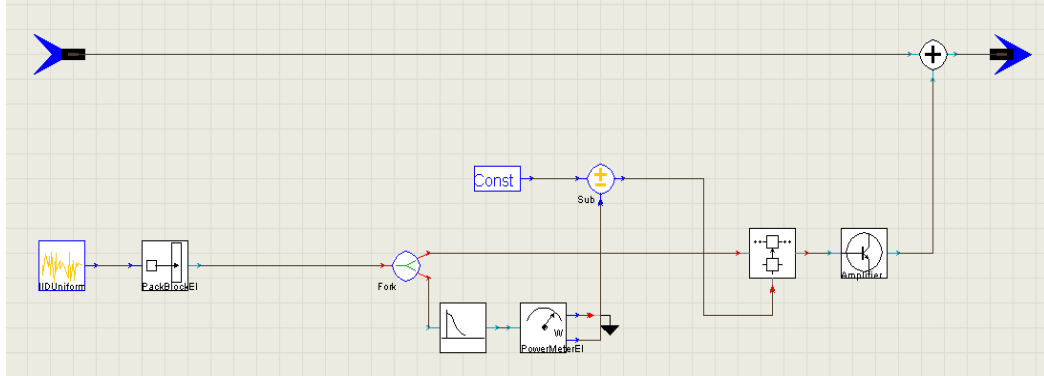
Figure 6-8: VPI model utilized to set the required noise floor for the wireless receiver

6.4 Transmission Simulation Results

6.4.1 EVM at Remote Antenna Inputs

As nonlinear optical modulators could significantly degrade network performance, EVM characteristics as a function of the MZM RF drive power in the OLT were initially estimated. Therefore, after the wavelength selection and frequency downshifting by both base stations, an EVM figure of higher than -31 dB for certain RF drive powers is achieved, as shown in Figure 6-9, matching closely the WiMAX standard [13] with 64-QAM modulation. This demonstrates the network capability to transparently deliver WiMAX signals based on FDM to remote base stations over multi-wavelength xPONs. As illustrated in Figure 6-9, at low RF drive powers the signal is mainly distorted by noise while at high powers EVMs increase with MZM nonlinear effects as expected.
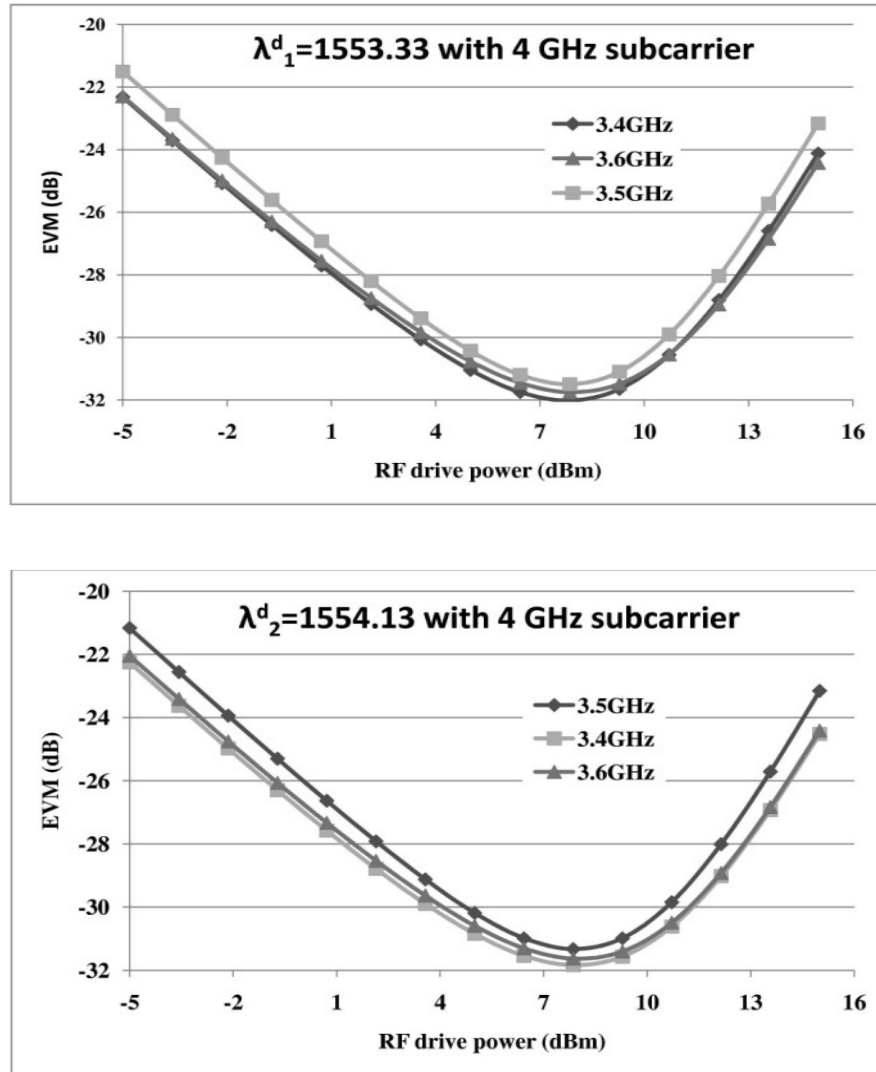
Figure 6-9: EVM versus RF drive power for the two wavelengths

6.4.2 WiMAX Transmission over the Overlapping Sector

To evaluate the quality of downstream transmission at a wireless receiver in the overlapping

sector, as described by the link-level model in Figure 6-1, two WiMAX channels, at 3.4 and 3.5

GHz, carried over the two wavelengths are transmitted to a single user with the power budget

parameters specified in Table 6-1. The BER curves were then plotted initially over a line-of-

sight (LOS) AWGN, as specified by the standard [13], and faded NLOS wireless paths.

Consequently, for both WiMAX channels in the presence of an AWGN wireless path, the

obtained results in Figure 6-10 display a power penalty of around 4 dB with respect to the 64-

QAM downstream receiver sensitivity of -71.7 dBm for BER of 1E-6 [13]. For a SUI-4 channel however a further power penalty is recorded due to the multipath propagation. The observed power penalties for both wireless paths are expected to be improved with the application of FEC techniques, as defined by the standard [13], which are excluded here to represent a worst case scenario. The BER characteristics of the remaining channels indicated similar performance since the model assumes identical coefficients and power budget parameters for all sectors.
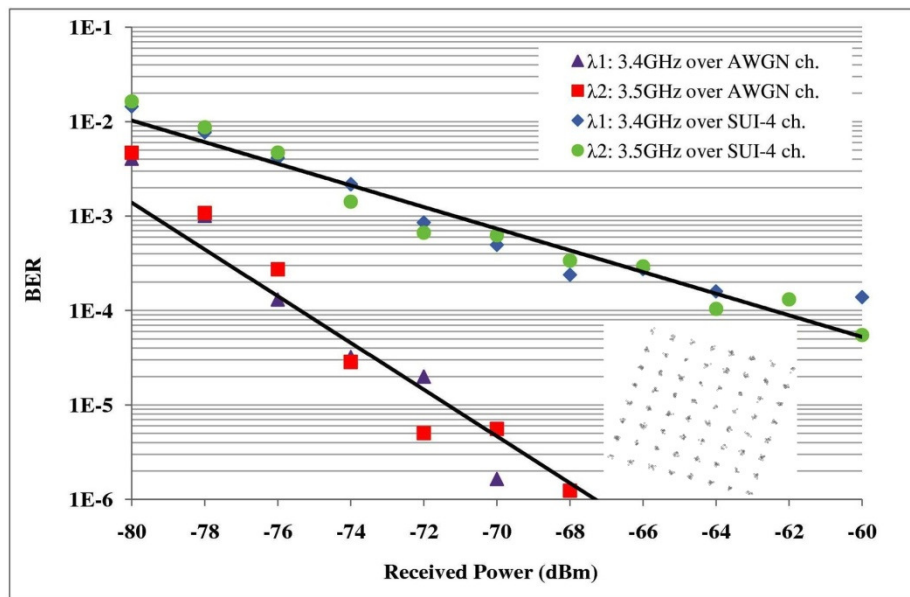
Figure 6-10: BER versus received power for the WiMAX channels in the overlapping sector downstream

In addition, to predict the extent of coverage across the overlapping sector, an empirically based path loss model, accepted by the IEEE802.16 working group for the fixed wireless transmission is modified according to the presented power budget analysis parameters and expanded to cover higher frequencies [14]. The path loss calculation equations are given in Appendix B.

As shown in Figure 6-10, for a BER of 1E-6 the received power in the presence of the LOS AWGN un-coded channel is -67.7 dBm which with maximum transmission power of +40 dBm corresponds to an attenuation value of 107.7 dB. For the category B channel and a base station antenna height of 30m [14], the maximum achievable transmission distance is 430m which is comparable with some practical deployment scenarios [21]. This is expected to be extended

however considerably with the application of FEC. The channel estimation algorithms at the wireless receiver and synchronization aspects were not considered as these are vendor specific and are therefore out of the scope of this thesis. Significantly, BERs of 1E-4 were achieved for both channels, with a received power of -63 dBm, confirming error-free transmission with a maximum coverage of around 330m for certain services [22, 23].

In upstream, the BER for the two WiMAX channels in the overlapping sector versus received power at the ONU/BSs is evaluated in the OLT wireless receiver. As shown in Figure 6-11, for an AWGN channel, the power penalty is about 0.7 dB which is lower than in downstream. For the SUI-4 channel a further power penalty is observed similar to downstream. However, the BER of 1E-4 could also be achieved for both channels with distinctive received powers. The obtained results in upstream demonstrate that signal distortion due to the interaction of laser chirp and fiber dispersion in long-wavelength direct VCSEL array modulation is not significant and is not degrading the proposed WiMAX-PON network.
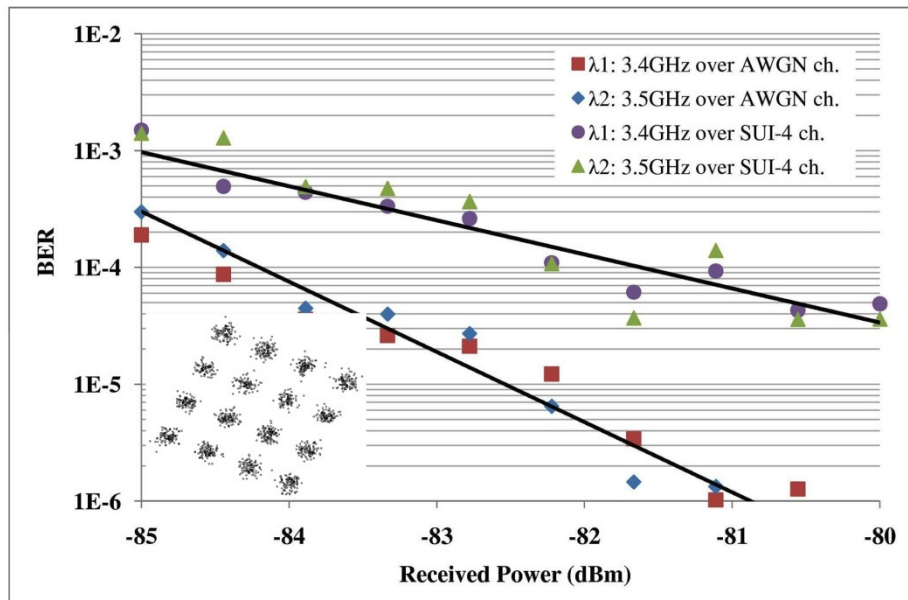
Figure 6-11: BER versus received power for the WiMAX channels in the overlapping sector upstream

Finally, the received constellation diagrams, displayed as insets in Figure 6-11 and obtained at the wireless receivers prior to any gain and phase compensation in both downstream and

upstream, show the rotation due to the optical filter phase response and direct laser modulation respectively. In both directions the received constellations are obtained at a BER of 1E-4. The pilot tones for the channel coefficients estimation, as described by the standard [13], were not used since perfect channel knowledge is assumed at the receiver.

6.5 Summary

A scalable network topology is described featuring transparent wireless transmission by means of FDM over multi-wavelength legacy PONs, requiring the slightest modifications in hardware through the use of a single AWG and low-cost long-wavelength VCSEL arrays in the OLT and ONU/BSs respectively. Significantly, extended wavelength band overlay provides for low frequency windows and consequently no dispersion compensation. In addition, it allows for small bandwidth optical and electrical devices.

The centrally controlled ONU/BSs, allow for the creation of overlapping cells which enable improved GPON redundancy in case of fibre failure between a distribution point and an ONU as well as enhanced WiMAX capacity beyond traditional deployment scenarios. The enhanced network dynamicity and resilience has been presented by routing multiple-wavelengths to a single user via a radio link.

The optical network transparency to WiMAX channels has been demonstrated through the obtained EVM figures of -31 dB for 64-QAM WiMAX downstream channels, measured at the ONU/BS antenna inputs as required by the standard. In addition, a 4 dB power penalty downstream and 0.7 dB upstream was monitored for 70 Mbit/s and 40 Mbit/s channels respectively transmitted over a combined 20km PON and 430m AWGN wireless path in the absence of channel error coding and relay techniques. Furthermore, minimum BERs of 1E-4 for the two channels were obtained bidirectionally over 330m, SUI-4 overlapping cell circumferences.

Finally, the ability of the architecture to support multiple radio-PONs on a single AWG offers a cost-effective solution for service delivery to a large number of remote users, since its deployment is of significantly lower cost in relation to traditional wireless solutions.

References

[1] M. Milosavljevic, P. Kourtessis, A. Gliwan, and J. M. Senior, "Advanced PON topologies with wireless connectivity," presented at 11th International Conference on Transparent Optical Networks, ICTON '09. , 2009.

[2] M. Milosavljevic, P. Kourtessis, and J. M. Senior, "Multi-Wavelength WiMAX–PONs With Overlapping Cells," *J. Opt. Commun. Netw.*, vol. 3, pp. 172-177, (2011).

[3] M. Milosavljevic, P. Kourtessis, and J. M. Senior, "Wireless-PONs with Extended Wavelength Band Overlay," presented at Access Networks and In-house Communications (ANIC), OSA Technical Digest (CD), (Optical Society of America, 2010), 2010.

[4] M. Milosavljevic, M. P. Thakur, P. Kourtessis, J. E. Mitchell, and J. M. Senior, "A Multi-Wavelength Access Network featuring WiMAX Transmission over GPON Links," presented at Proceedings of European Conference on Networks and Optical Communication (ECOC), 2010.

[5] W. Hofmann, E. Wong, G. Bohm, M. Ortsiefer, N. H. Zhu, and M. C. Amann, "1.55-um VCSEL Arrays for High-Bandwidth WDM-PONs," *Photon. Technol. Lett.*, vol. 20, pp. 291-293, (2008).

[6] M. Maier, "WDM Passive Optical Networks and Beyond: the Road Ahead (Invited)," *IEEE/OSA J. Opt. Commun. Netw.*, vol. 1, pp. C1-C16, (2009).

[7] *Enhancement band for gigabit capable optical access networks*, ITU-T G.984.5, 2007

[8] F. Effenberger, H. Mukai, P. Soojin, and T. Pfeiffer, "Next-generation PON-part II: candidate systems for next-generation PON," *IEEE Communications Magazine*, vol. 47, pp. 50-57, (2009).

[9] S. W. Peters and R. W. Heath, "The Future of WiMAX: Multihop Relaying with IEEE 802.16j," *IEEE Communications Magazine*, vol. 47, pp. 104-111, (2009).

[10] E. Kapon, "Developments of long-wavelength VCSELs," presented at IEEE 21st International Semiconductor Laser Conference, ISLC, 2008.

[11] T. Jayasinghe, C. J. Chae, and R. S. Tucker, "Scalability of RSOA-based multiwavelength Ethernet PON architecture with dual feeder fiber," *J. Opt. Netw.*, vol. 6, pp. 1025-1040 (2007).

[12] M. Milosavljevic, Y. Shachaf, P. Kourtessis, and J. M. Senior, "Interoperability of GPON and WiMAX for network capacity enhancement and resilience," *J. Opt. Netw.*, vol. 8, pp. 285-294, (2009).

[13] "IEEE Standard for Local and Metropolitan Area Networks Part 16: Air Interface for Fixed Broadband Wireless Access Systems," *IEEE Std 802.16-2004 (Revision of IEEE Std 802.16-2001)*, pp. 0_1-857, (2004).

[14] V. Erceg, L. J. Greenstein, S. Y. Tjandra, S. R. Parkoff, A. Gupta, B. Kulic, A. A. Julius, and R. Bianchi, "An empirically based path loss model for wireless channels in suburban environments," *J. Select. Areas Commun.*, vol. 17, pp. 1205-1211, (1999).

[15] *Gigabit-capable passive optical networks (GPON): Physical media dependent (PMD) layer specification*, ITU-T G.984.2, 2003

[16] *WiMAX Concepts and RF Measurements - IEEE 802.16-2004 WiMAX PHY layer operation and measurements* (Online). Available: http://cp.literature.agilent.com/litweb/pdf/5989-2027EN.pdf

[17] *JDSU Enabling Broadband and Optical Innovation* (Online). Available: http://www.jdsu.com/product-literature/awg100n_ds_cc_ae.pdf

[18] *IEEE 802.16 Broadband Wireless Access Working Group* (Online). Available: http://ieee802.org/16

[19] *VPI reference manual (VCSEL operation)* (Online). Available: http://www.vpiphotonics.com

[20] J. G. Proakis, *Digital Communications*, Fourth ed, 2001.

[21] S. Sarkar, S. Dixit, and B. Mukherjee, "Hybrid Wireless-Optical Broadband-Access Network (WOBAN): A Review of Relevant Challenges," *J. Lightw. Technol.*, vol. 25, pp. 3329-3340, (2007).

[22] K. N. Skalman, H. E. Sandstrom, and M. Gidlund, "Techno-Economical Study for Open Horizontal IPTV in the Access and Home Networks – from a Swedish Perspective," presented at Proceedings of European Conference on Networks and Optical Communication, 2008.

[23] *ARIB STD-T63-23.203 V8.5.0 "Policy and charging control architecture (Release 8)* (Online). Available: http://www.arib.or.jp/IMT-2000/V730Jul09/2_T63/ARIB-STD-T63/Rel8/23/A23203-850.pdf

Chapter 7

Experimental Investigation of WiMAX Transmission over Multi-Wavelength PONs

Contents

This chapter presents the network implementations presented in this thesis by experimentally demonstrating the application of wireless/wireline grooming across the architectures described in chapters 5 and 6. The OLT and ONU/BS sub-systems were widely implemented by readily-available Aeroflex PXI WiMAX transceivers, terminating either side the multi-wavelength, splitter-PON links. Performance evaluation criteria drawn to validate the experimental set-up include the EVM dependency of the WiMAX channels with respect to the MZM RF drive power in downstream, the equivalent EVM figure in upstream in view of the direct VCSEL modulation, and the BER characteristics drawn for extended fibre lengths and split ratios without any dispersion compensation techniques.

7.1 Network Architecture

A detailed diagram of the network architecture [1], incorporating the developed experimental setup is shown in Figure 7-1 (a snapshot of the set-up is included in appendix C.1). It has been previously established that inter-modulation products and link noise associated with the

137

transmission over the optical path could degrade the received radio signal quality at the remote base stations. VPI with MATLAB modelling results have confirmed EVM figures below -30 dB and -24 dB for downstream and upstream WiMAX channels respectively over 20 km of legacy PONs. The obtained EVM figures are in compliance with the WiMAX standard concluding that the optical fibre has negligible effect on the received WiMAX channels for certain drive powers of the MZM and drive currents of the DFB laser [2].
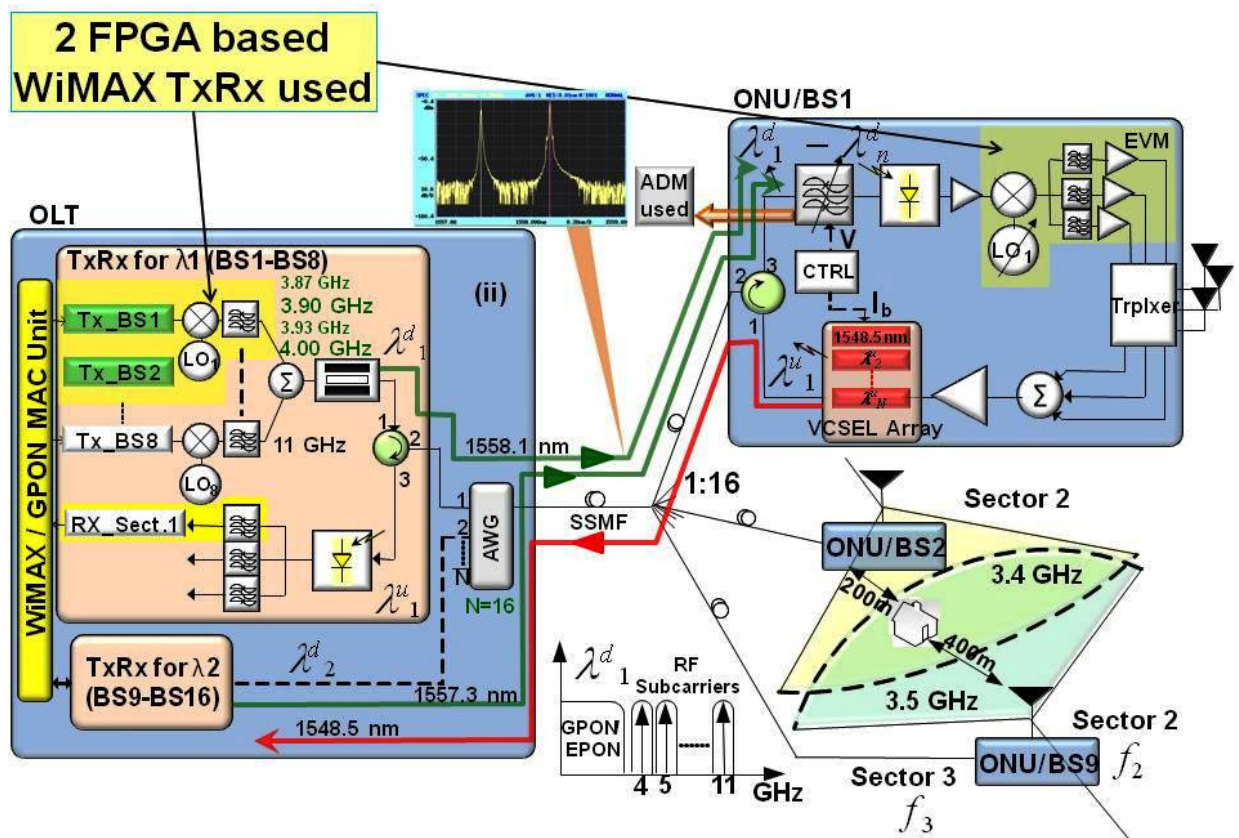
Figure 7-1: WiMAX over multi-wavelength splitter-PON and experimental setup

The experimental set-up portrays the key characteristics analysed in chapters 5 and 6 with the application of RoF by means of FDM to address individual base stations sharing a single wavelength being in the focus. To implement the ONU/BSs low-cost, long-wavelength VCSEL arrays and add/drop multiplexer, in the absence of a tuneable optical BPF, were employed. Transmission of the combined wireless/optical signals over the wavelength band overlay PON

was accomplished by the use of PXI Aeroflex [3] WiMAX transceivers, the specifications of which will be presented in subsequent sections.

7.2 Experimental Setup

In this experiment the mobile WiMAX IEEE802.16e specifications were consulted [4]. To that extent, this section emphasise on the generated WiMAX signals principle characteristics as well as the implemented experimental set-up backhauling the wireless channels over legacy PONs.

7.2.1 Radio Signal Generation

The specification data for each generated WiMAX channel distinguishing between upstream and downstream transmission is given in Table 7-1.

Table 7-1: Data sheet IEEE802.16-2005 WiMAX transceivers parameters [5]

	Downstream	Upstream
FFT size	1024	
Modulation	64-QAM	16-QAM
Coding	2/3	3/4
BW	10MHz	
RCE	-50dB	-25.8dB
Data rate	25.2Mbit/s	18.9Mbit/s

To outline its basic performance characteristics, of relative importance to the experimental set-up of this chapter, before being assigned to a subcarrier, the OFDMA symbols are coded and modulated. Channel coding is implemented by the application of convolutional codes. The encoded data is then passed to 64QAM and 16QAM modulators in downstream and upstream respectively. The modulated output in each case is then mapped and assigned to active subcarriers called sub-channels, formulating the OFDMA symbols. The latter are in the frequency domain and an inverse FFT is employed as a result to acquire their time domain equivalent.

The number of OFDMA subcarriers (corresponding to the FFT size) was selected according to standard deployments and was set to 1024. Consequently, for a 10MHz bandwidth, due to the limit of the Aeroflex RF output channels spacing, and 64-QAM modulation, the resulting aggregate data rate per sector for the downstream WiMAX link was specified at 25.2 Mbps. In view of 16-QAM modulation in upstream, the corresponding figure was defined at 18.9 Mbps. Important to stress out at this point, these data rates were calculated in view of guard and pilot subcarriers. These do not carry useful information but rather used for synchronisation and estimation purposes. A worst case scenario 25% cyclic prefix was also included. A standard 20 MHz WiMAX bandwidth [4], feasible with readily available VSGs and additional subcarriers would have increased the aggregate data rates. The downstream WiMAX channel transmitter relative constellation error (RCE) was -50 dB, a figure higher than the minimum required for 64-QAM modulation [4].

In addition, both TDM and FDM deployment options are available in a single service provider PHY. The FDM provision, adopted also by other 4G broadband wireless networks such as LTE [6], have a further capability of operating in either full or half-duplex modes.

According to the FDM mode, adopted for implementation in the experimental set-up, there are separate uplink and downlink sub-frames, which reside on different frequencies. Each frame begins with a preamble followed by a downlink transmission period and uplink transmission period. In each frame, the transmit transition gap (TTG) and receive transition gap (RTG) are inserted between the downlink and the uplink and at the end of the frame, respectively. This is done to allow the BS circuitry to change from transmit to receive mode.

7.2.2 WiMAX over PON Link Implementation

Four WiMAX channels, forming an FDM window, at the standard 3.5 GHz with 30 MHz subcarrier spacing were generated at the OLT. The number of generated WiMAX channels was defined by the limitation of the Aeoflex device. Ideally the number of generated WiMAX channels should match the passive optical network split and as a result for a targeted 1:16 split to comply with current deployments of legacy PONs, a minimum of 16 channels should be generated. This assumes that one or more ONU/BSs would require more than one WiMAX channels. The 30 MHz subcarrier spacing was chosen to match the Aeroflex receiver filter specifications.

To address individual ONU/BSs each WiMAX channel should be shifted in frequency from 3.5 GHz to any higher value that avoids adjacent channel interference. This was being achieved by using a predetermined local oscillator (LO) and BPFs in the OLT. In succession the WiMAX channels are combined and modulated onto an optical carrier. At ONU/BS, a LO is required, operating at the exact same frequency for a specific ONU/BS to downshift the appropriate WiMAX channels. Multiple BPFs are also needed to select each channel prior to transmission over the air.

The formed FDM signals in the OLT are then externally modulating by means of a Mach-Zehnder modulator (MZM) a commercially available distributed feedback (DFB) laser source.

The resulting signal (shown as inset in Figure 7-1) was then transmitted on λ_{d1}=1558.1 nm, through a circulator and a 16x1 AWG to an ONU/BS, using various lengths of standard single-mode fibre (SSMF) ranging from 23.2 km to 40.7 km. Having added the various optical component losses, including 7.75 dB for the MZM, 1 dB for the polarisation controller and 3.76 dB for the AWG in the system's OLT, 0.9 dBm optical power was launched into the fibre. Quite importantly if there was a requirement to accommodate legacy PONs over this

architecture for smooth network migration, this could be achieved by utilising the free spectral range of the AWG allowing 1490/1310 nm to be transmitted. To demonstrate the fixed to mobile convergence, a baseband (e.g. GPON) channel at 1.25 Gbit/s was also introduced.

Also significant to mention is that an additional un-modulated wavelength at λ_{d2}=1557.3 nm was connected at one of the unused AWG inputs to investigate interference at ONU/BSs.

Continuing downstream an optical attenuator was used after the fibre to account for various splitter loses. At the ONU/BS, a readily available add/drop multiplexer (ADM) was utilised prior to PIN detection as a substitute for a commercial 50 GHz optical band pass filter. The ADM drop port, at the wavelength of 1558.1 nm, produced a signal to interference ratio of 42 dB (as displayed Figure 7-2). The resulting up-converted WiMAX electrical spectrum was then down-shifted in frequency to get the original WiMAX channels and subsequently amplified by a 30 dB gain amplifier to perform performance evaluation measurements.
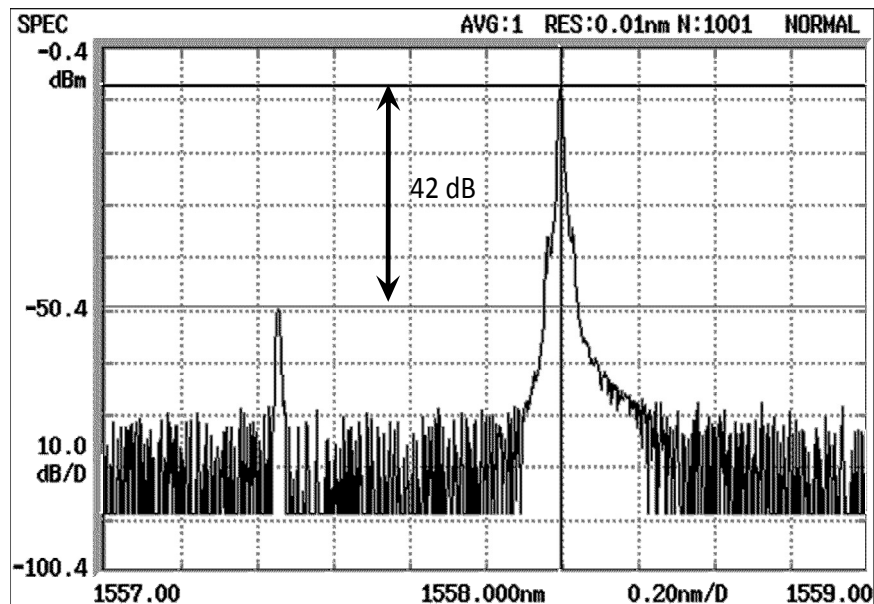
Figure 7-2: Output from the ADM

Complying with downstream, a single IEEE 802.16-2005, 3.5 GHz channel was generated in upstream to directly modulate a VCSEL at λ_{u1}=1548.5 nm. An 8.3 mA bias was used producing -0.94 dBm output power prior to being transmitted over the SSMF. Since the experimental investigations involve no signal transmission over a wireless channel, the upstream WiMAX transmitter RCE was set to -25.8 dB [4] to conform to the figure expected to be received at the base station in a practical scenario. The resulting optical signal was then routed through the corresponding AWG output port to the destination receivers (Rx_Sect.X) in the OLT where individual EVMs are measured.

7.3 Routing Performance Experimental Results

To establish accurate signal routing to and from an ONU/BS, received EVMs for the WiMAX channels and BERs for the GPON signals were experimentally investigated, aiming to confirm the routing simulation results produced in chapters 5 and 6.

To that extent, the four frequency shifted WiMAX channels generated prior to MZM modulation are initially observed and displayed in Figure 7-3. As expected and based on the RCE of the WiMAX channel shown in Table 7-1, the signal to noise ratio at the output of the Aeroflex PXI transmitter was 50 dB. The average power for the measurement channel at 4 GHz was +0 dBm. However, this power was varied in order to observe the effect of inter-modulation distortions due to the use of the MZM.
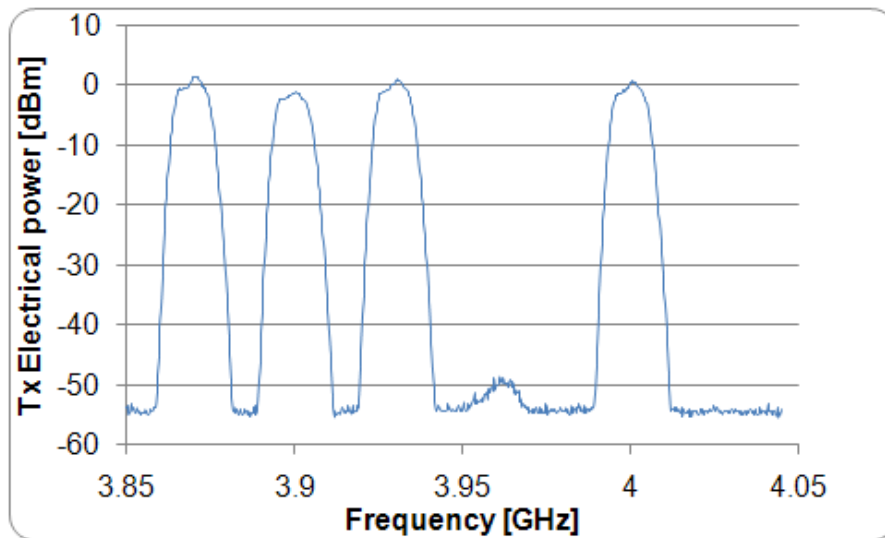
Figure 7-3: Obtained EVM for 3.5 GHz WiMAX channel at remote antenna downstream

After being modulated on the optical carrier and transmitted over the fibre, the spectrum of the combined electrical signal is shown in Figure 7-4 (left). The baseband signal extending up to 1.25 GHz can be clearly seen populating the corresponding spectrum alongside the up-converted WiMAX channels at 4 GHz. The power of the received signal before any electrical amplification is around -40 dBm. The measured BER of the GPON signal, after being

transmitted over 23.2 km fibre, was 1E-11, demonstrating error-free transmission for the wired users.
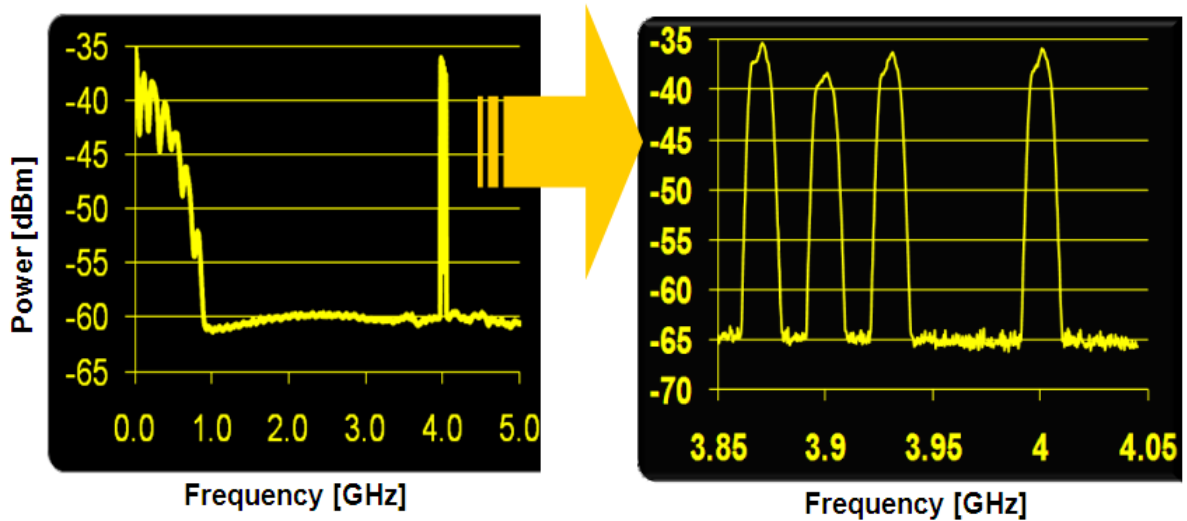
Figure 7-4: Electrical spectrum after PIN

Alternatively, in order to measure the effect of intermodulation distortion, following their application at the MZM RF input, and evaluate the associated degradation superimposed on the received WiMAX channels (Figure 7-4 (right)) at the ONU/BS receivers, the Aeroflex output power was varied between -2 dBm and +14 dBm.

To that effect the EVM characteristic of a selected WiMAX channel was drawn at the remote antenna input of the corresponding ONU/BS as a function of the MZM RF drive power. This is displayed in Figure 7-5 for varying fibre lengths and network splits to define the maximum reach and splitting ratio attainable with a fully passive infrastructure. The plots drawn in Figure 7-5 confirm in all cases that at low RF drive powers the signal is mainly distorted by noise while at high powers, EVM increases due to nonlinear effects.
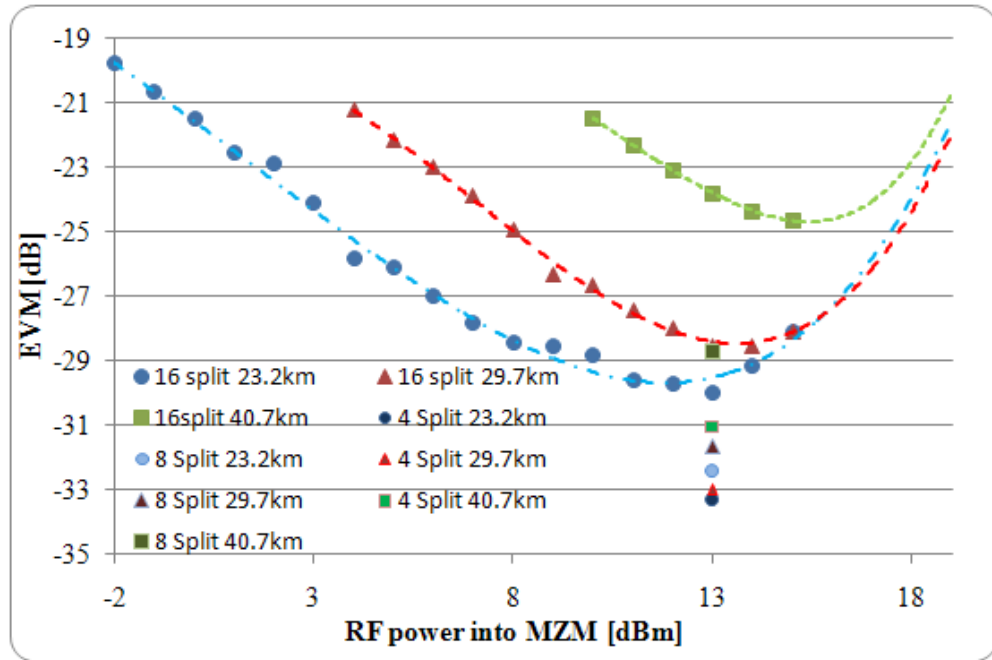
Figure 7-5: Obtained EVM for 3.5 GHz WiMAX channel at remote antenna downstream

To comply with the WiMAX downstream requirements for 64-QAM 2/3, an EVM figure above -30 dB should be achieved at the bottom of the bathtub curve. This is achieved in the experimental setup for a 23.2 km fibre and 16 split with RF input power into the MZM ranging between +11dBm and +13 dBm and a moderate +1dBm power lunched into the fibre. Suggested by the longer reach, reduced split responses in Figure 7-5, measuring 40.7 km and 8-split respectively, a justifiable increase in the fibre launch power would allow enhanced length-splitting ratios. This is expected to be achieved in a practical network by the optimisation of OLT network component losses according to specifications. Comparable results were confirmed for all WiMAX channels.

The power of the received WiMAX signals at an ONU/BS was determined at approximately -40 dBm being within the range of input powers required for linear operation of the high power amplifier for transmission over the air.

Similarly EVM measurements were performed at the OLT receiver in the upstream as shown in Figure 7-6, as a function of the VCSEL RF input power. This is purely investigated in order to establish the signal degradation between a base station and the OLT. To that extent, an EVM of -23 dB was recorded over 23.2 km of fibre with 16 split. The interaction of VCSEL laser chirp and fibre dispersion in analog optical modulation upstream had negligible effect on the received WiMAX channels in the OLT. Longer fibre lengths were not considered due to the VCSEL output power limitation. Taking into consideration that a +0 dBm VCSEL power was launched into the fibre, higher output power profile VCSEL arrays [7] are expected to significantly reduce the EVM penalties.
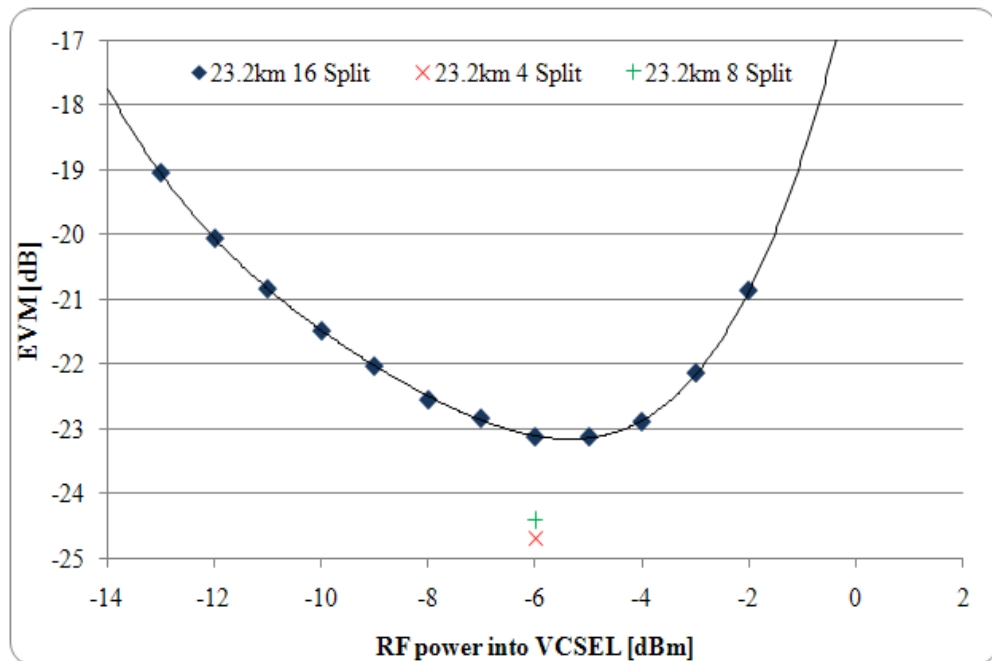
Figure 7-6: Obtained EVM at the WiMAX OLT receiver for 3.5 GHz channel

The resemblance of experimental and simulation results, in relation to EVM, confirm that network modelling, in view of the rigid selection of its design parameters, can approximate an equivalent experimental test-bed with accuracy. Therefore, it can be concluded, that the proposed optical network provides a transparent channel for standard wireless signal formats transmitted bi-directionally over a multi-wavelength power-splitting PON.

147

Finally, the constellation diagrams obtained at the WiMAX receivers after 23.2 km fibre and 16 split are displayed in Figure 7-7. The RF drive power in the MZM was +13 dBm and -6 dBm for downstream and upstream respectively since these powers are considered optimum for the lowest received EVM. It is important to note that no phase rotations could be observed since the constellation diagrams are obtained after the amplitude and phase correction, in contrast to the simulation results presented in the previous chapter. The two outermost points on the constellations are the pilot tones used for synchronisation and estimation purposes.
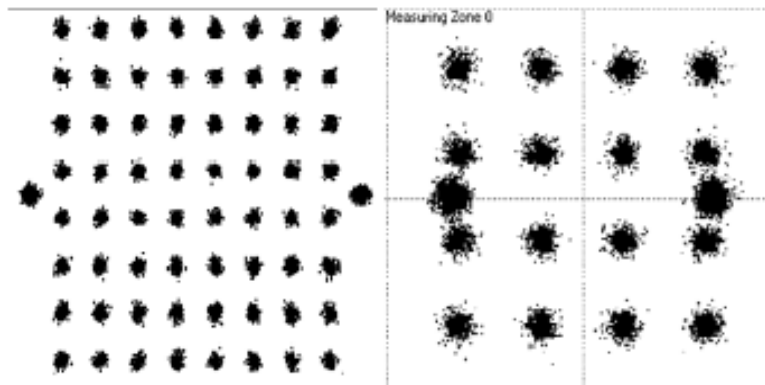
Figure 7-7: 64-QAM Downstream (left) and 16-QAM upstream (right) modulation

7.4 Summary

This chapter summarised the performance figures produced by the experimental demonstration of WiMAX transmission over legacy PONs and their resemblance to the modelling results presented in proceeding chapters. This was achieved by the application of the Aeroflex PXI IEEE802.16-2005 WiMAX transceivers, terminated at the OLT and ONU/BSs of the multi-wavelength PON with the aim of substantiating the simulation results that recommended the feasibility and performance validity of the original network architecture.

To demonstrate fixed-to-mobile convergence, a BER of 1E-9 has been initially demonstrated for wired users, featuring error-free GPON transmission by means of FDM propagation over multi-wavelength, power-splitting links.

In addition, experimental results have confirmed EVM figures, at remote base stations and the OLT receiver, below -29 dB and -23 dB for 25.2 Mbit/s and 18.9 Mbit/s, downstream and upstream WiMAX channels respectively, being in compliance with IEEE 802.16-2005 standards. Higher data rates however could be achieved with wider WiMAX bandwidths. Significantly, 40 km downstream transmission without any dispersion compensation was also readily achieved.

Finally, direct VCSEL laser modulation in upstream has shown negligible degradation on the received WiMAX channels in the OLT demonstrating low-cost colourless ONU/BS termination with simple couple optics.

References

[1] M. Milosavljevic, M. P. Thakur, P. Kourtessis, J. E. Mitchell, and J. M. Senior, "A Multi-Wavelength Access Network featuring WiMAX Transmission over GPON Links," presented at Proceedings of European Conference on Networks and Optical Communication (ECOC), Sept. 2010.

[2] M. Milosavljevic, P. Kourtessis, and J. M. Senior, "Wireless-PONs with Extended Wavelength Band Overlay," presented at Access Networks and In-house Communications (ANIC), OSA Technical Digest (CD), (Optical Society of America, 2010), 2010.

[3] *Aeroflex Test Solutions* (Online). Available: http://www.aeroflex.com/

[4] "IEEE Standard for Local and metropolitan area networks Part 16: Air Interface for Fixed and Mobile Broadband Wireless Access Systems Amendment 2: Physical and Medium Access Control Layers for Combined Fixed and Mobile Operation in Licensed Bands and Corrigendum 1," *IEEE Std 802.16e-2005 and IEEE Std 802.16-2004/Cor 1-2005 (Amendment and Corrigendum to IEEE Std 802.16-2004)*, pp. 0_1-822, (2006).

[5] *WiMAX forum* (Online). Available: http://www.wimaxforum.org/home/

[6] D. Astely, E. Dahlman, A. Furuskar, Y. Jading, M. Lindstrom, and S. Parkvall, "LTE: the evolution of mobile broadband - LTE part II: 3GPP release 8," *IEEE Communications Magazine*, vol. 47, pp. 44-51, (2009).

[7] W. Hofmann, E. Wong, G. Bohm, M. Ortsiefer, N. H. Zhu, and M. C. Amann, "1.55-um VCSEL Arrays for High-Bandwidth WDM-PONs," *Photon. Technol. Lett.*, vol. 20, pp. 291-293, (2008).

Chapter 8

Project Achievements and Future Work

Contents

This chapter serves the purpose of summarising the simulation and experimental work performed in the course of this research programme. In particular, a leading-edge wireless/optical access network architecture has been developed and demonstrated, providing high capacity backhauling links to support emerging broadband wireless solutions.

8.1 Research Drive

While both data (driven by an increasingly media-centric Internet) and video (driven by the adoption of new high definition hardware and content) services continue to see enormous increase in bandwidth demand, the access and metropolitan telecommunications network hierarchy remain relatively underdeveloped compared to the high capacity backbone networks. To overcome this ultra-broadband bandwidth "bottleneck" as far as the end user is concerned, optical fibre networks provide a future-proof solution for meeting the growing demand with guaranteed expansion possibilities, since the copper solution using digital subscriber line transmission techniques is approaching its theoretical capacity. However, the considerable fibre cabling cost and low levels of equipment sharing (especially in least densely populated areas) make the deployment of fully end-to-end active fibre optic networks currently impractical, pointing towards the solution of PONs.

This thesis has commenced by providing a justification as to why PONs have accomplished recognition from incumbents as a cost effective solution to form the basis for developing broadband access networks [1, 2] with subscriber bandwidths reaching more than 100 Mbit/s in the near future [3]. Owing to varying requirements and business plans of network operators and governments, Asia and North America constitute the worldwide leaders in the deployment of TDM-PON infrastructures, compared to Europe that although has developed plans for vast deployment in the coming years has only accommodated so far only a few fibre deployment projects as a result of the regulatory environment uncertainties. On the other extreme, South Korea has adopted primarily WDM-PON architectures to provide subscribers high dedicated bandwidth although the WDM-PON has not been yet standardised [2]. Elsewhere, WDM-PONs are currently not the preferable solution from the operators point of few since AWGs reduce network flexibility while providing for low resource utilisation per wavelength.

To allow higher bandwidth, greater coverage and penetration than the currently deployed standards, various potential research paths for building next-generation PONs have been undertaken, with a common aim to support new bandwidth-hungry online services and further reduce the cost for delivering the existing ones [4]. These initiatives include the increase of PON aggregate data rates to 10 Gbit/s [5-9] complemented by extending their physical reach and split to distances of at least 100 km [10, 11], offering economical bandwidth and service upgrade from the end-user all the way up to the core network at significantly reduced cost for network operators. An alternate path, aspects of which have very recently been standardised [12], considers multiple wavelength operation over standard splitter PONs to allow 2-D allocation of network resources and a smooth migration for the future.

In addition, broadband wireless standards have evolved from traditionally voice-based mobile networks to data-centric networks allowing hundreds of Mbits/s and large number of users

exploiting the OFDM modulation concept [13]. To that extent, several key network elements that emerged from various research paths are used to enhance data throughput, such as the application of multiple antenna techniques (MIMO) [14], adaptive modulation and coding [13], and relay re-transmission for increased coverage [15]. Alternatively, utilisation of lower frequency bands, around 700 MHz, has also provided the potential to support even higher data rates due to the large available bandwidth at these frequencies [16].

However, in order to achieve gigabit spectral efficiency across a cell or a sector, densely populated base stations need to be deployed [17]. This would result in higher network deployment cost as the number of base stations required to cover a certain area is increased. Significantly, high capacity backhauling links are then needed to connect these base stations to ISPs.

The wireless/optical integration has been investigated in this direction as a potential low-cost solution, expected to have a large impact on the economics of near-term access deployment [17]. As a result, combining the merits of the high bandwidth xPON solutions with the mobility and flexibility provided by the cost-effective, wireless networks, effectively address the challenges of next-generation access networks articulated by transparency, smooth upgradability, scalability and dynamicity [18].

Since the projected network could facilitate the support of multiple operators and multiple technologies within the same infrastructure, it is expected to provide a natural environment for healthy competition among European network and service providers that will revitalize the European market and reinforce its competitiveness.

8.2 Achievements

In order to meet the above challenges, this work introduced a novel hybrid optical access network architecture. It is intended not only to offer mobility over TDMA-PON solutions but also inherently provide the opportunity for convergence between optical and radio access, supporting seamless ubiquitous broadband services. The architecture provides a variety of desirable network characteristics, like high bandwidth backhauling links, increased radio spectral efficiency and scalability, enhanced resource allocation flexibility, lower equipment cost/complexity and reduced power consumption, while supporting multi-wavelength operation.

In that direction, this thesis has provided the justification, design criteria, implementation and evaluation both in the form of a comprehensive VPI/MATLAB simulation platform and test-bed experimentations for an innovative approach employing RoF transmission [19] complemented with FDM to address individual simplified remote base station antennas. Extended wireless network features in the form of overlapping cells were also evaluated to enhance the capacity and provide network resilience.

The property of the network to use FDM also added to the network dynamicity since multiple subcarriers could be dropped to a single base station thus increasing its capacity. This can be controlled centrally from the OLT. FDM also provides for wireless signal transparency avoiding interference with the legacy PON spectrum if transmitted on the same wavelength. Therefore, this novel network is easily extendable to support emerging broadband wireless standards including LTE and its upgrades.

A feature in upstream, is that ONU/BSs receive time-interleaved WiMAX channels, avoiding at the optical receiver in the OLT any potential OBI. This could, however, result in restricting the bandwidth utilisation efficiency for the wireless users. Also, a single wavelength approach could impose high dispersion penalties across the fibre as the number of frequency subcarriers

in the FDM window would be increased, to address larger number of ONU/BSs. As a result, increased network penetration could require sophisticated, high bandwidth optical and electrical components.

To overcome the above issues, an enhancement solution of the access network architecture was developed, both in software and hardware integrating the standard wireless signal formats over a multi-wavelength splitter-PON, again based on RoF. FDM was still applied to address individual base stations sharing each of the utilised wavelengths. Apart from different wavelengths transmitting different FDM windows, the proposed system also allows for a given FDM window to be propagated on multiple wavelengths. This relaxes significantly the bandwidth requirements of optical and electrical devices while enhancing the network scalability. This extended wavelength band overlay scheme overcomes the need for complex dispersion compensation techniques as it avoids the use of high frequency subcarriers in each FDM window.

The overall network performance has been initially evaluated by means of a powerful simulator incorporating extensive functionalities of RF transceivers and wireless propagation media as well as the complete building blocks of PONs including propagation degradation and end-to-end power budgeting engineering. The compliance of the developed simulator to the individual wireless and optical specifications has been established by the demonstration of an experimental set-up and the direct comparison of the obtained performance figures. For WiMAX routing over xPON architectures, inclusive OFDM transmitters and receivers are devised in VPI in co-simulation with MATLAB, utilising all necessary functional blocks. The latter include symbol mapping, a 256 point IFFT, 1/4 cyclic prefix and DAC conversion with 14-level quantisation. Square root-raised-cosine filters with 25% roll of were also used for I and Q ISI minimisation prior to RF up-conversion. The bandwidth of these filters is equivalent to the OFDM symbol

duration defined by its bit rate divided by the number of bits per symbol. The OFDM receivers perform similar scale FFT and interfaced to MATLAB through for further processing.

Critically, the additive distortion of the high power amplifier (HPA) on the transmitted WiMAX signals is modelled in VPI. A limiter block is used for representing nonlinear transfer function characteristics exhibiting amplitude clipping and consequently distorting transmitted signal to noise ratio. Limiter amplitudes of 0.68V and -0.68V were required to achieve -31dB EVM figures, the maximum allowed for 64-QAM modulation in WiMAX.

For wireless transmission, a SUI-4 wireless channel model is presented, evaluating practical multi-path radio signal transmission followed by BER estimation for various cycle prefixes. The maximum of three paths were included where a K of zero for all paths demonstrates non-line-of-sight wireless link between the transmitter and the receiver. Finally, the channel imposes maximum delay and attenuation of 4 µs and 20 dB respectively on the received signal. The OFDM symbol duration is initially calculated and used for variance calculations by the *CIRpowers* function that calculates variance for each path of the channel.

Finally, once the variance for each path has been calculated the *genh* function is then used to generate the Rayleigh channel coefficients according to the specific SUI type. This is achieved by utilising the Jakes Model to add sinusoids for generating the fading coefficients.

Following the simulator development and individual subsystem testing, propagation evaluation figures were drawn to establish its transmission merits. The network design was modified from its preliminary set-up, accounting for a dense AWG in the OLT and a tuneable filter with a VCSEL array [20] in each ONU/BS to provide for efficient wavelength routing and low-cost colourless upstream transmission. Significantly, to account for the wireless channel degradation properties and distance limitations, in order to emulate the overlapping cells/sectors properties, the VPI/MATLAB models were revised to include noise and therefore introduce the receiver

power sensitivity. The path loss of the channel was calculated based on empirical models taking into consideration parameters such as base station antenna height, gain and loss, to mention a few.

Multiple IEEE802.16d channels, with 70 Mbit/s downstream and 40 Mbit/s upstream data rates, were frequency shifted around the same RF carrier and transmitted on two different wavelengths. The obtained results have demonstrated standard EVMs of -31 dB at ONU/BS remote antenna inputs and minimum 1E-4 BERs bidirectionally over combined 20km optical and 330m faded overlapping micro-cells circumference without any error coding or relay techniques. The application of a low-cost, long-wavelength VCSEL array in upstream for colorless transmission demonstrated a 0.7 dB power penalty on the received WiMAX channels in the OLT.

Furthermore, in order to validate the new integrated access network core features, an experimental test-bed was implemented to demonstrate bidirectional WiMAX routing over xPON. Readily-available Aeroflex PXI WiMAX transceivers, terminating either side of the multi-wavelength, splitter-PON links were employed. Also, an add/drop multiplexer was used inside each ONU/BS instead of tuneable optical filters. Before being assigned to a subcarrier, the OFDMA symbols are coded and modulated using convolutional coding and 64QAM downstream, 16QAM upstream modulators respectively. The formulated OFDMA symbols are then applied to an inverse FFT producing their time domain equivalent. The number of OFDMA subcarriers (corresponding to the FFT size) was selected according to standard deployments and was set to 1024. Consequently, for a 10MHz bandwidth, due to the limit of the Aeroflex RF output channels spacing, and 64-QAM modulation, the resulting aggregate data rate per sector for the downstream WiMAX link was specified at 25.2 Mbps. In view of 16-QAM modulation in upstream, the corresponding figure was defined at 18.9 Mbps. These data

rates were calculated in view of guard and pilot subcarriers used for synchronisation and estimation purposes. A worst case scenario 25% cyclic prefix was also included. The downstream WiMAX channel transmitter relative constellation error (RCE) was -50 dB, a figure higher than the minimum required for 64-QAM modulation.

Four WiMAX channels, forming an FDM window, at the standard 3.5 GHz with 30 MHz subcarrier spacing were generated at the OLT. The number of generated WiMAX channels was defined by the limitation of the Aeoflex device. Ideally the number of generated WiMAX channels should match the passive optical network split and as a result for a targeted 1:16 split to comply with current deployments of legacy PONs, a minimum of 16 channels should be generated. This assumes that one or more ONU/BSs would require more than one WiMAX channels. The 30 MHz subcarrier spacing was chosen to match the Aeroflex receiver filter specifications.

To address individual ONU/BSs each WiMAX channel should be shifted in frequency from 3.5 GHz to any higher value that avoids adjacent channel interference. This was being achieved by using a predetermined local oscillator (LO) and BPFs in the OLT. In succession the WiMAX channels are combined and modulated onto an optical carrier. At ONU/BS, a LO is required, operating at the exact same frequency for a specific ONU/BS to downshift the appropriate WiMAX channels. Multiple BPFs are also needed to select each channel prior to transmission over the air. Also significant to mention is that an additional un-modulated wavelength at λ_{d2}=1557.3 nm was connected at one of the unused AWG inputs to investigate interference at ONU/BSs.

Complying with downstream, a single IEEE 802.16-2005, 3.5 GHz channel was generated in upstream to directly modulate a VCSEL at λ_{u1}=1548.5 nm. An 8.3 mA bias was used producing -0.94 dBm output power prior to being transmitted over the SSMF. Since the experimental

investigations involve no signal transmission over a wireless channel, the upstream WiMAX transmitter RCE was set to -25.8 dB to conform to the figure expected to be received at the base station in a practical scenario [3]. The resulting optical signal was then routed through the corresponding AWG output port to the destination receivers (Rx_Sect.X) in the OLT where individual EVMs are measured.

In order to measure the effect of intermodulation distortion, following their application at the MZM RF input, and evaluate the associated degradation superimposed on the received WiMAX channels at the ONU/BS receivers, the Aeroflex output power was varied between -2 dBm and +14 dBm. To that effect the EVM characteristic of a selected WiMAX channel was drawn at the remote antenna input of the corresponding ONU/BS as a function of the MZM RF drive power.

Experimental results indicated 40 km downstream transmission with 8-split without any dispersion compensation. A justifiable increase in the fibre launch power would allow enhanced length-splitting ratios. This is expected to be achieved in a practical network by the optimisation of OLT network component losses according to specifications. Comparable results were confirmed for all WiMAX channels. The application of directly modulated VCSEL lasers in upstream has shown negligible degradation to the received signal in the OLT over 23.2 km of fibre with 16 split. Longer fibre lengths were not considered due to the VCSEL output power limitation. Taking into consideration that a +0 dBm VCSEL power was launched into the fibre, higher output power profile VCSEL arrays readily available are expected to significantly reduce the incurred EVM penalties. In that direction, IEEE 802.16-2005 standards compliance was demonstrated with EVM figures below -29 dB and -23 dB for 25.2 Mbit/s and 18.9 Mbit/s, downstream and upstream respectively alongside 1E-11 BERs for the GPON signalling.

159

8.3 Future Work

This section summarises the key network features that could be further investigated, either through an independent research programme or through a FP7 consortium [21]. According to research initiatives the next generation network consolidation is seen as general trend for future OPEX and CAPEX optimization [1]. Extending the reach of the access segment will possibly facilitate simpler network structures, with fewer metro and core COs collecting the traffic from/to wide network areas. This consolidation will enable optimum use of network resources (shared by a large numbers of users), a relevant reduction on operation and maintenance costs and important real-state savings. Extended reach capabilities are crucial also for scenarios such as rural deployments that would not be feasible, either in a technical or economical way, using currently available technologies. Therefore, the scalability of the architecture should be further explored by investigating its ability to demonstrate a long reach converged optical/wireless network with low deployment cost.

However, the long fibre links, in the range of 100 km, could result in high latencies for radio signals and high power adjacent channel interference. Latency is typically introduced since the exchange of communication concerning the wireless channel management and control is delayed resulting, for example, in decreased spectral efficiency across a cell. This could be resolved by the introduction of an intermediate node, middle office (MO), between the CO and a remote base station where all the base station functionalities could be located. The MO will be also responsible for generation and transmission of RoF carriers over 20 km of fibre only, as has been demonstrated in Figure 8-1 below. The enhanced Node Bs (eNBs) are the typical base stations encountered in the next generation LTE deployments performing signal generation, detection and scheduling. The notation P1 in Figure 8-1 represents that signal processing is split between remote base station and MO.
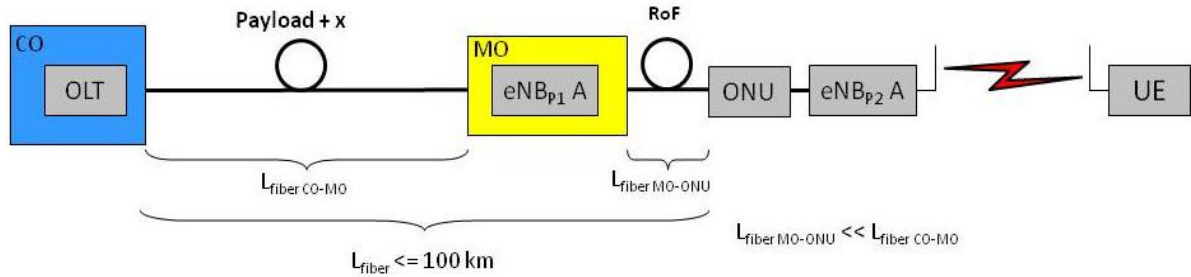
Figure 8-1: Long reach optical/wireless integration (MO: middle office, eNB: enhanced Node B, UE: user interface) [22]

To that extent, the delay associated with 100 km fibre transmission is reduced since the time sensitive wireless data is transmitted only over 20 km (between eNB_{p1} and eNB_{p2}). It is important to note that the centralised wireless processing is performed in the MO instead of CO.

Such a configuration would contribute massively towards the business plans of network operators in increasing bandwidth to support emerging media-rich services with mobility to potentially offer significant CAPEX and OPEX savings in an incorporate access/metro infrastructure.

The efficiency of the architecture should be further explored by investigating the benefits gained by centralised processing, considered also as an important aspect of the integrated optical/wireless networks. In particular, multi-site transmission schemes, such as co-ordinated scheduling with beamforming antennas and joint processing, could be simplified with the application of RoF, as detailed below [22]. These two schemes are important features in order to reduce interference and increase capacity respectively.

In standard wireless network deployments exchange of interference measurements is typically performed by X2 logical interfaces, as shown in Figure 8-2 [13]. Therefore, this imposes stringent requirements on the backhauling links (mainly the maximum distance and capacity) supporting these base stations.
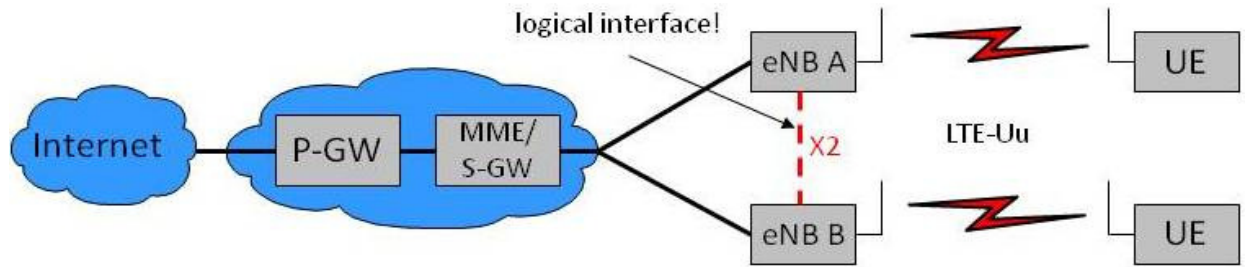
Figure 8-2: LTE network architecture (P-GW: packet gateway, S-GW: service getaway, MME: mobility management unit) [22]

However, with the application of centralised processing the X2 logical interface could be shifted at the CO, as shown in the Figure 8-3. Therefore, inter eNB communication is limited in CO which could result in decreased delay and higher capacity on the wireless links.
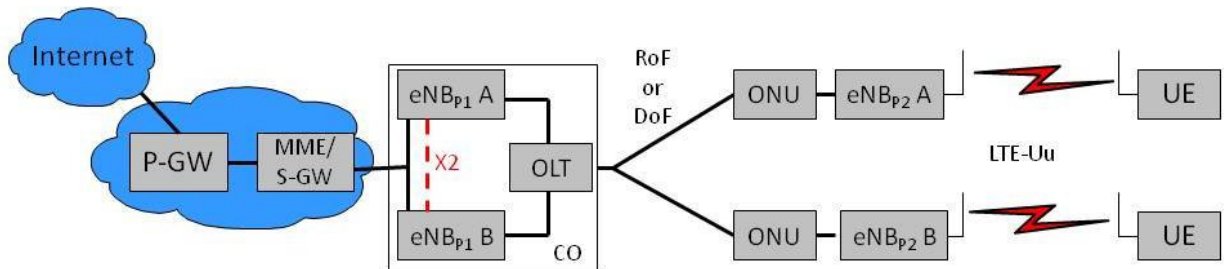
Figure 8-3: An example of xPON backhauling for LTE [22]

In addition to the above, the architecture presented in this thesis is based on the assumption that a frequency reuse pattern of 1:3:3 is used where each base station antenna covers three sectors operating at different frequencies. However, in some recent deployment scenarios frequency reuse of one has been considered where each sector is supported by the same frequency. In this case, additional LOs are needed at an ONU/BS for each sector in order to avoid interference with other base stations addressed with FDM on the same PON. Also, in order to reduce interference in overlapping sectors caused by the frequency reuse pattern of one, in a similar manner to co-ordinated scheduling, efficient network management at the CO without introducing unnecessary delay into the system should be investigated.

Finally, as an alternative to RoF a digital-over-fibre (DoF) variants could be considered as well where analog wireless RF/IF data are first digitised prior to transmission over the fibre. This offers the advantages of exploiting mature digital optical communications hardware and network interfaces while providing for a high performance microwave signal distribution framework [23]. However, as a direct result of digitization, the data rate of the optical link is a product of sampling resolution and the sampling frequency. The relative cost advantage of DoF over analog RoF from the optoelectronics perspective will depend on whether the data-rate or the maximum RF frequency is high. In FDM systems the sampling rate depends strongly on the wireless RF frequencies as well as their fractional bandwidth used to carry data. As the RF frequency increases when applications move to high frequency bands, the implementation of DoF becomes more challenging.

Firstly, the electronic sampling sub-systems need to be able to accommodate these high RF frequencies increasing their cost in parallel with that of the RF. The second aspect arises from the fact that overall data rate for the digital optical link can be excessively high, thereby negating the cost benefit of DoF over analog RoF implementations [23].

On the other hand, digital transmission based on the CPRI [24] is clearly allowing deployment of distributed base station antennas with high flexibility and low deployment cost. The CPRI technology is defining key internal interface of radio base stations between the Radio Equipment Control (REC) and the Radio Equipment (RE), as shown in Figure 8-4. With a clear focus on layer 1 and layer 2 the scope of the CPRI specification is restricted to the link interface only, which is basically a point to point interface. Such a link shall have all the features necessary to enable a simple and robust usage of any given REC/RE network topology, including a direct interconnection of multiport REs. To that extent CPRI provides for simple remote radio heads since all the signal processing is performed centrally.

163
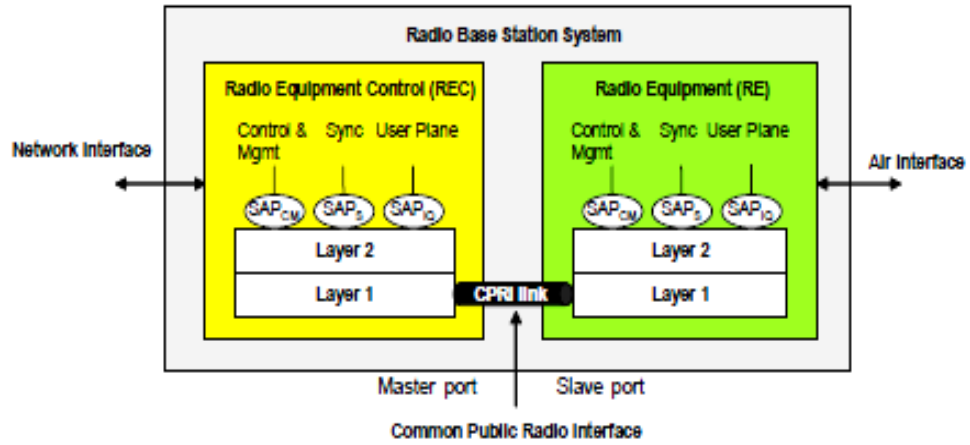
Figure 8-4: CPRI general block diagram [24]

The main drawback of this solution is in order to support the most recent OFDMA-based standards such, as WiMAX and LTE with 20 MHz bandwidth, the total throughput required on the optical link is in the range of 2.5 Gbits/s. Therefore, high bandwidth backhauling links are required.

It can be concluded from the above discussion that the potential integration of RoF and DoF variants on the same integrated architectural platform could be beneficial and should be investigated further.

References

[1] J. i. Kani, F. Bourgart, A. Cui, A. Rafel, M. Campbell, R. Davey, and S. Rodrigues, "Next-generation PON-part I: technology roadmap and general requirements," *IEEE Communications Magazine*, vol. 47, pp. 43-49, (2009).

[2] C.-H. Lee, S.-M. Lee, K.-M. Choi, J.-H. Moon, S.-G. Mun, K.-T. Jeong, J. H. Kim, and B. Kim, "WDM-PON experiences in Korea (Invited)," *J. Opt. Netw.*, vol. 6, pp. 451-464, (2007).

[3] *Cisco Systems: Global IP Traffic Forecast and Methodology* (Online). Available: www.hbtf.org/files/cisco_IPforecast.pdf

[4] F. Effenberger, H. Mukai, P. Soojin, and T. Pfeiffer, "Next-generation PON-part II: candidate systems for next-generation PON," *IEEE Communications Magazine*, vol. 47, pp. 50-57, (2009).

[5] M. Hajduczenia, P. R. M. Inacio, H. J. A. Silva, M. M. Freire, and P. P. Monteiro, "10G EPON Standardization in the Scope of IEEE 802.3av Project," presented at National Fiber Optic Engineers Conference, 2008.

[6] *FSAN NGA* (Online). Available: http://www.fsanweb.org/nga.asp

[7] *IEEE Standard for Information technology - Telecommunications and information exchange between systems - Local and metropolitan area networks - Specific requirements Part 3: Carrier Sense Multiple Access with Collision Detection (CSMA/CD) Access Method and Physical Layer Specifications Amendment 1: Physical Layer Specifications and Management Parameters for 10 Gb/s Passive Optical Networks*, IEEE Std 802.3-2009 (Amendment to IEEE Std 802.3-2008), 2009

[8] K. Y. Cho, Y. Takushima, and Y. C. Chung, "10-Gb/s Operation of RSOA for WDM PON," *Photon. Technol. Lett.*, vol. 20, pp. 1533-1535, (2008).

[9]   F. Effenberger, H. Mukai, J. i. Kani, and M. Rasztovits-Wiech, "Next-generation PON-part III: system specifications for XP-PON," *IEEE Communications Magazine*, vol. 47, pp. 58-64, (2009).

[10] *Photonic Integrated Extended Metro and Access Network (PEIMAN)* (Online). Available: http://ist-pieman.org/techapp.htm

[11] L. G. Kazovsky, W. T. Shaw, D. Gutierrex, N. Cheng, and S. W. Wong, "Next-Generation Optical Access Networks," *J. Lightw. Technol.*, vol. 25, pp. 3428-3442, (2007).

[12] *Enhancement band for gigabit capable optical access networks*, ITU-T G.984.5, 2007

[13] D. Astely, E. Dahlman, A. Furuskar, Y. Jading, M. Lindstrom, and S. Parkvall, "LTE: the evolution of mobile broadband - LTE part II: 3GPP release 8," *IEEE Communications Magazine*, vol. 47, pp. 44-51, (2009).

[14] A. J. Paulraj, D. A. Gore, R. U. Nabar, and H. Bolcskei, "An Overview of MIMO Communications – A Key to Gigabit Wireless," presented at Proceedings of IEEE 2004.

[15] Y. Yang, H. Honglin, X. Jing, and M. Guoqiang, "Relay technologies for WiMax and LTE-advanced mobile systems," *IEEE Communications Magazine*, pp. 100-105, (2009).

[16] *WiMAX Forum Position Paper for WiMAX Technology in the 700 MHz Band* (Online). Available: www.wimaxforum.org

[17] N. Ghazisaidi, M. Maier, and C. Assi, "Fiber-wireless (FiWi) access networks: a survey," *IEEE Communications Magazine*, vol. 47, pp. 160-167, (2009).

[18] Y. Kun, O. Shumao, K. Guild, and C. Hsiao-Hwa, "Convergence of ethernet PON and IEEE 802.16 broadband access networks and its QoS-aware dynamic bandwidth allocation scheme," *J. Select. Areas Commun.*, vol. 27, pp. 101-116, (2009).

[19] C. Bock, T. Quinlan, M. P. Thakur, and S. D. Walker, "Integrated Optical Wireless Access: Advanced topologies for future access networks," presented at ICTON '09. 11th International Conference on Transparent Optical Networks, 2009.

[20] W. Hofmann, E. Wong, G. Bohm, M. Ortsiefer, N. H. Zhu, and M. C. Amann, "1.55-um VCSEL Arrays for High-Bandwidth WDM-PONs," *Photon. Technol. Lett.*, vol. 20, pp. 291-293, (2008).

[21] *ACCORDANCE: A Converged Copper-Optical-Radio OFDMA-based access Network with high Capacity and Flexibility* (Online). Available: http://ict-accordance.eu

[22] *ACCORDANCE: Deliverable 2.1 (D2.1)* (Online). Available: http://ict-accordance.eu

[23] *Fibre-Optic Networks for Distributed Extendible Heterogeneous Radio Architectures and Service Provisioning (FUTON)* (Online). Available: http://www.ict-futon.eu

[24] *Common Public Radio Interface (CPRI); Specificaiton v4.1*, http://www.cpri.info, 2009

Appendix **A**

Appendix A presents the MATLAB coding for wireles trancreceivers as well as multupath channel modelling. These models were used throughout the thesis for WiMAX signal generation and reception as well as for radio channel evaluation. Aspects of the this coding have been presented in [1]. Modifcations are included here to adopt the program to the proposed simulation platform.

A.1 MATLAB Coding for Co-Simulation with VPI

A.1.1 WiMAX OFDM Transmitter

```
%%%%%%%%%%%%%%%%%%%%%%%%%%%%%%%%%%%%%%%%%%%%%%%%%%%%%%%%%%%%%%%%%%%%%%%%%%%%
%%                                                                      %
%%      Name: ofdm_tx.m                                                 %
%%                                                                      %
%%      Description: It generates OFDM symbols by performing symbol mapping%
%%      and IFFT. It also adds CP and multi-path channel if needed. The    %
%%      output is fed to the VPI cosimulation interface                 %
%%                                                                      %
%%                                                                      %
%%      Parameters:                                                     %
%%                                                                      %
%%       TimeWindow, BitRate, NFFT, BitPerSymbol, CyclicPrefix, BitStream= %
%%       are passed from the VPI                                        %
%%       Cx=output complex IQ symbols        data_mapped=mapped symbols %
%%                                                                      %
%%%%%%%%%%%%%%%%%%%%%%%%%%%%%%%%%%%%%%%%%%%%%%%%%%%%%%%%%%%%%%%%%%%%%%%%%%%%

function Cx=ofdm_tx(TimeWindow,BitRate,Nfft,BitPerSymbol,CyclicPrefix,BitStream)

OFDM=[];
%
% SUI=4;
% BW=10;   %enabled only in upstream
%
% channel=channelSUI(SUI, CyclicPrefix, BW); % see A.3 for ch modelling

FrameLength=floor(Nfft*(1+CyclicPrefix));
NFrames=ceil(TimeWindow*BitRate/BitPerSymbol/FrameLength);

for i=1:NFrames
```

```
    data_mapped=cod(BitStream((i-
1)*BitPerSymbol*Nfft+1:i*BitPerSymbol*Nfft),BitPerSymbol);  %symbol mapping

    ofdm_symbol=sqrt(Nfft).*ifft(data_mapped,Nfft);

    margin=length(ofdm_symbol)*CyclicPrefix;

    SymbolTx=[ofdm_symbol((end-margin+1):end) ofdm_symbol]; %cyclic prefix
adding

    %Channel effect (enabled for upstream transmission)
%     NextSymbol = 8 .* sqrt(Nfft) .* ifft(randint(1,Nfft));
%     SymbolTx = [NextSymbol NextSymbol SymbolTx];      %introduce ISI
%     symbol_channel = filter(channel,1,SymbolTx);     %apply multi-path ch
%     symbol_channel = symbol_channel(end-(256*(1+CyclicPrefix))+1:end);

    OFDM=[OFDM  SymbolTx]; %concentating OFDM symbols


end

Cx=OFDM(1,1:TimeWindow*BitRate/BitPerSymbol); %ensuring sample rate
consistency with VPI
```

A.1.1.1 Symbol Mapping

```
%%%%%%%%%%%%%%%%%%%%%%%%%%%%%%%%%%%%%%%%%%%%%%%%%%%%%%%%%%%%%%%%%%%%%%%%%%%%
%%                                                                      %
%%     Name: cod.m                                                      %
%%                                                                      %
%%     Description: The function used in ofdm_tx for symbol mapping to   %
%%     required constellation.                                          %
%%                                                                      %
%%                                                                      %
%%     Parameters:                                                      %
%%      Y = output QAM symbols.         Bits = input PRBS bits          %
%%      m = constellation size.                                         %
%%                                                                      %
%%%%%%%%%%%%%%%%%%%%%%%%%%%%%%%%%%%%%%%%%%%%%%%%%%%%%%%%%%%%%%%%%%%%%%%%%%%%

function Y=cod(Bits,m)


Ns=length(Bits)/m; %Number of symbols
QAM=zeros(1,Ns);      %Variable initiation
Q=zeros(1,length(Bits)/2);
I=zeros(1,length(Bits)/2);

for k=1:(length(Bits)/2)
I(1,k)=Bits(1,2*k-1);   %I bitsream.  def used by QAM coder of TM in VPI
Q(1,k)=Bits(1,2*k);     %Q bitstram
end

for k=1:Ns
    x=0;
    y=0;
    for l=1:m/2
        x=x+2^(m/2-l)*(2*I(1,(k-1)*m/2+l)-1);
        y=y+2^(m/2-l)*(2*Q(1,(k-1)*m/2+l)-1);
```

```
      end
    QAM(1,k) = x + i*y;
  end
Y=QAM/(2^(m/2)-1);
```

A.2 WiMAX OFDM Receiver

```
%%%%%%%%%%%%%%%%%%%%%%%%%%%%%%%%%%%%%%%%%%%%%%%%%%%%%%%%%%%%%%%%%%%%%%%%%%%%
%%                                                                      %
%%      Name: OFDM_Rx.m                                                 %
%%                                                                      %
%%      Description: This function performs OFDM reception and channel  %
%%      equalisation. It also introduces ISI.                          %
%%                                                                      %
%%                                                                      %
%%      Parameters:                                                     %
%%       TimeWindow, BitRate, NFFT, BitPerSymbol, CyclicPrefix, BitStream= %
%%       are passed from the VPI                                        %
%%       IQ=output recovered symbols      channel=radio ch coef.        %
%%       SUI=type of radio ch            channel_reverse=equalisation   %
%%       SymbolTx=ISI distorted Tx symbol                               %
%%                                                                      %
%%                                                                      %
%%%%%%%%%%%%%%%%%%%%%%%%%%%%%%%%%%%%%%%%%%%%%%%%%%%%%%%%%%%%%%%%%%%%%%%%%%%%


function IQ = OFDM_Rx(TimeWindow,BitRate,I,Q,Nfft,BitPerSymbol,CyclicPrefix)

InputSignal=[I+j*Q];


SUI=4;  %type of SUI channel (out of 6)
BW=14;  %bandwidth in MHz

channel=channelSUI(SUI, CyclicPrefix, BW);  %Channel coefficient creation

FrameLength=floor(Nfft*(1+CyclicPrefix));
NFrames=floor(TimeWindow*BitRate/BitPerSymbol/FrameLength);

for i=1:NFrames

    Frame=InputSignal((i-1)*FrameLength+1:i*FrameLength);

    %Channel effect
    NextSymbol = 8 .* sqrt(Nfft) .* ifft(randint(1,Nfft));
    SymbolTx = [NextSymbol NextSymbol  Frame];
    symbol_channel = filter(channel,1,SymbolTx);  %applied channel
    symbol_channel = symbol_channel(end-(256*(1+CyclicPrefix))+1:end);

    S_symbolsRx(i,:)=receiver(symbol_channel,CyclicPrefix, Nfft);

    channel_reverse(i,:) = channelestimate(S_symbolsRx(i,:),channel);

end


ReceivedSignal=zeros(1,TimeWindow*BitRate/BitPerSymbol);

for u=1:NFrames
    ReceivedSignal(1,(u-1)*Nfft+1:u*Nfft)=    channel_reverse(u,:);
```

```
        end

IQ=ReceivedSignal;
```

A.2.1 FFT and Channel Equalisation

A.2.1.1 FFT

```
%%%%%%%%%%%%%%%%%%%%%%%%%%%%%%%%%%%%%%%%%%%%%%%%%%%%%%%%%%%%%%%%%%%%%%%%%%
%%                                                                    %
%%     Name: receiver.m                                               %
%%                                                                    %
%%     Description: This function performs FFT and CP removal         %
%%                                                                    %
%%     Parameters:                                                    %
%%      SymbolRx = QAM symbols.         SymbolTx = OFDM symbol        %
%%      margin = CP size in samples.                                  %
%%                                                                    %
%%                                                                    %
%%%%%%%%%%%%%%%%%%%%%%%%%%%%%%%%%%%%%%%%%%%%%%%%%%%%%%%%%%%%%%%%%%%%%%%%%%

function SymbolRx=receiver(SymbolTx, Guard, Nfft)

%Cyclic prefix removal
margin=length(SymbolTx)*Guard;

margin=margin/(1+Guard);

cyclic_removed=SymbolTx(margin+1:end);

%FFT
SymbolRx=fft(cyclic_removed,Nfft);
```

A.2.1.2 Channel equalisation

```
%%%%%%%%%%%%%%%%%%%%%%%%%%%%%%%%%%%%%%%%%%%%%%%%%%%%%%%%%%%%%%%%%%%%%%%%%%
%%                                                                    %
%%     Name: chanelestimate.m                                         %
%%                                                                    %
%%     Description: This code estimates the channel coefficients and  %
%%     perform data recovery.                                         %
%%                                                                    %
%%                                                                    %
%%     Parameters:                                                    %
%%      data_rx = Equalised symbols.    estimate = channel coeficients %
%%                                                                    %
%%%%%%%%%%%%%%%%%%%%%%%%%%%%%%%%%%%%%%%%%%%%%%%%%%%%%%%%%%%%%%%%%%%%%%%%%%

function data_rx = channelestimate(dataafterFFT,channel)

estimate = fft(channel,256);
estimate = conj(estimate');

data_rx = dataafterFFT ./ estimate;
```

A.3 Multi-path SUI Channel Modelling

```matlab
function channel = channelSUI(N_SUI,G,BW)


%%%%%%%%%%%%%%%%%%%%%%%%%%%%%%%%%%%%%%%%%%%%%%%%%%%%%%%%%%%%%%%%%%%%%%%%
%%                                                                  %
%%     Name: channelSUI.m                                           %
%%                                                                  %
%%     Description: The function generates the Channel Impulse Response  %
%%     of the channel variant by using Jakes Model.                 %
%%                                                                  %
%%     SUI channels from 1-6 with different bandwidths could be simulated %
%%                                                                  %
%%                                                                  %
%%     Parameters:                                                  %
%%      n = Oversampling factor.        channel = output coefficients    %
%%                                                                  %
%%%%%%%%%%%%%%%%%%%%%%%%%%%%%%%%%%%%%%%%%%%%%%%%%%%%%%%%%%%%%%%%%%%%%%%%

Nfft = 256;  % fixed WiMAX
BW = BW*1e6;

% oversampling factor defined by 802.16d
if mod(BW,1.75)==0
    n = 8/7;
elseif mod(BW,1.5)==0
    n = 86/75;
elseif mod(BW,1.25)==0
    n = 144/125;
elseif mod(BW,2.75)==0
    n = 316/275;
elseif mod(BW,2)==0
    n = 57/50;
else
    n = 8/7;
end

    Fs = floor(n*BW/8000)*8000; % Oversampling rate
    deltaF = Fs / Nfft;      % OFDM subcarrier spacing
    Tb = 1/deltaF;            % Symbol duration
    Ts = Tb * (1+G);          % Symbol duration with CP
    T = 1/(Fs*1e-6);          % OFDM symbol duration


    [variances,Lc,Dop]=CIRpowers(N_SUI,T); % variance calculated

    hfr=[];
    for ih=1:Lc+1
      hfr=[hfr;genh(FrameLength,Dop,Ts)]; % generates coefs according to
Jakes Model
    end
    hfr=diag(variances.^0.5)*hfr;

    % Channel coefficients are normilised.
    channel = hfr ./ norm(hfr);
```

172

```matlab
%%%%%%%%%%%%%%%%%%%%%%%%%%%%%%%%%%%%%%%%%%%%%%%%%%%%%%%%%%%%%%%%%%%%%%%%
%%                                                                  %
%%      Name: CIRpowers.m                                           %
%%                                                                  %
%%      Description: It generates variance of each path of the channel  %
%%                                                                  %
%%                                                                  %
%%      Parameters:                                                 %
%%       SUI = Channel type to simulate.   T = Symbol duration      %
%%       tap_variances = Output variance.  BW = Bandwidth of the channel  %
%%       L= length of the variance                                 %
%%                                                                  %
%%%%%%%%%%%%%%%%%%%%%%%%%%%%%%%%%%%%%%%%%%%%%%%%%%%%%%%%%%%%%%%%%%%%%%%%


function [tap_variances,L,Dop]=CIRpowers(SUI,T)

  [powers,K,delays,Dop,ant_corr,Fnorm] = SUI_parameters(SUI);
  Dop = max (Dop);

  delays=delays/T; % delay expressed in terms of samples

  nbtaps=length(powers);      % Number of paths
  len_cir=1+round(max(delays)); % Length of the channel impulse response
  tap_variances=zeros(1,len_cir); % Output variance variable initialisation

  variances=10.^(powers/10);   % convert power to linear units

  variances=variances/sum(variances); % normalise the variance

  for i=1:nbtaps

      tap_variances(1+round(delays(i)))=tap_variances(1+round(delays(i)))+
      variances(i);
  end

  L=length(tap_variances)-1;



%%%%%%%%%%%%%%%%%%%%%%%%%%%%%%%%%%%%%%%%%%%%%%%%%%%%%%%%%%%%%%%%%%%%%%%%
%%                                                                  %
%%      Name: SUI_parameters.m                                      %
%%                                                                  %
%%      Description: It defines parameters for all SUI types according to  %
%%      the standard.                                               %
%%                                                                  %
%%%%%%%%%%%%%%%%%%%%%%%%%%%%%%%%%%%%%%%%%%%%%%%%%%%%%%%%%%%%%%%%%%%%%%%%

function [P,K,tau,Dop,ant_corr,Fnorm] = SUI_parameters(SUI)

% Standardised SUI parameters for each type (ie. SUI1-6)
switch SUI

    case 1
        P = [ 0 -15 -20 ];   % Power in each path
        K = [ 4 0 0 ]; % LOS factor. This one represent high LOS link
        tau = [ 0.0 0.4 0.9 ]; % Delay in each path
```

```matlab
        Dop = [ 0.4 0.3 0.5 ];   % Doppler shift
        ant_corr = 0.7; % Correlation factor
        Fnorm = -0.1771; % Normalisation factor

    case 2
        P = [ 0 -12 -15 ];
        K = [ 2 0 0 ];
        tau = [ 0.0 0.4 1.1 ];
        Dop = [ 0.2 0.15 0.25 ];
        ant_corr = 0.5;
        Fnorm = -0.3930;

    case 3
        P = [ 0 -5 -10 ];
        K = [ 1 0 0 ];
        tau = [ 0.0 0.4 0.9 ];
        Dop = [ 0.4 0.3 0.5 ];
        ant_corr = 0.4;
        Fnorm = -1.5113;

    case 4
        P = [ 0 -4 -8 ];
        K = [ 0 0 0 ];
        tau = [ 0.0 1.5 4.0 ];
        Dop = [ 0.2 0.15 0.25 ];
        ant_corr = 0.3;
        Fnorm = -1.9218;

    case 5
        P = [ 0 -5 -10 ];
        K = [ 0 0 0 ];
        tau = [ 0.0 4.0 10.0 ];
        Dop = [ 2.0 1.5 2.5 ];
        ant_corr = 0.3;
        Fnorm = -1.5113;

    case 6
        P = [ 0 -10 -14 ];
        K = [ 0 0 0 ];
        tau = [ 0.0 14.0 20.0 ];
        Dop = [ 0.4 0.3 0.5 ];
        ant_corr = 0.3;
        Fnorm = -0.5683;
end

%%%%%%%%%%%%%%%%%%%%%%%%%%%%%%%%%%%%%%%%%%%%%%%%%%%%%%%%%%%%%%%%%%%%%%%%%%%%
%%                                                                      %
%%     Name: genh.m                                                     %
%%                                                                      %
%%     Description: Unique fading coefficients with sum of sinusoids    %
%%                                                                      %
%%     Parameters:                                                      %
%%      tb = Symbol duration.        I = Frame length                   %
%%      Dop = Doppler shift.         Fadingcoeff = Output ch coefficients %
%%                                                                      %
%%%%%%%%%%%%%%%%%%%%%%%%%%%%%%%%%%%%%%%%%%%%%%%%%%%%%%%%%%%%%%%%%%%%%%%%%%%%

function fadingcoeff=genh(I,Dop,tb)

  fdmax = Dop;
```

```matlab
    N = 100;
    t = tb:tb:tb*I;

    len = length(t);
    theta = rand(1,N)*2*pi;    % phase of each sinusoid
    fd = cos(2*pi*((1:N)/N))*fdmax;

    E = exp(j.*(2*pi*fd(:)*t(:)'+repmat(theta(:),1,len)));
    E = E/sqrt(N);
    fadingcoeff = sum(E);   % sum of sinusoids from Jakes Model

end
```

A.4 References

[1] *MATLAB Central* (Online). Available: http://www.mathworks.co.uk/

Appendix **B**

Appendix B presents the path loss calculations based on emperical models. These were used in chapter 6 to estimate the maximum transmission distance across the overlapping cell circumference with constant wireless receiver noise floor.

B.1 Wireless channel Path Loss Calculations

An empirical based path los model described in [1] is experimental data collected gathered across typical sub-urban area. The model was initially derived at 1.9 GHz transmission however further extensions were followed to support higher frequencies up to 5 GHz and different antenna heights [2]. To that extent, the path loss as a function of distance can be derived as shown in B.1:

$$PL = A + 10\gamma \log\left(\frac{d}{d_0}\right) + s \qquad \text{(B.1)}$$

where variable **d** is distance in meters between transmitter and receiver while **s** represents the fading loss and is typically assumed in the range of 8dB [1].

The intercept **A** (in B.1) is a fixed quantity and is given by a free space path loss formula [1]:

$$A = 20 \log\left(\frac{4\pi d_0}{\lambda}\right) \qquad \text{(B.2)}$$

where d_0=100m (which is Fresnel zone) and λ is the wavelength in meters.

Furthermore, γ is the path-loss component calculated as in the B.3:

$$\gamma = \left(a - bh_b + \frac{c}{h_b} \right) \quad\quad (B.3)$$

From B.3 **h_b** is a base station antenna height in meters and **a**, **b** and **c** are constant units depending on terrain category as given in the figure below.

Table B-1: Various terrain categories used in the path loss calculation

MODEL PARAMETER	TERRAIN CATEGORY		
	A (Hilly/Moderate-to-Heavy Tree Density)	B (Hilly/Light Tree Density or Flat/Moderate-to-Heavy Tree Density)	C (Flat/Light Tree Density)
a	4.6	4.0	3.6
b (in m^{-1})	.0075	.0065	.0050
c (in m)	12.6	17.1	20.0

Finally, to account for frequencies above 2GHz the correction parameters were defined [2] as shown in equations B.4 - B.6:

$$P_{correction} = PL + \Delta PL_f + \Delta PL_h \quad\quad (B.4)$$

$$\Delta PL_f = 6\log\left(\frac{f(MHz)}{2000} \right) \qu\quad (B.5)$$

$$\Delta PL_h = -10.8\log\left(\frac{h_b}{2} \right) \qu\quad (B.6)$$

B.2 References

[1]   V. Erceg, L. J. Greenstein, S. Y. Tjandra, S. R. Parkoff, A. Gupta, B. Kulic, A. A. Julius, and R. Bianchi, "An empirically based path loss model for wireless channels in suburban environments," *J. Select. Areas Commun.*, vol. 17, pp. 1205-1211, 1999.

[2]   J. G. Andrews, A. Ghosh, and R. Muhamed, "Fundamentals of WiMAX: Understanding Broadband Wireless Networking", Prentice Hall, 2007.

Appendix C
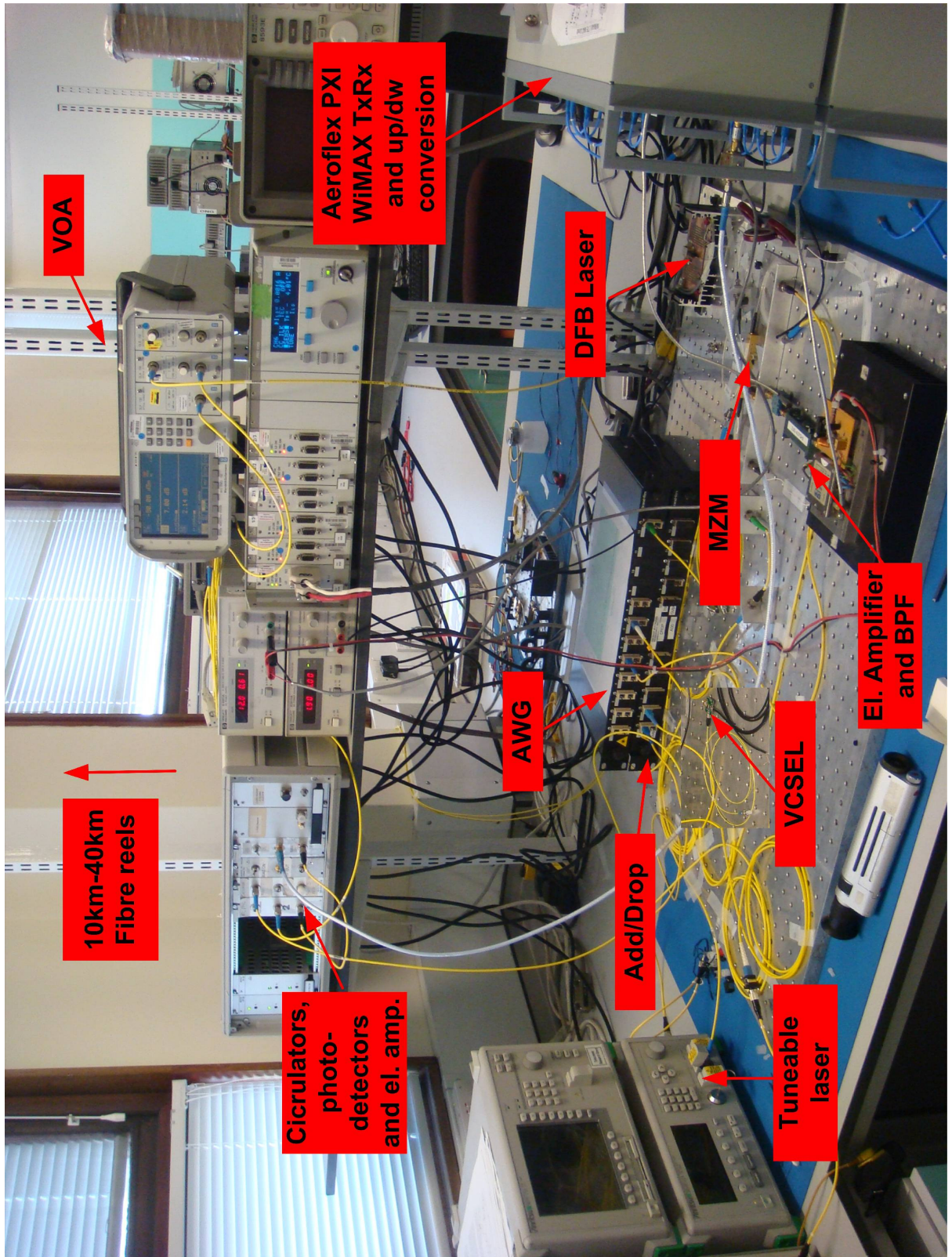
Figure C-1: Experimental setup photo
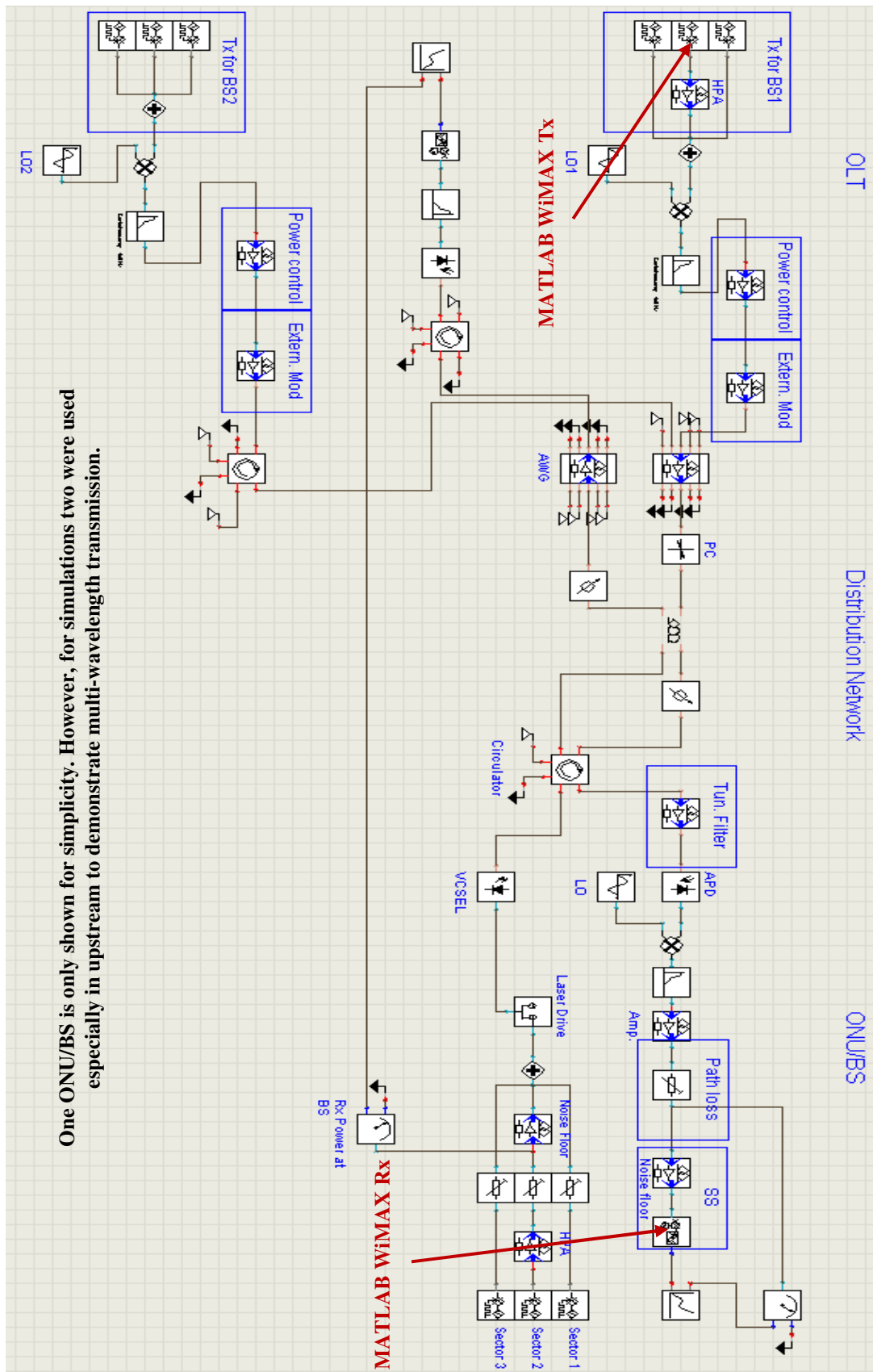
Figure C-2: VPI network modelling